

**PURDUE UNIVERSITY
GRADUATE SCHOOL
Thesis/Dissertation Acceptance**

This is to certify that the thesis/dissertation prepared

By Stephanie Marge Flaig

Entitled
Development of Therapies to Treat Polycystic Kidney Disease

For the degree of Master of Science

Is approved by the final examining committee:

Bonnie Blazer-Yost

Chair

Vincent H. Gattone II

Teri Belecky-Adams

To the best of my knowledge and as understood by the student in the *Research Integrity and Copyright Disclaimer (Graduate School Form 20)*, this thesis/dissertation adheres to the provisions of Purdue University's "Policy on Integrity in Research" and the use of copyrighted material.

Approved by Major Professor(s): Bonnie Blazer-Yost

Approved by: Simon Atkinson

Head of the Graduate Program

10/23/2012

Date

**PURDUE UNIVERSITY
GRADUATE SCHOOL**

Research Integrity and Copyright Disclaimer

Title of Thesis/Dissertation:

Development of Therapies to Treat Polycystic Kidney Disease

For the degree of Master of Science

I certify that in the preparation of this thesis, I have observed the provisions of *Purdue University Executive Memorandum No. C-22, September 6, 1991, Policy on Integrity in Research*.*

Further, I certify that this work is free of plagiarism and all materials appearing in this thesis/dissertation have been properly quoted and attributed.

I certify that all copyrighted material incorporated into this thesis/dissertation is in compliance with the United States' copyright law and that I have received written permission from the copyright owners for my use of their work, which is beyond the scope of the law. I agree to indemnify and save harmless Purdue University from any and all claims that may be asserted or that may arise from any copyright violation.

Stephanie Marge Flaig

Printed Name and Signature of Candidate

10/23/2012

Date (month/day/year)

*Located at http://www.purdue.edu/policies/pages/teach_res_outreach/c_22.html

DEVELOPMENT OF THERAPIES TO TREAT POLYCYSTIC KIDNEY DISEASE

A Thesis

Submitted to the Faculty

of

Purdue University

by

Stephanie Marge Flaig

In Partial Fulfillment of the

Requirements for the Degree

of

Master of Science

December 2012

Purdue University

Indianapolis, Indiana

For everyone that has inspired me to be my best, live up to my greatest potential, and
always follow my dreams.

ACKNOWLEDGEMENTS

First, I want to acknowledge my loving family who has supported me throughout my years in school and has always believed in me.

I offer my greatest thanks to my committee members, who have been patient, thoughtful, and helpful in their advisory roles towards me. Dr. Bonnie Blazer-Yost has been a wonderful advisor, besides being extremely patient and helpful with every aspect of my project she was always encouraging me to go above and beyond. I do not believe I could have accomplished as much as I did during my time at IUPUI without her. It was Dr. Blazer-Yost that further stimulated my interest into renal physiology, which begun when I was an undergraduate and took her physiology class, which encouraged me to further changed my academic path for the better. Dr. Vincent Gattone has also been instrumental in my graduate career, always offering valuable advice and encouragement. He has been a great factor in my research and my academic career while making decisions that affect my future goals. I only met Dr. Teri Belecky-Adams in my first year of graduate school, but in the very short time she has been supportive and provided suggestions that have resulted in higher quality projects.

I also want to sincerely give thanks to all the other students and lab technicians that have helped me throughout my degree. I greatly appreciate Dr. Amiraj Banga, for she initially trained me in lab procedures and protocols, as well as encourage and helped me. I also want to give thanks to Alexander Carr, for the animal projects he was a great asset to the study and it could not have been completed without his help. Other students that were helpful throughout my graduate studies were Shanta Lewis and Gabriel Martinez.

TABLE OF CONTENTS

	Page
LIST OF TABLES	vi
LIST OF FIGURES	vii
ABSTRACT	x
CHAPTER 1: INTRODUCTION	1
1.1 Polycystic Kidney Disease (PKD)	1
1.2 Lysophosphatidic Acid	3
1.3 PPAR γ agonists	4
1.4 Current PKD Therapies	4
CHAPTER 2: METHODOLOGY	6
2.1 Cell Culture	6
2.2 Electrophysiology	7
2.3 Immunohistochemistry	8
2.4 cAMP assay	8
2.5 Fluid Secretion	10
2.6 Animals	10
2.7 Study Design and Protocols	11
2.7.1 Rosiglitazone	11
2.7.2 Pioglitazone	12
2.8 Histological Analysis	13
2.9 CT Imaging	14
2.10 CT Analysis	14
2.11 Statistical Analysis	15
CHAPTER 3: RESULTS	16
3.1 Electrophysiology	16
3.2 Immunohistochemistry	19
3.3 cAMP	19
3.4 Fluid Secretion	20
3.5 Rosiglitazone Data	21
3.6 Pioglitazone Data	23
CHAPTER 4: DISCUSSION	28
4.1 Electrophysiology	28
4.2 Immunohistochemistry	32
4.3 cAMP	32
4.4 Fluid Secretion	33

	Page
4.5 Rosiglitazone Data	34
4.6 Pioglitazone Data	36
CHAPTER 5: SUMMARY.....	40
LIST OF REFERENCES	42
TABLES	48
FIGURES	51
VITA	97

LIST OF TABLES

Table		Page
1.	Summary of overall data completed for the 24 week, rosiglitazone study on the PCK rat model	48
2.	Summary of overall 10 day data completed for the pioglitazone study on the W-WPK rat model	49
3.	Summary of overall 18 day data completed for the pioglitazone study on the W-WPK rat model	50

LIST OF FIGURES

Figure	Page
1. Postulated LPA receptors (LPA ₁ -LPA ₅) pathways from Choi, et al. (9)	51
2. Human Cyst Fluid Addition to Apical and Basolateral side of the mpkCCD _{cl4} renal cell line.....	52
3. Stimulatory response to the addition of 50µM LPA to the basolateral side of the mpkCCD _{cl4} renal cell line	53
4. Inhibition of cyst fluid (CF-12) stimulated chloride secretion in mpkCCD _{cl4} cells with known inhibitors of CFTR and CaCCs	54
5. Inhibition of LPA stimulation with CFTR and CaCC inhibitors	55
6. Testing the Stimulatory Capacity of Human Cyst Fluid from Multiple Patients	56
7. Comparison of LPA and ADH stimulation of ion transport in the mpkCCD _{cl4} renal cell line.....	57
8. Inhibition of the fetal bovine serum (FBS) stimulation with CFTR and CaCC inhibitors	58
9. Comparison of the basolateral stimulatory response of ether LPA and ester LPA	59
10. Inhibition of LPA stimulation with LPA 1/3 Receptor Antagonists (Ki6425 and VPC51299)	60
11. Basolateral addition of Bapta-AM and Ionomycin with LPA	61
12. Basolateral addition of Bapta-AM and Ionomycin with CF-12.....	62
13. Inhibition of the fetal bovine serum (FBS) stimulation with T16AinhA-01	63
14. Inhibition of the cyst fluid (CF-12) stimulation with digalliac acid	64
15. Immunohistochemical confocal staining of the mpkCCD _{cl4} renal cell line for TMEM16A	65
16. Standard curve generated from the cAMP standard solutions	66
17. Fluid secretion after 5 minutes of LPA stimulation on the basolateral side of the mpkCCD _{cl4} renal cell line	67
18. Fluid secretion after 5 minutes of LPA stimulation on the basolateral side of the mpkCCD _{cl4} renal cell line	68
19. Fluid secretion after 24 hours of LPA stimulation on the basolateral side of the mpkCCD _{cl4} renal cell line	69
20. Rosiglitazone treated PCK rats body weight comparison for control, high, intermediate, and low dose treatment	70

Figure	Page
21. Rosiglitazone treated PCK rats total kidney weight (A) and kidney weight as a percent of Body weight (KW%BW) (B) comparison for control, high, intermediate, and low dose treatment	71
22. Rosiglitazone treated PCK rats renal cyst volume percentage (Vv) (A) and renal cyst volume (B) comparison for control, high, intermediate, and low dose treatment	72
23. Histological Kidney Sections from Rosiglitazone (Control, High, Low), treated PCK rats	73
24. Rosiglitazone treated PCK rats total liver weight (A) and liver weight as a percent of Body weight (LW%BW) (B) comparison for control, high, intermediate, and low dose treatment	74
25. Rosiglitazone treated PCK rats liver percent fibrocystic comparison for control, high, intermediate, and low dose treatment	75
26. Rosiglitazone treated PCK rats heart weight comparison for control, high, intermediate, and low dose treatment	76
27. Day Pioglitazone treated W-WPK rats glucose (A) and hematocrit (B) comparison for control, high, and low dose treatment.....	77
28. 10 Day Pioglitazone treated W-WPK rats body weight comparison for control, high, and low dose treatment	78
29. 10 Day Pioglitazone treated W-WPK rats total kidney weight (A) and kidney weight as a percent of body weight (KW%BW) (B) comparison for control, high, and low dose treatment	79
30. 10 Day Pioglitazone treated W-WPK rats renal cyst volume percentage (Vv) (A) and renal cyst volume (B) comparison for control, high, and low dose treatment	80
31. 10 Day Pioglitazone treated W-WPK rats total liver weight (A) and liver weight as a percent of body weight (LW%BW) (B) comparison for control, high, and low dose treatment	81
32. 10 Day Pioglitazone treated W-WPK rats total heart weight (A) and heart weight as a percent of body weight (HW%BW) (B) comparison for control, high, and low dose treatment	82
33. 10 Day Pioglitazone treated W-WPK rats CT renal cyst volume percentage comparison for control, high, and low dose treatment	83
34. 18 Day Pioglitazone treated W-WPK rats glucose (A) and hematocrit (B) comparison for control, high, and low dose treatment	84
35. 18 Day Pioglitazone treated W-WPK rats body weight comparison for control, high, and low dose treatment	85
36. 18 Day Pioglitazone treated W-WPK rats total kidney weight (A) and kidney weight as a percent of body weight (KW%BW) (B) comparison for control, high, and low dose treatment	86
37. 18 Day Pioglitazone treated W-WPK rats renal cyst volume percentage (Vv) (A) and renal cyst volume (B) comparison for control, high, and low dose treatment	87

Figure	Page
38. 18 Day Pioglitazone treated W-WPK rats total liver weight (A) and liver weight as a percent of body weight (LW%BW) (B) comparison for control, high, and low dose treatment	88
39. 18 Day Pioglitazone treated W-WPK rats total heart weight (A) and heart weight as a percent of body weight (HW%BW) (B) comparison for control, high, and low dose treatment	89
40. 18 Day Pioglitazone treated W-WPK rats brain perimeter (A) and brain area (B) comparison for control, high, and low dose treatment.....	90
41. 18 Day Pioglitazone 3-D Cystic Tissue Image generated from Philips program using CT value ranges	91
42. 18 Day Pioglitazone 3-D Cystic Normal Image generated from Philips program using CT value ranges	92
43. 18 Day Pioglitazone 2-D Image of CT values labeling for cystic tissue from Philips program	93
44. 18 Day Pioglitazone 2-D Image of CT values labeling for normal tissue from Philips program	94
45. 18 Day Pioglitazone 2-D Image of CT values labeling for normal tissue from Philips program, with all other CT labeled tissue removed, besides the kidney	95
46. 18 Day Pioglitazone treated W-WPK rats CT renal cyst volume percentage comparison for control, high, and low dose treatment	96

ABSTRACT

Flaig, Stephanie Marge. M.S., Purdue University, December 2012. Development of Therapies to Treat Polycystic Kidney Disease. Major Professor: Bonnie Blazer-Yost.

Polycystic kidney diseases (PKD) are genetic disorders characterized by fluid-filled cysts in the kidney tubules and liver bile ducts. There are two forms of PKD, autosomal dominant polycystic kidney disease (ADPKD) and autosomal recessive polycystic kidney disease (ARPKD). The focus of the studies in this thesis has been on ADPKD. The disease progresses slowly and the fluid-filled cysts grow in size due to increased rates of cell proliferation and fluid secretion into the cyst lumen. The expanding cysts compromise the normal kidney function and result in a decrease of renal function to the point of end-stage renal failure in midlife. Cyst enlargement is due, at least in part, to chloride secretion via the cystic fibrosis transmembrane conductance regulator (CFTR) chloride channel. Currently therapy is limited to renal cyst aspiration, dialysis, and eventually renal transplantation after organ failure, thus it has critical to determine possible drug therapies for the treatment of PKD.

Previous studies showed that cyst fluid caused a secretory response in cells lining the cysts. We hypothesized that once the cyst have expanded and become so large that they burst or leak, which could also occur due to renal injury or aging, the cyst fluid may stimulate additional cyst growth. Lysophosphatidic Acid (LPA) was determined to be the active component of human cyst fluid, and we investigated the LPA stimulated signaling pathway.

Our data suggest that the LPA stimulates chloride and fluid secretion by a combination of CFTR and Ca²⁺-Activated chloride channels (CaCC) and that the two channels may functionally be linked to each other. The secretion is not occurring through a cAMP stimulated pathway, and it is possible that TMEM16A, a CaCC, plays a larger role than previously expected.

Previous studies demonstrated that PPAR γ agonists, insulin sensitizing drugs used to treat diabetes, inhibit chloride secretion by the collecting duct principal cells by decreasing CFTR synthesis. It was logical therefore to consider PPAR γ agonists as long-term treatment for PKD. The first preclinical study showed that high (20 mg/kg BW) dose pioglitazone, a PPAR γ agonist, inhibited cyst growth in the PCK rat model, a slow progressing model, of PKD. To continue to look at the effects of the PPAR γ agonists another preclinical study was completed, which tested if there was a class action of PPAR γ agonists and if a lower dose was effective in treating the cystic burden. Using the PCK rat model, and another PPAR γ agonist, rosiglitazone, a 24 week study was completed using 3 doses (4, 0.4, and 0.04 mg/kg BW). 4 mg/kg BW rosiglitazone is analogous to 20 mg/kg BW pioglitazone. The data indicated that the rosiglitazone is effective in lowering the cystic burden, and importantly the low dose proved to be effective. An additional rat model, the W-WPK rapidly progressing model was used to determine efficacy across multiple models, and to determine if there was a way to track the progress of the disease in a manner analogous to that used in human patients. The animals were treated with pioglitazone using 2 doses (2 and 20 mg/kg BW), and were imaged using CT scans to track the progress of the disease. The data suggest that pioglitazone was not as effective in the W-WPK rat model as it was the PCK rat model. There was a trend however, that low dose PPAR γ agonist was as effective as high dose. Even more important, the CT scans proved to be an effective way to track the progress of the disease in animal models.

CHAPTER 1. INTRODUCTION

1.1 Polycystic Kidney Disease (PKD)

Polycystic kidney disease (PKD) is a genetic disorder that is characterized by the accumulation and growth of fluid-filled cysts predominately in the kidney tubules and liver bile ducts. It is normally diagnosed in adults with an incidence of 1:400 to 1:1000, making it one of the most common genetic diseases (5, 18, 42). The disease progresses slowly and the fluid-filled cysts grow in size due to increased rates of proliferation and secretion. The expanding cysts compromise the normal kidney function and result in a decrease of renal function to the point of end-stage renal failure in midlife (32).

There are two forms of PKD, autosomal dominant polycystic kidney disease (ADPKD) and autosomal recessive polycystic kidney disease (ARPKD) (18). ARPKD is rare and affects children, especially in the neonatal period. It is characterized by tubular dilation in the kidneys (5, 18, 42). ADPKD is the common form in the population and is characterized by the closed cysts that grow during a patient's lifetime. ADPKD is not specific to any race or gender (20), but there are gender dimorphisms in disease progression.

ADPKD is caused by genetic mutations that occur on chromosomes 16 and 4. In 85% of the patients the genetic mutation occurs on chromosome 16, the PKD1 gene, which makes the protein polycystin 1. The other 15% of genetic mutations occur on chromosome 4, the PKD 2 gene, which makes the protein polycystin 2 (4). The proteins polycystin 1 and 2 are found on the primary cilia, and other locations throughout the cell. They either act as a transient receptor potential Ca^{2+} channel or they are proteins that

regulate the same class of Ca^{2+} channels (18, 32, 42, 43). Mutations that affect Ca^{2+} levels in the cells will ultimately affect intracellular signaling pathways, such as ones that are involved in regulation of cAMP. In the renal epithelial cells of the distal nephron and cortical collecting duct, Ca^{2+} influx inhibits the adenylyl cyclase/cAMP pathway. The lack of PKD 1 or PKD 2 in the primary cilia mechano-sensitive organelles in renal cysts, inhibits the Ca^{2+} influx. Thus, increasing the activity of the adenylyl cyclase leading to an increase in intracellular cAMP. It is further exacerbated by a decrease in an intracellular Ca^{2+} -stimulated phosphodiesterase. The increase in cAMP, has been widely documented as a common finding in cystic cells (5, 18). With an increase in cAMP, there is an increase in protein kinase A (PKA), which thereby will alter intracellular signaling pathways that control ion flow as well as fluid secretion (18).

It is speculated that patients are born with every cyst that will ever develop (13) and over time these cysts slowly expand and fill with fluid. Surprisingly, this cyst expansion does not compromise renal function until later in life, but once the renal function declines it does so at a severe rate (5). The symptoms of PKD that precede renal failure, include cyst formation in organs other than the kidney, aneurysms, flank pain, hematuria, renal colic, urinary tract infections, and hypertension (18). The renal pathology is the primary cause for the deaths associated with PKD in both ADPKD and ARPKD. The other most common area of concern besides renal pathology is the liver cysts that arise in the lining of the hepatic bile duct. Currently therapy is limited to renal cyst aspiration, dialysis (currently approximately 4% of dialysis patients are due to PKD), and eventually renal transplantation after organ failure (20). Thus, it is critical to look at possible therapies for the treatment of PKD.

1.2 Cyst Fluid/Lysophosphatidic Acid (LPA) and PKD Disease Progression

The growth of individual cysts is determined to be combined rates of epithelial proliferation and fluid transport into the cyst cavity (14). The fluid transport is secondary to aberrant ion secretion into the cyst lumen. In renal cysts it has been observed that cAMP is increased resulting in over stimulation of ion channels (12). By inhibitor and electrophysiology studies, it has been shown that the cystic fibrosis transmembrane conductance regulator (CFTR) is one of the major ion channels responsible for the increase of chloride secretion in both the kidney tubules and liver bile ducts (10, 24).

It was shown that cyst fluid from human patients stimulate a secretory activity from normal renal epithelial cells and enhance cyst growth *in vitro* (12, 34, 54). In Madin Darby Canine Kidney (MDCK) cells it was shown by Grantham et al., that the component of the human cyst fluid is lipid-like that stimulates the chloride secretion via CFTR (14). In a subsequent paper, the group proposed that the lipid-like active component of cyst fluid was forskolin, but could not reveal the origin of this lipid-like plant compound (34).

Our laboratory has extended the Grantham studies using electrophysiological techniques (46) to examine the effect of human cyst fluid when added to the mpkCCD_{c14} (mouse principal cells of the kidney cortical collection duct, clone 4) cell line (1). It was found that human cyst fluid stimulated at least two chloride channels and that lysophosphatidic acid (LPA) is an active component in the human cyst fluid. LPA, present in both cyst fluid and serum, stimulated a chloride secretory response (2) LPA, a small glycerophospholipid, plays a role in cell signaling pathways and is released into the interstitial space during renal injury. Under normal conditions, LPA does not interact with the basolateral receptors because it is attached to serum proteins or proteins such as albumin and gelsolin found in the cyst fluid (30, 40, 41). Thus it is reasonable that an occurrence of renal injury to a PKD patient could release the cyst fluid or simply the cyst could burst, allowing the basolateral membrane to be in contact with LPA (39). LPA could be potential target for therapy, but the intracellular pathway has to be elucidated in more detail. For example there are at least five known G-protein- coupled receptors:

LPA₁-LPA₅ (9), and their general pathway has already been established (Figure 1) from the Choi, et al. Yet, the intracellular signaling pathway for the activation of LPA from the cyst fluid remains uncharacterized.

1.3 PPAR γ agonists

Peroxisome proliferator activator receptor gamma (PPAR γ) agonists are insulin-sensitizing agents and are commercially available for the treatment of type 2 diabetes mellitus (6, 8, 35, 52, 53). PPAR γ is expressed in the renal collecting duct (16). The nephron controls the salt and water balance via the ion transport systems and in the collecting duct, sodium and water reabsorption are under hormonal control (31).

At high concentrations, PPAR γ agonist therapy causes fluid retention, initially the focus of PPAR γ agonist induced fluid retention was on the epithelial sodium channel (ENaC) (7, 15, 19, 29, 38, 47, 56). However inhibitor and electrophysiology studies in various principal cell types suggest that ENaC is not the target of the PPAR γ agonists. Studies completed in cell culture models of the principal cell type of the distal nephron have shown the PPAR γ agonists inhibit cAMP-stimulated anion transport by inhibiting the synthesis of the CFTR protein (28). As noted above CFTR is the chloride channel responsible for the cyst growth in the kidney and liver cysts in PKD (10, 21, 24). Thus, it is reasonable to hypothesize PPAR γ agonists could be used as treatment for PKD.

1.4 Current PKD Therapies

Currently there are several drugs in clinical trials for the treatment of PKD. There are three general areas that drugs are targeting; proliferative pathways, fluid and electrolyte transport pathways, and a combination of both. One of the proliferative pathway targeting drugs, mTOR (rapamycin) inhibitors, blocks cell growth and proliferation. The pre-clinical trials were conducted in the mouse models and the results were positive (33, 50). However, in clinical trials the drug did not do as well as expected. Some of the patients left the trial due to the side effects associated with the drug and

efficacy did not match the preclinical assays (36, 48). On a more positive outlook, the drugs that are targeting the fluid and electrolyte pathways are showing more promising data. The vasopressin, V2 receptor antagonist, Tolvaptan has shown to be the most promising. It works by inhibiting the adenylyl cyclase pathway, thus decreasing the amount of chloride secretion and it has progressed from animal models into phase III clinical trials (44, 45).

In consideration of therapies for the treatment of PKD, there are many factors that play key roles. A drug that has adverse side effects that eventually will cause more damage than the disease itself would not be effective. This is the reason the mTOR inhibitors have been abandoned. To be beneficial, the drug needs to be at a higher dose, which is dangerous (33, 50). ADPKD is a slowly progressing disease, thus the earlier the treatment the better, but this also means that a patient needs to remain consistently on a drug from the time of diagnosis. Tolvaptan has an adverse effect on a patient's lifestyle that makes the drug less pleasing to the patients. The most serious side effect is the risk of dehydration due to the inability to concentrate urine. There is also the issue of cost for a drug. The more expensive the drug the less likely the patients will be able to afford it for a long period of time. And the current cost of Tolvaptan is approximately \$300,000 a year. Ultimately it is clear that there needs to be other drugs that could be used in the treatment of PKD, that are less harmful and more patient friendly.

CHAPTER 2. MATERIALS AND METHODS

2.1 Cell Culture

The well-characterized mpkCCD_{cl4} renal cell line of mouse principle cells of the cortical collecting duct were grown at 37°C in a humidified incubator continuously gassed with 5% CO₂. The culture media consisted of DMEM/F12 base media supplemented with 2% fetal bovine serum (FBS), 0.4 M penicillin/streptomycin, 0.5 M glutamax, 3.1x10⁻⁸ M ciproflaxin, 6.37 x10⁻⁵ M transferrin, 1.16 x10⁻⁴ M selenium, and 1.0 x10⁻⁹ M T₃. In some cases additional supplements were added to the media, such as 1.57 x10⁻⁸ M epidermal growth factor, 4.1 x10⁻⁸ M dexmasome, and 0.0224 M glucose. Media was replaced every 2 to 3 days. Cell cultures were maintained in plastic 75 cm² flasks until confluence. At confluence, the cells were subcultured and reseeded into another 75 cm² flask, and permeable supports in 6-well plates. They were subcultured by first warming the media, 20 mL of Hanks Balanced Salt Solution (HBSS) and 2 mL trypsin with EDTA to 37°C. The flask containing the confluent mpkCCD_{cl4} renal cell is taken out of the incubator and placed into the biosafety cabinet. The old media is removed and 10mL of HBSS is added to the flask. During this time, quickly the trypsin with EDTA is filtered and diluted with 8 mL of HBSS. Then the HBSS is removed from the flask and the diluted trypsin is placed in the flask and then put back in the incubator for approximately 5 minutes. As soon as the cells were released from the flask, 10mL of serum containing culture media is added to the flask to deactivate the trypsin. The culture media with cells and diluted trypsin with HBSS is then placed into a 50 mL centrifuge tube and is placed into a centrifuge for 5 minutes at 1000 rpm. The supernatant is removed, leaving behind a solid pellet of cells, which is then mixed with

10 mL of culture media. From the resuspended cells, only a few drops are placed into a new flask already containing 10 mL of culture media. Then 14 mL of culture media is added to the remaining cell pellet suspension. 1.5 mL of this solution is placed in each well of a transwell 6-well plate and 2 mL of media on the bottom. The plates are cultured for 13-16 days in order to form high resistant monolayers.

2.2 Electrophysiology

After approximately 14 days of growth on the transwells the cells formed a confluent monolayer. At this time the permeable membrane was excised, mounted into Ussing chambers and clamped into electrophysiology set-ups. The cells were bathed in serum-free media, which contained only DMEM/F12, sodium bicarbonate, penicillin/streptomycin, and glutamax. They were maintained at 37°C via a water jacket buffer reservoir that was continuously gassed with 95% O₂/5% CO₂. The trans-epithelial potential difference (PD) was measured and clamped to zero leaving the resulting short-circuit current (SCC) which is a measure of net ion flow. A positive change in SCC is defined as an anion moving in a secretory direction (basolateral to apical) or a cation moving in an absorptive direction (basolateral to apical). During the experiments the trans-epithelial PD was switched from 0 to 2 mV every 200 seconds, thus using Ohm's law the trans-epithelial resistance (TEER) was calculated from the resulting current change. Cultures with resistances lower than 1000 Ω/cm² were discarded. For each experiment, the inhibitor, enhancer, or hormone was added to either the basolateral or apical side of the cells depending on where their presence was effective.

2.3 Immunohistochemistry

After approximately 14 days of growth on the permeable supports, the cells were fixed and stained for zonula occludens protein 1 (ZO1), a tight junction protein, and TMEM16A, a Ca²⁺-activated chloride channel. Permeable supports containing confluent monolayers were washed twice with cold 1% phosphate buffer saline (PBS) for 10 minutes for each wash. After which 1mL of 3.7% paraformaldehyde in PBS was added to the cells for 5 minutes. The cells were then washed twice with cold 1% PBS for 10 minutes each. The cells were permeabilized with 0.25% NP-40 in PBS for 15 minutes. Again, the cells were washed twice with cold 1% PBS for 10 minutes each. The primary antibody was made up to a 1:50 dilution in 1% PBS with 10% fat-free dry milk. The primary antibody was added to the permeable supports and allow to incubate overnight at 4°C while gently being swirled on a plate shaker. After overnight incubation the cells were washed three times with cold 1% PBS for 5 minute each. The secondary antibody was made up to a 1:200 dilution in 1% PBS with 10% fat-free dry milk. The secondary antibody was added to the wells and the plate incubated at 37°C for 30 minutes. After 30 minutes the wells were washed three times with cold 1%PBS while avoiding light exposure. The permeable supports were mounted face up onto microscope slides to be viewed on the fluorescent microscope.

2.4 cAMP assay

Cells cultured on permeable supports for 14 days were used for analysis of intracellular cAMP (Direct cAMP EIA kit purchased from Enzo Life Sciences). The cells were stimulated with LPA, forskolin, antidiuretic hormone (ADH), or diluent for 20 seconds, 1 minute, or 5 minutes. For stimulation, the effectors were added to the basolateral side of the cells and the plate was gently swirled. After which, 1 mL of lysis buffer (1% Triton X-100 in 0.1 M HCl), was added to the well and the plate was placed in the incubator for 10 minutes. The plate was taken out of incubator and the cells were rubbed off by rotating a rubber policeman on the transwell 30 times, alternating direction ever 5 times. The media, cells, and lysis buffer were removed and collected. The

collected fluid was centrifuge on high speed for 2 minutes. The standards were made by using the stock 2,000 pmol/mL warmed to room temperature. Five standards were made by serial dilutions in 0.1M HCl, to produce 200 pmol/mL, 50 pmol/mL, 12.5 pmol/mL, 3.13 pmol/mL, and 0.78 pmol/mL. Wash buffer was prepared by diluting 5mL of the supplied concentrated wash buffer with 95 mL of deionized water. The 96-well plate to be used to analyze the samples was a goat anti-Rabbit IgG microtiter plate. Initially 50 μ L of neutralizing reagents was added into each well except the total activity (TA) and blank well. Then 100 μ L of the 0.1 M HCl was added into the non-specific (NSB) and the Bo (0 pmol/mL standard) wells. Another 50 μ L of 0.1 M HCl was added to the NSB well. Then for the correct corresponding wells, 100 μ L of each of the 5 standards was pipetted into their appropriate labeled well. Next, 100 μ L of the supernatant of the centrifuge samples was added to the appropriate wells. Then, 50 μ L of the cAMP direct conjugate was added to each well except the TA and blank wells, and 50 μ L of the antibody was added into each well except the blank, TA, and NSB well. The plate was sealed and covered with parafilm and aluminum foil and incubated for 2 hours on a plate shaker at approximately 500 rpm at room temperature. After the 2 hour incubation period the contents of the wells was removed by using a glass pipette and a vacuum. Each well was washed with the diluted wash buffer by added 400 μ L to each well. This washing procedure was repeated 2 times, after the final wash was completed the plate was gently tapped onto lint free paper towel to make sure to remove any of the wash buffer. At this point 5 μ L of the cAMP direct conjugate was added to the TA well, and 200 μ L of substrate solution was added into each well. The plate was then sealed again and incubated at room temperature for one hour without shaking. After the one hour incubation, stop solution was added into every well. Once the stop solution was added the plate then could placed into the plate reader and the optical density was read at 405 nm. After which, a standard curve could be generated by graphing the standard concentration vs. the mean optical density on a log scale.

2.5 Fluid Secretion

A fluid secretion protocol was modified from Neufeld, et.al. (27). After approximately 14 days of growth on the permeable supports, the mpkCCD_{cl4} renal cells have grown to confluence. At this time, the 6-well plates, containing the permeable supports were removed from the incubator and placed into a biosafety cabinet. As the cells grow on the supports, the basolateral side of the cells is facing the permeable supports, and the apical is facing the upper media. 0.114 mM LPA or diluent were added to the basolateral side of the transwell. Every 30 second time point the transwells were either stimulated with diluent or with LPA. During stimulation the plate was gently swirled. After 5 minutes of stimulation the media was removed using a P1000 pipette and placed into a pre-weighed microcentrifuge tube. The tubes were then re-weighed, and the weights were compared to the microcentrifuge tube without the collected media. The difference was taken to determine exactly how much fluid was in the tube, and it was determined that every μg would be a μL of fluid. There were two protocols: 1) the cells were stimulated for 24 hours; 2) the media was left on top and then stimulated. In the 24 hour fluid secretion protocol, the cells were stimulated the day before and 500 μL of autoclaved oil was placed on the top of the well to help reduce the lost of fluid due to evaporation. The media and oil was removed and placed into a microcentrifuge, and centrifuge to separate the oil from the fluid. The oil was removed and the microcentrifuge tube was weighed and compared to the unweighed tube. In the fluid secretion protocol in which the media was left on top before stimulation with LPA, the wells were stimulated and after 5 minutes the media was removed and placed in a pre-measured microcentrifuge tube and compared to its original mass.

2.6 Animals

The PCK rats were purchased from Charles River Laboratories, Inc. (Wilmington, MA) and a breeding colony maintained at Indiana University School of Medicine (IUSM). The PCK rat model was chosen for its orthologous genetic mutation to ARPKD and the presence of many the phenotypic characteristics of human ADPKD. The Pck

gene of the rat is an orthologue to the PKHD-1 gene responsible for ARPKD (49). The animal model develops both kidney and liver fibrocystic diseases, and is slow progressing. There is also a gender dimorphism of the rat model; females develop more severe liver disease while males develop more severe kidney disease, which resembles what is seen in human ADPKD (22).

The W-WPK rat colony was already established at IUSM. The W-WPK rat model is a rapidly progressing model, that has full development of terminal disease at the age of 21 days (11). The mutant gene is the MKS3 gene in humans and Mks3 gene in rats. The protein associated with the gene mutation is called Meckelin, which has 995 amino acids in humans and 997 amino acids in the rat and they are 84% identical and 91% similar (37). The W-WPK rat was developed for its renal cystic disease, but it has demonstrated phenotypic CNS malformations, such as hypoplasia, agenesis of the corpus callosum, and severe hydrocephalus. As such, it proved to be a good model for both renal cystic disease and Meckel-Gruber Syndrome (11).

Institutional Animal Care and Use Committees approved all protocol procedures for both animal models. Animals were monitored and each day with the help of the laboratory animal resource center (LARC).

2.7 Study Design and Protocols

2.7.1 Rosiglitazone

Rosiglitazone (Avandia®) are purchased in tablet form. After weaning, at four weeks of age, the PCK rats were randomly separated out into groups. Only females were used due to their development of more severe liver disease. There were three treatment groups, and one control group. All animals were kept in the same room, with the same type of bedding, and water. Control animals were fed a diet of Purina no. 5002 LabDiet. The treatment groups were fed Purina no. 5002 LabDiet supplemented with rosiglitazone calculated to provide 4 mg/kg body weight (BW), 0.4 mg/kg BW, and 0.04

mg/kg BW daily. The concentrations were dependent on the estimated animal consumption of their base diets. The rats were kept on control or supplemented diet for 24 weeks, throughout the study various parameters were recorded. At 8 weeks a 24-hour urine sample was collected and glucose levels were measured. A hematocrit was measured to assess possible fluid retention. The day before they were 24 weeks old, the animals were placed in metabolic chambers to collect urine to later be centrifuge and collected and analyzed. At week 24, the animals were anesthetized with 100 mg/kg intraperitoneally injected sodium pentobarbital. After the animals no longer had tail, foot, and eye reflexes the sacrifice was begun. Blood was collected via intracardiac puncture for serum analysis. Body weight was measured and a laparotomy was performed. Urine protein was assessed using an uristix, then the left kidney and right liver lobe was removed, weighed, and frozen in liquid nitrogen. The body was then flushed with a saline solution through a catheter in the left ventricle followed by 4% paraformaldehyde in phosphate buffer to perfusion fix the animal. The right kidney, the left liver lobe, and heart were removed, weighed and kept in 4% paraformaldehyde. The kidney and liver were to be later used for histological analysis.

2.7.2 Pioglitazone

Pioglitazone (Actos®) was purchased as 15 mg tablets. The drug was made up in grape juice to enhance palatability. Animals received either 20 mg/kg BW or 2.0 mg/kg BW. It was fed to the animals by daily weighing the animals and feeding them the grape juice supplemented with Pioglitazone at 1 µL per gram of body weight. The W-WPK rat model was used and treatment was started on day 5, because of the rapid progression. On day 5 the entire litter was started due to the fact that it was difficult at this age to determine which ones were cystic or normal. On day 5, they were weighed and received grape juice either supplemented with drug or nothing. A tail clip was performed and blood glucose was determined and blood was collected for hematocrit. The animals continued to stay on the treatment either till day 10 or day 18. For everyday of treatment, the animals were weighed and treated with either grape juice or grape juice

supplemented with pioglitazone. They were treated by using a pipette and received 1 μ L per gram of BW. The animals were sacrificed on day 10 or day 18 of treatment. Some were randomly chosen to be scanned for CT images. The animals were initially anesthetized with 100 μ g/g intraperitoneally injected sodium pentobarbital. After the animals no longer had tail, foot, and eye reflexes the sacrifice begun. Body weights were determined, urine if present was collected directly from their bladder, and blood was collected for serum analysis, hematocrit and blood glucose levels. A kidney was removed, weighed, and frozen in liquid nitrogen. The body was then flushed with a saline solution, followed by 4% paraformaldehyde in phosphate buffer to perfusion fix the animal. The other kidney, liver, heart, and head were collected and kept in 4% paraformaldehyde. The kidney and head were to later to be used for histological analysis.

2.8 Histological Analyses

Slides were prepared at the histology center in the Anatomy and Cell Biology Department, IUSM. In the rosiglitazone study, the liver and the kidney were embedded in paraffin, transversely sectioned and stained with hematoxylin, and eosin as well as with picosiruis red for fibrosis analysis. In the pioglitazone study the kidney and head sections were embedded in paraffin. The kidney was sectioned transversely and either unstained or stained with hematoxylin, and eosin. The head was coronally sectioned and either unstained or stained with hematoxylin, and eosin. The kidneys for both studies were analyzed by completing point count stereology. Point count stereology is when a grid is placed on top the image of the kidney and then for every point of intersection it was either counted as a point for tissue or one for cyst. This provides a numerical value to the tissue and the cyst, so the renal cyst percentage could be calculated. The liver for the rosiglitazone study was analyzed in a similar manner, except that the pictures of the livers were from the picosiruis red staining, which also stains for the fibrosis. At every point of intersection, it was either counted as a point for tissue or one for cyst and fibrosis, thus the percent fibrocystic could be determined. Finally, the brains for the

pioglitazone study were analyzed by using ImageJ (NIH), in which the outline of the ventricles was drawn and the program was able to calculate the perimeter and the area in square centimeters.

2.9 CT Imaging

In the pioglitazone study, the W-WPK rats were imaged at two time points, 10 days and 18 days. The rats were taken from the rest of the litter and moved to the CT imaging facility in the IU Health Hospital to be scanned on the Siemens Biograph Truepoint PET•CT. Before the imaging could begin the rats were slightly anesthetized by injecting them with 70% diluted sodium pentobarbital and were kept warm by placing them under a heating lamp. Once the rat was no longer moving a contrasting fluid was injected into the tail vein, and then the rat was imaged approximately 10 times by the scanner.

2.10 CT Analysis

The CT scans were copied on to disks and analyzed using the Philips Extended Brilliance™ Workspace (V2.0.1). Each animal's data was uploaded to the program and the best series of images was determined. The CT value range was determined for the functioning renal tissue and for the cyst tissue. The CT ranges were different between the 10 day animals compared to the 18 day animals. The CT ranges were applied to each animal analysis, which then a 3-dimensional kidney was built slice by slice for both the normal renal tissue and the cystic tissue per animal. The program calculated the volume of the 3-dimensional image in cubic millimeters and thus the renal cyst volume percentage could be calculated by comparing the normal renal tissue volume with the cyst tissue volume.

2.11 Statistical Analysis

Comparisons between data groups were performed using a Student's t-test for unpaired samples. Where indicated further statistical analysis was performed using Anova one-tailed probability test. *P value* less than 0.05 were used to denote statistical significance. Statistics were completed using the ProStat (version 5.5).

CHAPTER 3. RESULTS

3.1 Electrophysiology

The laboratory was investigating the active component of human cyst fluid, lysophosphatidic acid (LPA), to determine the pathway controlling cyst expansion. For all studies the well characterized mpkCCD_{c14} (mouse principal cells of the kidney cortical collection duct, clone 4) cell line (1) were used. Previously the laboratory showed that cyst fluid (10% v/v) was more effective in stimulating ion transport when added on the basolateral side (Figure 2). The response had several secretory components (2). Since the laboratory already has shown the LPA was the active component of cyst fluid in previous experiments (2) it was logical to test the response after the addition of LPA to the basolateral side of the cells (Figure 3). The same response was shown in comparison to the addition of cyst fluid, in which there was a strong initial ion transport and then a smaller secondary ion transport.

The laboratory showed the cyst fluid response was not due to sodium absorption, but chloride secretion (2), thus the next step was to look at the identity of the chloride channels. The cells were pretreated with two chloride inhibitors, GlyH-101 and tannic acid, then stimulated with cyst fluid. GlyH-101 is a specific inhibitor of the CFTR chloride channel, and tannic acid is an inhibitor of Ca²⁺-activated chloride channels (CaCC), including the recently described TMEM16A (Figure 4). GlyH-101 inhibited majority of the secretory response, and tannic acid partially inhibited the chloride transport. The laboratory also previously completed an experiment in which different concentrations of LPA were added to determine the maximal concentration that mimicked the addition of human cyst fluid (10% v/v). It was determined that the LPA

concentration of 0.05 to 50 mM maximally stimulated the mpkCCD_{cl4} cells (2). Having established LPA as the active component of cyst fluid the next step was to look the chloride channels in response to the basolateral addition of LPA. The cells were pretreated with GlyH-101 and tannic acid prior to the addition of LPA (Figure 5). The results were similar to the effects in the human cyst fluid experiment. If one envisions the chloride secretory response as composed of two overlapping ion secretory transports, GlyH-101 partially inhibited the first secretory response completely and inhibited the second response, while tannic acid inhibited the second ion transport, but affected the first ion transport slightly.

To further investigate the cyst fluid response, it was critical to determine if cyst fluid from multiple sources elicited the same response when added to the basolateral side of the cells. Cyst fluid from different patients was added to the basolateral side of the cells (Figure 6). There was a substantial variability in the responses tested, and it was determined that cyst fluid 12 (CF-12) would be used in later experiments.

Antidiuretic hormone (vasopressin) stimulates CFTR through the cAMP pathway. Thus a comparison of basolateral addition of LPA and ADH was completed (Figure 7). Antidiuretic hormone seems to be a more abrupt and intense ion transport.

Fetal bovine serum (FBS) contains enough LPA to maximally stimulate the chloride channels (2). It was important to look at the chloride channels, thus the cells were pretreated with the chloride channel inhibitors, GlyH-101 and tannic acid and added together (Figure 8). GlyH-101 partially inhibits the first secretory response and inhibits second secretory response, and tannic acid slightly inhibits the first secretory response and completely inhibits the second.

It was important to classify the LPA receptor responsible for the chloride secretory response. There are at least five known G-protein- coupled receptors for LPA: LPA₁-LPA₅ (9). Initially, LPA receptor 5 was investigated. This was done by comparing the ion transport the responses to ester LPA and ether LPA. Ether LPA is known to preferentially stimulate LPA receptor 5. A comparison of stimulatory effects of eqimolar amounts of ether and ester LPA indicated that ester LPA had a much greater stimulatory effect than ether LPA suggesting LPA receptor 5 was not involved (Figure 9).

Other, LPA receptors of interest, where LPA receptor 1 and 3. The cells were pretreated with LPA 1/3 receptor antagonists, Ki16425 and VPC51299 supplied by Professor Kevin Lynch, to the basolateral side then there was an addition of ester LPA to the basolateral side (Figure 10). The out come of the experiments indicated that neither LPA receptor 1 or 3 was contributing to the secretory response.

To further characterize the ion secretory response to LPA stimulation, we studied two compounds that alter intracellular Ca^{2+} in the cells. Ionomycin, which increases intracellular Ca^{2+} by forming channels that allow Ca^{2+} influx from the extracellular medium and Bapta-AM, which chelates intracellular Ca^{2+} . One would expect the ionomyocin would potentiate the Ca^{2+} -activated chloride channels (CaCC), and that Bapta-AM would inhibit the same channel.

Ionomycin caused an initial transport event, then with the addition of LPA, the normal secretory response was decreased, which was unexpected. Since ionomyocin increases intracellular Ca^{2+} stores, thus if chloride is secreted by CaCC, it is expected that the transport events associated with basolateral addition of LPA would increase, which was not the case. Bapta-AM as expected when added to the renal cell line the chloride secretory response to LPA was diminished (Figure 11). Bapta-AM chelates the Ca^{2+} stores, thus if the LPA secretory response is due, in partial, to CaCC, if there is no Ca^{2+} present, then the secretory event would be expected to be diminished. The next step was to preincubate with ionomyocin and Bapta-AM before the addition of human cyst fluid (Figure 12), to see if it reacted in the same way as the LPA did, since the laboratory has already showed the LPA is the active component of cyst fluid. The results showed a similar response as seen with LPA, the ionomyocin decreased the secretory event, again unexpectedly, and Bapta-AM diminished the response as expected.

Although the situation is complex, the Ca^{2+} is involved and the identity of the CaCC remains unknown. Previous inhibitor experiments suggested that it might be TMEM16A. And several references indicated there are more specific inhibitors for TMEM16A. This was investigated by using two different TMEM16A inhibitors, besides the original tannic acid, namely T16Ainh-A01 and digalliac acid (25). The cells were pre-treated with T16Ainh-A01 inhibitor and then human cyst fluid was added

(Figure 13). Which, unexpectedly the inhibitor did not have an effect on the chloride secretory response. Also, the cells were pretreated with digalliac acid and then FBS was added to the basolateral side (Figure 14), similar to the T16Ainh-A01, the inhibitor did not have an effect on the chloride secretory response.

3.2 Immunohistochemistry

By the electrophysiology data, it is clear that there are potentially two channels in which chloride secretion occurs, CFTR and TMEM16A. It has already been established the renal cells have small amounts of CFTR (10, 24), but the presence of TMEM16A is unknown. Thus using immunohistochemistry, the TMEM16A channel could be stained. After approximately 14 days of growth, the staining protocol was tested on the mpkCCD_{cl4} renal cell line by staining for ZO1, a tight junction protein, that is present in every epithelial cell. The cells were stained properly and the protocol worked. The next step, completed by Dr. Criss Hartzell, was to use a primary antibody that attaches to the TMEM16A protein, and using the secondary antibody, fluorescein isothiocyanate (FITC) to determine if TMEM16A is present in the renal cell line while viewing the cells using a confocal microscopy (Figure 15).

3.3 cAMP

A cAMP assay was completed to further investigate the LPA stimulatory pathway. The only receptor that activates cAMP production is LPA receptor 4, thus determining the amount of cAMP released due to stimulation of LPA is critical if the receptor in question is LPA receptor 4. Multiple trials were completed where the cells were stimulated with nothing for control, LPA, ADH, and forskolin for various times. In each trial, a standard curve was created by comparing the standard cAMP concentration with their optical density values (Figure 16). Then by graphing the optical density values of the LPA, ADH, and forskolin by interpolation, the cAMP concentrations could be determined.

The cAMP concentrations are expressed as cm^2 (Figure 17). Thus, contrary to our hypothesis, LPA does not stimulate an increase in intracellular cAMP levels.

3.4 Fluid Secretion

From the electrophysiology experiments it has been clear that there is a transepithelial ion flux in response to the basolateral addition of FBS, LPA, and human cyst fluid. We next explored the hypothesis that the ion flux is accompanied by water flux. The mpkCCD_{cl4} renal cells lines were grown to confluence for approximately 14 days then the cells were stimulated basolaterally with LPA. There were two different protocols for fluid secretion. The first method was to leave the media completely untouched before stimulation. Thus there was 2 mL of media on the basolateral side and 1.5 mL of media on the apical side, this is the typical fluid level in the transwell chamber. The cells were stimulated LPA on the basolateral side of the cells or nothing for control and gently swirled for 5 minutes. After five minutes the media was collected and placed in a pre-weighed microcentrifuge tube. Thus after weighing the tube, by simple subtraction the amount of media was determined. There was a statistically significant increase of 39 μL per transwell of media compared to the control (Figure 18). In an alternative protocol, the cell volume was measured 24 hours after stimulation. Since the stimulation occurred over such a long period of time, there was risk of losing fluid due to evaporation, thus oil was to the top of the transwell. After 24 hours the fluid on top was collected and was centrifuged for 1 minute on max speed to separate the fluid and the oil, thus the oil could be removed before weighing the tubes. In this long-term protocol there was a fluid secretion of approximately 50 μL per transwell compared to control (Figure 19).

3.5 Rosiglitazone Data

A previous study was performed using the PCK rat to determine the effect of oral feeding of the PPAR γ agonist, pioglitazone, for 7 or 14 weeks. The 7 week pioglitazone feeding study was completed at the Mayo Clinic, while our laboratory in collaboration with Dr. Vincent Gattone, at the Department of Anatomy and Cell Biology, IUSM completed the 14 week protocol (3). PCK rats were either fed a control diet or a diet supplemented with pioglitazone at the concentration of 4 mg/kg for the 7 week study and 20 mg/kg for both the 7 and 14 week studies. The animals were sacrificed at the end of the 7 and 14 week study. In the 14 week study, blood was collected by cardiac puncture for serum analysis. The left kidney and right liver lobe were collected and frozen in liquid nitrogen, whereas the remaining kidney and liver were fixed, then removed and kept in 4% paraformaldehyde. The kidney and liver were later embedded in paraffin and transversely sectioned and stained with hematoxylin, and eosin. Cyst volume was calculated using point count stereology methods. Fibrosis was assessed on a 1-4 scale (1 was normal and 4 was severe) after completing a picosirius red staining. Immunohistochemistry by light microscopy and immunocytochemistry by transmission electron microscopy were conducted to stain for the CFTR channel. The results showed that there was improvement in the renal and liver cyst burden due predominantly to decreased cyst size. There was a variation between the male and female rats used in the study. The gender dimorphism in the animal mimicked the observations in humans, where renal disease is relatively worse in males and liver disease is relatively worse in females. The serum analysis showed well-preserved kidney function, but liver enzymes were increasing indicating a compromised of hepatic function. The bile ducts showed a decrease in apical expression of CFTR by electron microscopy (3).

This study showed promising data, but some parameters were not assessed fully. For example, the fibrosis of the liver and kidneys were not severe enough to analyze effectively at 7 or 14 weeks of age in this slowly progressing model. It is also important to determine whether there is a class action effect of PPAR γ agonists on cyst growth in the PCK rat model. Also, previous studies in renal cell culture studies have shown that the PPAR γ agonists' effect on CFTR occurs at a concentration lower than what is

necessary for diabetic treatment (4). Thus, it was important to assess the effect of a low dose agonist. Therefore, our laboratory used another PPAR γ agonist, rosiglitazone, to investigate whether this compound would cause similar outcomes at a lower dose.

Following weaning PCK rats were fed a control diet or a diet supplemented with rosiglitazone at three different concentrations, 4.0 mg/kg BW, 0.4 mg/kg BW, and 0.04 mg/kg BW. Only females were used in this 24 week study, due to gender dimorphism. Females developed more severe liver cystic disease, which in the previous pioglitazone study uncovered an area of concern, which we needed to follow. There was no significant change in the glucose or hematocrit of the animals at any concentration indicating that the insulin-sensitizing drug did not cause hypoglycemia and did not cause fluid retention respectively (data not shown). However, as shown in the body weight the animals supplemented with the highest dose, 4.0 mg/kg BW had a significant increase in their body weight compared to control, while the other two doses were not statistically different (Figure 20).

The body weight is perhaps a more sensitive measurement of fluid retention than hematocrits. Total kidney weight (Figure 21A), was significantly lower in the highest and the lowest dose, but yet unchanged in the intermediate dose. Kidney weight as a percent of body weight was determined for all animals. Again, as seen in the total kidney weight, kidney weight as a percent of body weight was significantly decreased in the highest and lowest dose (Figure 21B), yet not statistically different in the intermediate dose.

Following point count stereology methods, the renal cyst volume was calculated as a percent of total kidney. This provides a more accurate indication of how much of the total kidney weight is due to cystic burden. From the renal cyst volume percentage the highest and lowest dose were significantly decreased, but a conflicting result was that the intermediate dose was actually significantly increased. (Figure 22A) Taking the renal cyst volume percentage and multiplying it with the total kidney weight, the renal cyst volume was calculated. Renal cyst volume showed the same statistical changes as the renal cyst volume percentage (Figure 22B). It is even more apparent to see the

effects of the rosiglitazone when looking at the actual histological kidney sections (Figure 23). Both the high and low dose decreased the cystic burden.

Other organs that were taken into account were the liver and the heart. The organ that shows cyst development almost as frequently as the kidney is the liver, specifically the bile ducts. Total liver weight (Figure 24A) was not significantly changed in any of the three different treatment doses. Liver weight as a percent of body weight was determined, and as seen in total liver weight, neither of the three doses were significantly altered this parameter (Figure 24B). Livers were stained with picosiruis red to access the liver fibrocystic disease, by using point count stereology methods. The percent liver fibrocystic disease (Figure 25) was not significantly different in any of the three doses. The serum liver enzymes, as measure of liver function, were also not significantly changed (data not shown). PPAR γ agonists have been widely noted for their fluid retention side effect, which is, in some cases severe enough to cause cardiac hypertrophy. Thus the heart weight was determined (Figure 26). Heart weight was not significantly changed in any of the three treatment doses. The data is all summarized (Table 1).

A serum and urine analysis was performed on the samples collected from the animals at their 24 week time point. For the serum the test detected sodium, potassium, chloride, CO₂, anion gap, BUN, creatinine, calcium, phosphate, alanine transaminase (ALT), aspartate transaminase (AST), bilirubin, total protein, albumin, and glucose. For the urine the test detected sodium, potassium, chloride, protein, and urea nitrogen. No changes were observed in the serum and urine values (data not shown).

3.6 Pioglitazone Data

The rosiglitazone data showed that PPAR γ agonists had a class action effect and that a low dose was effective in the treatment of renal cyst burden. But, another aspect of the preclinical trials of PPAR γ agonists treatment, was to show that there is potential for the drug to be effective in a fast-progressing rat model, since previous studies were completed in the PCK rat, a slow-progressing rat model. So the following study used the

W-WPK rat model, with pioglitazone, because it was shown in the previous studies to be less potent than the rosiglitazone. Also it is important to determine a way to track the progress of the disease without sacrificing the animals, to be more relatable to treatment in humans. So, CT scans would be used to determine the progress of the treatment and the disease along with histology to compare the two methods to determine if it is a reasonable to use CT scans to determine the extend of renal cyst burden.

W-WPK rats were given grape juice or grape juice supplemented with pioglitazone at two different concentrations, 20 mg/kg BW and 2.0 mg/kg BW starting on day 5. All animals were started on the drug at 5 days of age, because it was difficult to determine which of the animals were cystic or normal. Animals were continued on the treatment until it was determined if they were actually cystic or normal. Animals were sacrificed at two time points, either at 10 days or at 18 days, and of the animals a subset were chosen for CT imaging.

The 10-day data were collected in order to determine if the disease could be assessed in an earlier stages. There was no significant change in the glucose or hematocrits of the animals fed either concentration indicating that the insulin-sensitizing drug did not cause hypoglycemia or fluid retention (Figure 27A,B). Unlike the rosiglitazone data, in the 10 day animals there was no change in body weight (Figure 28) in either of the treatments compared to control. After only being on treatment for 5 days, the only kidney parameter in which drug treated was different from control was kidney weight as a percent of body weight (Figure 29B). High dose treatment, 2.0 mg/kg BW pioglitazone, was significantly increased. Total kidney weight (Figure 29A) remained unchanged between the different treatments. Renal cyst volume percentage determined by point count stereology methods (Figure 30A), and the renal cyst volume (Figure 30B) determined by taking the percentage multiplied with the total kidney weight both remained statistically unchanged in the drug treated animals compared to control.

Other organs taken into account were the liver and heart. For total liver weight (Figure 31A) and for liver weight as a percent of body weight (Figure 31B) just as seen in the kidney, neither dose was statistically different from control. Total heart weight

was statistically increased for both the high and low dose treatment (Figure 32A), but when looking at heart weight as a percent of body weight (Figure 32B) there was no statistically significant changes.

The extra parameter that was different from all the previous PPAR γ agonist studies was the use of CT scans. From the CT scans, a 3-dimensional image was developed for both the cystic tissue and the normal tissue, and the program was able to determine the volume in cubic millimeters. Thus the percent renal cyst volume could be determined. In the 10 day animals there were no statistically significant changes, but also the n values were low for this group of animals, because based in the data provided above, we did not expect to find differences (Figure 33). All the 10 day data is summarized (Table 2).

The 18 day data was collected as the end of the study to examine the full effect of the disease. Since it was a fast progressing animal model, at this time point the animals were close to renal failure. Blood glucose was statistically decreased for both the low and high dose treated animals (Figure 34A). Interestingly, this is the first model where we have observed a change in glucose. Hematocrits were not statistically different (Figure 34B), indicating that fluid retention was not a problem with the pioglitazone treatment. Body weight was not statistically different in animals treated with either dose compared to control (Figure 35). After these animals were on treatment for longer period of time, unlike the animals sacrificed on 10 days of age, there was more interesting changes in the kidney parameters. Total kidney weight (Figure 36A) was statistically decreased for the low dose treatment, and trended lower in high does as well, but not statistically. Kidney weight as a percent of body weight was not statistically different, but the low dose was definitely trending in the decreasing direction (Figure 36B). The renal cyst volume percentage calculated by point count stereology was not statistically different in either the low or high dose animals, but again both of them were decreasing compared to control (Figure 37A). Using the renal cyst volume percentage and the total kidney weight, the cyst volume was determined for this parameter, low dose significantly decreased the cyst burden (Figure 37B).

Other organs that were taken into account were the liver, heart, and brain. For total liver weight (Figure 38A) and for liver weight as a percent of body weight (Figure 38B), there was no statistical difference between the treatment groups and the control. Total heart weight (Figure 39A) was significantly decreased for the low dose treatment group, but heart weight as a percent of body weight (Figure 39B) was not significantly different. This specific animal model develops severe hydrocephalus along with the cystic kidney disease, thus the brain was analyzed by measuring the perimeter of the ventricles and the brain area. In both cases there was no significant difference in brain perimeter or brain area (Figure 40A,B).

Just as in the 10 day animals, some of the 18 day animals received CT scans. From the CT scans a 3-dimensional image was developed for both the cystic tissue (Figure 41) and the normal tissue (Figure 42). The 3-dimensional images were developed by assigning the appropriate CT values and building the kidney slice by slice, by removing everything from the image except the kidney tissue. This method is shown for the cystic tissue in which the colored section, determined from the CT number range, only marks cyst tissue (Figure 43). The CT number range was also applied for normal tissue, which the colored areas only showed the normal, functioning renal tissue (Figure 44). Then by using the Philips program, once the CT number range was applied for either cyst or normal renal tissue, the kidney was segregated by removing all the areas besides the kidney of interest (Figure 45). The Philips program was able to determine the volume in cubic millimeters based on the 3-dimensional image produced. Thus the percent renal cyst volume could also be assessed. In the 18 day animals there was no statistically significant changes (Figure 46), but the treated animals were showing a trend of decreasing renal burden. The 18 day data is all summarized (Table 3).

One of the most important aspects of this study, besides the drug treatment, was the use of the CT scans to assess the progress of the disease and if it was comparable to the histological analysis. Using regression statistics on the renal cyst volume percentage calculated from the CT scans and the renal cyst volume percentage calculated from the histology showed an R^2 value of 0.6993 and a correlation of 0.8362. The CT scans can further be compared with the whole animal, by showing the correlation of the left kidney

weight to the total left kidney volume determined from the CT scans, which showed an R^2 value of 0.9719 and a correlation of 0.9859. Finally by taking the total kidney weight and multiplying the renal cyst volume percentage determined using point count stereology and comparing that volume to the CT cyst volume it showed a R^2 value of 0.9360 and a correlation of 0.9674.

CHAPTER 4. DISCUSSION

4.1 Electrophysiology

Electrophysiology is a useful tool for following transepithelial electrogenic ion flux. Our laboratory has been studying the effects of human cyst fluid with goals of identifying the active component, which was previously stated as a lipid-like molecule, and to characterize the intracellular pathway stimulated in response to cyst fluid (14). Human cyst fluid is normally in contact with the apical side of the renal epithelial cells, thus one would wonder why does a person who has had cysts their whole life not go into renal failure until midlife. Previous studies had reported that cyst fluid stimulated transport when added to either side of the polarized epithelial cells. Our laboratory decided to investigate this question further, using the mpkCCD_{cl4} renal cell line. Human cyst fluid (10%) was added to the both the apical and basolateral side of the cells. In contrast to previous studies, there was no reaction to human cyst fluid when the cells were explored on the apical side, but instead there was a response when applied to the basolateral side. The ion transport response was relatively complex consisting of several temporally distinct components (2). This suggested that the human cyst fluid reacted with the epithelial plasma membrane on the outside of the cyst. The question was how could the cyst fluid reach the basolateral side and what importance does this have to the renal failure in midlife. This led to the hypothesis that when the cysts become too large they begin to leak or burst releasing cyst fluid into the abdominal cavity, causing the cyst fluid to come into contact with basolateral side of the cystic, renal cells. The subsequent increase in ion flux accompanied by compensatory water movement causes the expansion of the remaining intact cysts. This could also occur in response to renal injury.

Before more experiments could be completed, human cyst fluid was tested to determine which cyst fluid was most active and could be used for other experiments. Cyst fluid from different human patients was added basolaterally to determine which samples gave an optimal response. One thing that was consistent was cyst fluid that had blood contamination, even after centrifuging, was not that active. The results suggest that the red blood cells may contain a factor that inactivates the stimulatory component. After the testing, it was determined that human cyst fluid 12 (CF-12) had an optimal response and there was plenty of it to complete multiple experiments.

Previous studies showed that the response seen after the addition of human cyst fluid was not due to sodium absorption, but it was due to chloride secretion (2). It is also well documented that cyst expansion is due to chloride secretion via CFTR (10, 24). However a variety of studies including the complex response observed in our electrophysiological experiments suggested the presence of additional channels. One prime candidate for an additional transporter is the recently described Ca^{2+} -activated chloride channel (CaCC), TMEM16A. This was investigated using various inhibitors in electrophysiology experiments. The two compounds we used were GlyH-101 which specifically inhibit CFTR (23), and tannic acid, which has been recently described to inhibit TMEM16A (25,26). The renal epithelial cells were pretreated with the two inhibitors, both separately and in combination before the addition of CF-12. The results suggested that the first transepithelial ion flux indicated by the first peak was due predominantly to chloride secretion via CFTR, because the inhibitor GlyH-101 inhibited majority of the ion transport event indicated by the first peak. The second, broader ion transport event, indicated by the second peak, most likely represented chloride secretion via TMEM16A, because tannic acid inhibited majority of the ion transport event, indicated by the second peak. When the inhibitors were added together almost the entire response was inhibited.

It was recently discovered by our laboratory that LPA was the active component in human cyst fluid (2). LPA and human cyst fluid both generate identical responses each with multiple components. An LPA dose response study was completed and it was determined that the LPA concentration of 0.05 to 50 μM maximally stimulated ion

transport in the mpkCCD_{c14} cells. We also used the chloride channel inhibitors to determine the inhibitory effects compared with the cyst fluid. The GlyH-101 inhibitor almost completely inhibited all stimulated transport. These results suggested that there might be a correlation between the CFTR and TMEM16A. Further experimentation will be necessary to fully characterize the transporters and any interactions between them.

Fetal bovine serum (FBS) contains maximal concentration of LPA and we have used this as a more available alternative to cyst fluid. FBS showed the same transport responses that were seen when either cyst fluid or LPA were added basolaterally. To further ensure that FBS acts in the same way as cyst fluid and LPA, the chloride channel inhibitors, GlyH-101 and tannic acid, were used. As seen when cyst fluid and LPA were pretreated with the inhibitors, FBS showed the same type of inhibitory response.

Previous data suggests that the two chloride channels may be functionally dependent on each other. Therefore it is reasonable to look at the CFTR or the CaCC channel more in detail. Since the CaCC's are dependent on Ca²⁺ activation of this channel. Ca²⁺ can be looked at in more detail by using compounds that alter intracellular Ca²⁺. Ionomycin increases intracellular Ca²⁺, by enhancing Ca²⁺ influx from extracellular fluid. Bapta-AM decreases intracellular Ca²⁺ by chelating intracellular Ca²⁺. One would expect that ionomycin would potentiate the CaCC's, and that Bapta-AM would inhibit the same channel. The results were somewhat more complex. When ionomycin was added there was an immediate increase in transepithelial transport. However, after the addition of either LPA or human cyst fluid, the normal stimulated ion movement was decreased. It is likely that the addition of ionomycin stimulated the CaCC in the absence of LPA and cyst fluid stimulation and no further activation of this channel was possible by LPA or cyst fluid. With the pretreatment of Bapta-AM followed by LPA or human cyst fluid the reactions were similar and showed inhibition of all components of the stimulated transport. These results suggest that Ca²⁺ is involved in all aspects of the chloride secretory response including CFTR-mediated transport. Since Ca²⁺ regulation of CFTR is unusual this may indicated that there is a correlation between CFTR and CaCC in the renal cells.

The identity of the CaCC remains unknown, but previous inhibitor experiments suggested that it may be TMEM16A. It has been suggested that there are more specific inhibitors for TMEM16A than the previously used tannic acid. They were T16Ainh-A01 and digalliac acid. When the cells were pre-treated with either inhibitor, there was no effect on the FBS and human cyst fluid stimulated current, thus indicating at least in the mpkCCD_{c14} cell line, that these inhibitors are not effective. This finding is surprising, because immunohistochemical studies indicate a high abundance of TMEM16A in the cell line. We have requested additional specific inhibitors, and these will be explored in subsequent experiments.

Knowing that cyst fluid and LPA stimulates a chloride secretory response, it was important to identify the LPA receptor which initiates the response. There are 5 known LPA receptors with a 6th postulated (9). LPA receptor 5 was investigated by comparing the response of ester LPA against ether LPA. Ether LPA is known to preferentially stimulate LPA receptor 5, so if ether LPA addition resulted in the chloride secretory response, then the intracellular pathway by which LPA stimulates fluid secretion is by LPA receptor 5. Ultimately ether LPA did not show the characteristic response that is seen when human cyst fluid is added basolaterally, suggesting the receptor in question is not LPA receptor 5. The receptors were further investigated by using LPA receptor 1 and 3 antagonists, Ki16425 and VPC51299. The antagonists were added basolaterally, followed by the addition of LPA. Antagonist pretreatment did not alter a subsequent LPA response suggesting that the receptor in question is not LPA receptor 1 or 3. The laboratory previously showed that LPA receptor 2 was not likely the receptor either, by pretreating the mpkCCD_{c14} renal cells with DDP (dodecylphosphate) an LPA2 agonist/LPA3 antagonist, which had no effect on cyst fluid stimulated ion transport (2). By process of elimination the receptor experiments suggest that LPA receptor 4 is the only receptor in which the intracellular signaling pathway can occur, unfortunately there is not a known agonist or antagonist of LPA receptor 4. To further these studies we have requested more specific agonists and antagonists from GSK.

4.2 Immunohistochemistry

TMEM16A is a relatively new CaCC and it might play a bigger role in the principal renal epithelial cell function than previously noted. So showing the presence of TMEM16A in the mpkCCD_{cl4} renal cell line is critical. Confluent cells were stained for the TMEM16A protein, and the results strongly agreed that there is TMEM16A in the cells. The data shows that there is a lot of TMEM16A throughout all the renal cells, and that majority of it is concentrated on the apical membrane. It will also be important to determine if TMEM16A is located in other tissue, besides mouse, such as rat and human tissue.

4.3 cAMP

According to Choi, the only LPA receptor that signals through the cAMP pathway is LPA receptor 4 (9). Based on our finding that CFTR is activated in response to LPA and the well-documented knowledge that the main component that activates CFTR in the phosphokinase-A (PKA) phosphorylation after PKA activation by increasing cAMP, we assumed that LPA 4 was the most likely receptor candidate. It happens that the LPA receptor 4 is also the only one of the receptors that does not have a known agonist or antagonist available. If we stimulate the cells with LPA and then perform a cAMP assay on them and there is an increase in cAMP, we can predict that it is likely the receptor in question responsible for the chloride secretion seen with the addition of LPA is working through LPA receptor 4. Thus the cells were stimulated with LPA for 1 and 5 minutes. Unexpectedly in all cases the cAMP levels were the same or lower than control, indicating that LPA might actually inhibit cAMP. According to Choi, LPA receptor 4 actually can inhibit the cAMP pathway as well as stimulate it (9). However, these results are contrary to what is expected for an agent that increases CFTR activity. Thus there was a cAMP assay completed on the cells stimulated with LPA for only 20 seconds. The cAMP levels were still the same as the control. At this point, it was critical to make sure the methodology was working correctly. Agents that are known to increase cAMP were used to stimulate the cells, namely forskolin and ADH. With

stimulation of both forskolin and ADH there was an increase in cAMP levels as predicted, thus indicating the methodology was working and that LPA does not stimulate an increase in cAMP levels.

Overall, the cAMP assay raises multiple questions. Initially, it indicates that the receptor in question may not be LPA receptor 4. This also now contradicts the electrophysiology data which correlated with the LPA receptor not being 1,3, or 5 and our laboratory also already showed that it was not LPA receptor 2 (2). Thus, in the future our laboratory will need to reassess which receptor is responsible for the secretory response associated with the basolateral addition of LPA. We are in the process of requesting a variety of receptor agonists and antagonists from GSK. These are not commercially available. Another question the cAMP assay presents is whether or not the LPA stimulates chloride secretion via CFTR. Previous electrophysiology inhibitor studies indicated that the chloride secretory response was due to a combination of both CFTR and CaCC. CFTR has been well documented that it is activated by the adenylyl cyclase, cAMP pathway (2), while according to the assay with the addition of LPA there was no cAMP present. This presents a problem that potentially the inhibitors being used in electrophysiology were not as specific as they were indicated to be, and may have potentially inhibited both CFTR and CaCC. In this case we have also requested additional, more specific, but not commercially available inhibitors from a colleague.

4.4 Fluid Secretion

Electrophysiology is an extremely useful tool in determining net ion flow, then with the use of inhibitors and enhancers, the nature of the particular channel can be determined. The data has strongly supported that there is chloride secretion after the addition of LPA to the basolateral side of the cells. LPA is the active component of human cyst fluid and the hypothesis is that when a LPA is released and allowed to come into contact with the outside of the cyst, this causes chloride ions to be secreted and the cyst begin to expand. This hypothesis assumes that fluid follows the chloride ions that are being secreted, but electrophysiology cannot determine the net fluid flow. Thus, a

protocol was developed to determine the amount of fluid secreted, if any. There were multiple ways to approach the fluid secretion, and all methodology that were used showed the same results, that there was actual fluid secretion following the stimulation of LPA on basolateral side of the cells. In one method LPA was added and then after 5 minutes of stimulation the media was collected and weighed. In this method the cells were not stressed before stimulation, because the media was changed 24 hours prior to the fluid removal. There was a secretion of approximately 39 μL per transwell from the basolateral to the apical side of the cells, thus showing that LPA also stimulates fluid secretion, which would cause a cyst to expand. In this first series of experiments the fluid secretions were done in a 5 minute time frame, because according to the electrophysiology data, the chloride secretion occurs immediately after the addition of LPA. However, one would assume that fluid secretion would continue over time, so a fluid secretion study that allowed the cells to be stimulated for LPA for 24 hours was completed. The data does support that fluid continues to secrete over 24 hours, but not much more was secreted compared to the fluid collected after 5 minutes. It went from secreting 39 μL per transwell in 5 minutes to 50 μL per transwell in 24 hours. Thus it appears that majority of the fluid secretion happens rather quickly. Fluid secretion does support the hypothesis that LPA is the active component of cyst fluid when in comes into contact with the basolateral side of the cyst.

4.5 Rosiglitazone Data

The previous study performed using the PCK rat determined the effect of oral feeding of the PPAR γ agonist, pioglitazone, for 7 or 14 weeks. PCK rats were either fed a control diet or a diet supplemented with pioglitazone at the concentration of 4 mg/kg for the 7 week study and 20 mg/kg for both the 7 and 14 week studies. The results showed that there was improvement in the renal and liver cyst burden due predominantly to decreased cyst size. There was a variation between the male and female rats used in the study. The serum analysis showed well-preserved kidney function, but liver enzymes were increasing indicating a compromised of hepatic function. The effect of pioglitazone

on fibrosis was more difficult to assess, since fibrosis is mild in this early stage of the disease. The bile ducts showed a decrease in apical expression of CFTR by electron microscopy (3). This study showed promising data, but some parameters were not assessed fully. For example, the fibrosis of the liver and kidneys were not severe enough to analyze effectively at 7 or 14 weeks of age in this slowly progressing model. It is also important to determine whether there is a class action effect of PPAR γ agonists on cyst growth in the PCK rat model (3). Also, previous studies in renal cell culture studies have shown that the PPAR γ agonists' effect on CFTR occurs at a concentration that is approximately 10 fold lower than the EC_{50s} for receptor transactivation (2). Thus, it was important to assess the effect of a low dose agonist. Therefore, our laboratory used another PPAR γ agonist, rosiglitazone at three different concentrations; 4 mg/kg BW, 0.4 mg/kg BW, and 0.04 mg/kg BW, to investigate whether this compound would be effective at a lower dose. Rosiglitazone is more potent than pioglitazone, thus 4.0 mg/kg BW rosiglitazone is analogous to 20 mg/kg BW pioglitazone. The PCK rats were treated from post-weaning, approximately 3 weeks, until 24 weeks of age with 0 mg/kg BW, 4 mg/kg BW, 0.4 mg/kg BW, and 0.04 mg/kg BW rosiglitazone.

There was no significant change in the blood glucose for any dose as well as no change in hematocrit. No change in hematocrit was a promising result, because it indicates that the rosiglitazone is potentially not causing the well-known side effect of fluid retention. The heart weight was also not altered by drug treatment, thus further indicating that the drug was not causing fluid retention. A conflicting result with the hematocrit was the total body weight. It was not affected in either the intermediate or in the low dose, but it actually was significantly higher in the high dose. The increase of body weight could have been due to an increase in fluid retention because of the high dose drug treatment, which was not severe enough to alter heart weight or hematocrit. There was another difficulty with this high dose that affects all results of the study. High dose, or 4.0 mg/kg BW, treated animals only had an n of 3, because 7 of the animals were removed from the study due to the development of cholangitis, an infection of the common bile duct. Even though many of the high dose treated animals developed

cholangitis, the liver fibrocystic disease was not statistically different for any of the three doses, but again the cholangitis animals were removed from the statistical analysis.

Even taking the problems with the high dose into account, the data related to the kidney and the cystic volume showed promising data. In all renal parameters, the lowest dose, 0.04 mg/kg BW, was significantly effective. This indicates that the drug is working, so it is a class action in the PPAR γ agonists, since both rosiglitazone and pioglitazone worked in a similar fashion by decreasing the renal cystic burden. Also, an extremely important piece of data was that the lowest dose of treatment, which was two ten-fold decrease compared to the concentration used in the pioglitazone study, was effective in decreasing the renal cystic burden. As noted in some of the renal parameters, the intermediate dose actually significantly increased cystic burden, and currently reasons are still unknown.

4.6 Pioglitazone Data

Following the rosiglitazone study, it was determined that it was important to look at another rat model as well as determine a more effective way to track the progress of the disease. For maximal contrast to the slow-progressing PCK rat we chose the fast-progressing model the W-WPK rat. Also, this study added a new research parameter by introducing CT scans. Previously the severity of the disease and the effectiveness of the PPAR γ agonists was determined through histological analysis, after the animal was sacrificed. Thus, if this study were to go into human clinical trials there would have to be another way to track the progress of the disease, and one way to do this would be CT scans if they proved to be effective. Also, it was clear that the rosiglitazone had more side effects than the pioglitazone in the PCK rat, so the study also went back to using the PPAR γ agonist, pioglitazone.

In the WPK model the disease progressed so rapidly that by day 18 their kidneys were approximately 15% of the body weight (Figure 29B). All animals had to be treated at the age of 5, because it was nearly impossible, by palpation, to determine whether individual animals were cystic or normal. Once the animals were on treatment, by

approximately day 9 it is easy to determine which ones were cystic, and eventually the treatment numbers were reduced. The first time point was 10 days when the animals had been on treatment for 5 days. At this time point glucose and hematocrit were not different, indicating that the animals are not hypoglycemic or retaining fluid, which was further substantiated by the consistency in body weight. The only renal parameter that was significantly different was the high dose kidney weight as a percent of body weight, in which it was increased in comparison with the control. This is the opposite of the expected finding if the drug is working properly to decrease renal cystic burden.

The total liver weight and liver weight as a percent of body weight was statistically not different. The heart weight was actually significantly increased at both the high and low dose. This indicates that potentially the drug is causing fluid retention, even if not seen in the hematocrit or body weight. However, heart weight as a percent of body weight was not significantly changed. The one important aspect of the 10 day time point was the CT renal cyst volume percentage. The renal cyst volume percentage calculated by histology resembled CT renal cyst volume. In both cases the low dose treated animals decreased in compared to the control animals, which is a trend that was seen in the rosiglitazone 24-week study.

The 18 day time point showed promising results throughout all parameters, even if they were not all significant. Blood glucose was significantly decreased at both high and low dose, indicating that potentially these animals are hypoglycemic. The hematocrit was not different, thus indicating that the animals are not experiencing the fluid retention side effect associated with the PPAR γ agonists. And further agreeing with the hematocrit data, the heart weight was significantly decreased for low dose and was decreasing for high dose. Heart weight as a percent of body weight was not significantly different. Ultimately it seems that the fluid retention side effect is not an issue with the W-WPK rat. Liver weight and liver weight as a percent of body weight were not different. Most important was the renal parameters, in which there was very little that was statistically significant, but their trends showed great promise. Total kidney weight trended lower for each treatment group, even was significantly lower in the low dose treated animals. Kidney weight as a percent of body weight was showing

the trend that the low dose was more effective than the high dose. Renal cyst volume percentage calculated from the histological sections did not show any statistical difference, but did show the trend that was seen in the rosiglitazone study, where the low dose was more effective than the high dose. Renal cyst volume was statistically lower than the control for the low dose treated group. Ultimately the kidney data showed promising trends that were consistent with what was seen in the previous rosiglitazone study. The low dose was more effective in the treatment of renal cystic burden.

The W-WPK rat developed hydrocephalus along with the renal cystic disease, thus it was important to make sure that the PPAR γ agonists were not affecting the hydrocephalus. To measure the severity of the hydrocephalus the brain perimeter and area were determined. The ventricles were measured using the histological sections. Neither the brain perimeter nor area were different due to the pioglitazone treatment, thus indicating that PPAR γ agonists do not affect the cerebral spinal fluid accumulation in the brain. These animals were also imaged at the 18 day time point and their CT images were analyzed to determine the renal cyst volume percentage. Similar to what was seen in the kidney parameters, the CT renal cyst volume percentage had a trend where the low dose was more effective than the high dose.

Overall, one of the most important parts of the study was the CT scans. If the study is to go to human clinical trials, there has to be an effective way to track the progress of the disease during the course of treatment. CT imaging is a good method to use for many reasons, it is less expensive and takes less time compared to an MRI and can be used on any patient (51) and is able to create a 3-dimensional image of the kidney. The best way to determine if the CT scans were comparable to the histological sections was to determine the correlation between multiple different CT parameters. First we directly compared the CT renal cyst volume percentage with the renal cyst volume percentage determined from histology. Next we compared the kidney weight with the total volume determined from the CT. Finally, the cyst volume from CT was compared with the cyst volume determined from the mass of the kidney and the renal cyst volume percentage. Overall, the correlation was good, thus indicating CT scans are

can be used effectively in analyzing renal cyst burden of the rat, and thus should be able to be used in humans.

In conclusion all the animal preclinical data, indicate that PPAR γ agonists may be effective in decreasing cyst growth. The results were positive in the low dose treatment, which is the dose that would be more beneficial, because of the side effects associated with high dose PPAR γ agonists. Also, it is clear that CT scans could be used throughout PPAR γ treatment to track the disease and progress of the renal cyst burden. So the next step is to take PPAR γ agonist to phase 1 human clinical trails to see if the results that have been seen in the rat models can be reproduced in humans.

CHAPTER 5. SUMMARY

Treatment for polycystic kidney disease currently is limited, and drugs that are in clinical trials are either not showing efficiency, or they are not patient friendly, so the ultimate goal was to develop new targets for potential therapies. Treatment could be for the early onset of the disease, thus a long term drug therapy, or it could be late stage treatment.

The LPA study is targeting the late stage of the disease. The hypothesis that once the cyst have expanded and become so large that they burst or leak, which could also occur due to renal injury, the cyst fluid would stimulate the other cyst to secrete fluid. This is consistent with the clinical observations that once renal decline begins, the disease progresses to end-stage renal failure rather quickly. LPA was determined to be the active component of cyst fluid, thus studying the pathway by which LPA stimulates the chloride secretion could eventually lead to a drug that targets the last stage of disease progression. My results suggest that LPA is stimulating chloride and fluid secretion via a combination of CFTR and CaCC and that the two channels may be functionally linked. The secretion is not occurring through a cAMP stimulated pathway and potentially TMEM16A is playing a larger role than expected. The LPA receptor has still not been identified. Ultimately, the LPA story is still being developed, but has becoming intriguingly interesting.

The PPAR γ agonist study was looking at long-term treatment that begins earlier in the disease and continues as life-long treatment. By electrophysiology and inhibitor studies, it was previously discovered the PPAR γ agonists decrease synthesis of CFTR (28). CFTR has been determined to be the channel responsible for cyst growth, so it was logical to study the effects of PPAR γ agonists in the treatment of PKD. Thus, our laboratory along with the Mayo Clinic completed a preclinical animal trial using the PCK

rat and pioglitazone and the results were promising. My studies begun with further studying the PPAR γ agonists, completing a long-term study, using rosiglitazone at three different doses and adding a different rat model. The data were encouraging, first of all the rosiglitazone proved to be effective thus indicating that there is a class action of PPAR γ agonists in the treatment of PKD. Also, in multiple experiments the low dose agonists proved to be effective, which is extremely important, because PPAR γ agonist are associated with a dose dependent side effect of fluid retention. The next step was to determine if the PPAR γ agonist were effective in another rat model with a different genetic mutation, that was fast-progressing, and ultimately determine a way to track the disease that could be used in human patients. My results suggested that pioglitazone was not as significantly effective in the W-WPK rat model as it was in the PCK rat model, but that there was a trend that the low dose was showing promise in agreement with the rosiglitazone data. More importantly CT scans were used to track the progress of the disease and were compared with the histological data, which it was promising results. There was a strong correlation between the CT and the histological analyses, thus suggesting if this study was to go to human clinical trials, CT scans could be used to analyze and track the progress of the disease. The next step to the story is to, hopefully, go into human clinical trials.

LIST OF REFERENCES

LIST OF REFERENCES

- 1) Bens M., Vallet B., Cluzeaud F., Pascual-Letallec L., et al., "Corticosteroid-dependent sodium transport in a novel immortalized mouse collecting duct principal cell line." *Journal of American Society of Nephrology*, vol 10, pp 923-934, 1999.
- 2) Blazer-Yost B.L., Blacklock B.J., Flaig S.M., et al., "Lysophosphatidic Acid is a Modulator of Cyst Growth in Autosomal Dominant Polycystic Kidney Disease." *Cellular Physiology and Biochemistry*, vol 28, pp 1255-1264, 2011.
- 3) Blazer-Yost B.L., Haydon J., Eggleston-Gulyas T., et al., "Pioglitazone Attenuates Cystic Burden in the PCK Rodent Model of Polycystic Kidney Disease." *PPAR γ Research*, doi:10.1155/2010/274376, 2010.
- 4) Braun W.E., "Autosomal dominant polycystic kidney disease: Emerging concepts of pathogenesis and new treatments." *Cleveland Clinical Journal of Medicine*, vol 76, no 2, pp 97-104, 2009.
- 5) Chapman A.B. "Approaches to testing new treatments in autosomal dominant polycystic kidney disease: Insights from the CRISP and HALT-PKD studies." *Clinical Journal of the American Society of Nephrology*, vol 3, pp 1197-1204, 2008.
- 6) Chawla A., Schwarz E.J., Dimaculangan D.D., Lazar M.A. "Peroxisome proliferator-activated receptor (PPAR γ) gamma: adipose-predominant expression and induction early in adipocyte differentiation." *Endocrinology*, vol 135, pp 798-800, 1994.
- 7) Chen L., Yang B., McNulty J.A., et al., "GI262570, a peroxisome proliferator-activated receptor γ agonist, changes electrolytes and water reabsorption from the distal nephron in rats." *Journal of Pharmacology and Experimental Therapeutics*, vol 312, pp 718-725, 2005.
- 8) Chetty V.T., Sharma A.M., "Can PPAR γ agonists have a role in the management of obesity-related hypertension?" *Vascular Pharmacology*, vol 45, pp 46-53, 2006.

- 9) Choi, J.W., Herr D.R., Noguchi K., et al., "LPA Receptors: Subtypes and biological actions." *Annual Review of Pharmacology Toxicology*, vol 50, pp 157-186, 2010.
- 10) Davidow, C.J., Maser R.L., Rome L.A., et al., "The cystic fibrosis transmembrane conductance regulator mediates transepithelial fluid secretion by human autosomal dominant polycystic kidney disease epithelium in vitro." *Kidney International*, vol 50, pp 208-218, 1996.
- 11) Gattone V.H., Tourkow B.A., Trambaugh C.M., et al., "Development of Multiorgan Pathology in the wpk Rat Model of Polycystic Kidney Disease." *The Anatomical Record*, vol 277, pp 384-395, 2004.
- 12) Grantham J.J., Ye M., Davidow C., et al., "Evidence for a potent lipid secretagogue in the cyst fluids of patients with autosomal dominant polycystic kidney disease." *Journal of American Society of Nephrology*, vol 6, pp 1242-1249, 1995.
- 13) Grantham J.J., Mulamalla S., Grantham C.J., et al., "Detected Renal Cyst Are Tips of the Iceberg in Adults with ADPKD." *Clinical Journal of the American Society of Nephrology*, vol 7, pp 1087-1093, 2012.
- 14) Grantham J.J., Ye M., Gattone II V.H., et al., "In vitro fluid secretion by epithelium from polycystic kidneys." *Journal of Clinical Investigation*, vol 95, pp 195-202, 1995.
- 15) Guan Y., Hao C., Cha D.R., et al., "Thiazolidinediones expand body fluid volume through PPAR γ stimulation of ENaC-mediated renal salt absorption." *Nature Medicine*, vol 11, pp 861-866, 2005.
- 16) Guan Y. "Targeting peroxisome proliferator-activated receptors (PPAR γ 's) in kidney and urologic disease." *Journal of Nephrology and Urology*, vol 54, pp 65-79, 2002.
- 17) Hanaoka, K., Devuyst O., Schwiebert E. M., et al., "A role for CFTR in human autosomal dominant polycystic kidney disease." *American Journal of Physiology-Cell Physiology*, vol 270, pp C389-C399, 1996.
- 18) Harris P.C. and Torres V.E., "Polycystic Kidney Disease." *Annual Review of Medicine*, vol 60, pp 321-337, 2009.
- 19) Hong G., Lockhart A., Davis B., et al., "PPAR γ activation enhances cell surface ENaC α via up-regulation of SGK1 in human collecting duct cells." *FASEB Journal*, vol 17, pp 1966-1968, 2003.

- 20) Lentine, K.L., Xiao H., Machnicki G., et al., "Renal function and healthcare costs in patients with polycystic kidney disease." *Clinical Journal of American Society of Nephrology*, vol 5, pp 1471-1479, 2010.
- 21) Mangoo-Karim, R., Ye M., Wallace D.P., et al., "Anion secretion drives fluid secretion by monolayers of cultured human polycystic cells." *American Journal of Physiology-Renal Physiology*, vol 269, pp F381-388, 1995.
- 22) Mason S.B., Liang Y., Sinderson R.M., et al., "Disease Stage Characterization of Hepatorenal Fibrocystic Pathology in the PCK Rat Model of ARPKD." *The Anatomical Record*, vol 293, pp 1279-1288, 2010.
- 23) Muanprasat C., Sonawane N.D., Salinas D., et al., "Discovery of glycine hydrazide pore-occluding CFTR inhibitors: mechanism, structure-activity analysis, and in vivo efficacy." *The Journal of General Physiology*, vol 124, no 2, pp 125-37. 2004.
- 24) Muchatuta M.N., Gattone II V.H., Witzmann F.A., et al., "Structural and functional analysis of liver cysts from BALB/c-cpk mouse model of polycystic kidney disease." *Experimental Biology and Medicine*, vol 234, no 1, pp 17-27, 2009.
- 25) Namkung W., Phuan P.W., Verkman A.S., "TMEM16A inhibitors reveal TMEM16A as a minor component of calcium-activated chloride channel conductance in airway and intestinal epithelial cells." *The Journal of Biological Chemistry*, vol 286, no 3, pp 2365-74, 2011.
- 26) Namkung W., Thiagarajah J.R., Phuan P.W., et al., "Inhibition of Ca²⁺-activated Cl⁻ channels by gallotannins as a possible molecular basis for health benefits of red wine and green tea." *FASEB Journal*, vol 24, no 11, pp 4178-86, 2010.
- 27) Neufeld T.K., Grant M.E., and Grantham J.J., "A method to measure the rate of net fluid secretion by monolayers of cultured renal epithelial cells." *Journal of Tissue Culture Methods*, vol 13, pp 229-234, 1991.
- 28) Nofziger C., Brown K.K., Smith C.D., et al., "PPAR γ agonists inhibit vasopressin – mediated anion transport in the MDCK-C7 cell line." *American Journal of Physiology*, vol 297, no 1, pp F55-F62, 2009.
- 29) Nofziger C., Chen L., Shane M.A., et al., "PPAR γ agonists do not directly enhance basal or insulin-stimulated Na²⁺ transport via the epithelial Na²⁺ channel." *European Journal of Physiology*, vol 451, pp 445-453, 2005.

- 30) Osborn T.M., Dahlgren C., Hartwig J.H., et al., "Modifications of cellular responses to lysophosphatic acid and platelet-activating factor by plasma gelsolin." *American Journal of Physiology-Cell Physiology*, vol 292, pp C1323-1330, 2007.
- 31) O'Shaughnessy K.M. and Karet F.E., "Salt handling and hypertension." *Journal of Clinical Investigation*, vol 113, pp 1075-1081, 2004.
- 32) Patel V., Chowdhury R., and Igarashi P., "Advances in the pathogenesis and treatment of polycystic kidney disease." *Current Opinion in Nephrology and Hypertension*, vol 18, no 2, pp 99-106, 2009.
- 33) Pei, Y. "Of mice and men: Therapeutic mTOR inhibition in polycystic kidney disease." *Journal of American Society of Nephrology*, vol 21, pp 383-394, 2010.
- 34) Putnam W.C., Swenson S.M., Reif G.A., et al., "Identification of a forskolin-like molecule in human renal cysts." *Journal of American Society of Nephrology*, vol 18, pp 934-943, 2007.
- 35) Ryan M.J., Didion S.P., Mathur S., et al., "PPAR γ agonist rosiglitazone improves vascular function and lowers blood pressure in hypertensive transgenic mice." *Hypertension*, vol 43, pp 661-666, 2004.
- 36) Serra, A.L., Poster D., Kistler A.D., et al., "Sirolimus and kidney growth in autosomal dominant polycystic kidney disease." *New England Journal of Medicine*, vol 363, pp 820-829, 2010.
- 37) Smith U.M., Consugar M., Tee L.J., et al., "The transmembrane protein meckelin (MKS3) is mutated in Meckel-Gruber syndrome and the wpk rat." *Nature Genetics*, vol 28, no 2, pp 191-196, 2006.
- 38) Song J., Knepper M.A., Hu X., et al., "Rosiglitazone activates renal sodium- and water-reabsorptive pathways and lowers blood pressure in normal rats." *Journal of Pharmacology and Experimental Therapeutics*, vol 308, pp 426-433, 2004.
- 39) Takakura A, Contrino L., Zhou X., et al., "Renal injury is a third hit promoting rapid development of adult polycystic kidney disease." *Human Molecular Genetics*, vol 18, pp 2523-2531, 2009.
- 40) Thumser A.E.A., Voysey J.E., Wilton D.C., "The binding of lysophospholipids to rat liver fatty acid-binding protein and albumin." *Biochemical Journal*, vol 301, pp 801-806, 1994.

- 41) Tigyi G., Miledi R., "Lysophosphatidates bound to serum albumin activate membrane currents in xenopus oocytes and neurite retraction in PC12 pheochromocytoma cells." *Journal of Biological Chemistry*, vol 267, pp 21360-21367, 1992.
- 42) Torres, V.E., and Harris P.C., "Autosomal dominant polycystic kidney disease: the last 3 years." *Kidney International*, vol 76, pp 149-168, 2009.
- 43) Torres, V.E., "Treatment Strategies and clinical trial design in ADPKD." *Advance Chronic Kidney Disease*, vol 2, pp 190-204, 2010.
- 44) Torres, V.E., Meijer E., Bae K.T., et al., "Rationale and design of the TEMPO (tolvaptan efficacy and safety in management of autosomal dominant polycystic kidney disease and its outcomes) 3-4 study." *American Journal of Kidney Disease*, vol 57, pp 692-699, 2011.
- 45) Torres, V.E., Winklhofer F., and Chapman A.B., "Phase 2 open-label study to determine long term safety, tolerability and efficacy of split-dose tolvaptan in ADPKD." *Journal of American Society of Nephrology*, vol 20, pp 746A, 2009.
- 46) Ussing H.H. and Zerahn K., "Active transport of sodium as the source of electric current in the short-circuited isolated frog skin." *Acta Physiologica Scandinavica*, vol 23, pp 110-127, 1951.
- 47) Vallon V., Hummler E., Rieg T., et al., "Thiazolidinedione- induced fluid retention is independent of collecting duct α ENaC activity." *Journal of American Society of Nephrology*, vol 20, pp 721-729, 2009.
- 48) Walz, G., Budde K., Mannaa M., "Everolimus in patients with autosomal dominant polycystic kidney disease." *New England Journal of Medicine*, vol 363, pp 830-840, 2010.
- 49) Ward C.J., Hogan M.C., Rossetti S., et al., "The gene mutated in autosomal recessive polycystic kidney disease encodes a large, receptor-like protein." *Nature Genetics*, vol 30, pp 259-269, 2002.
- 50) Watnick, T. and Germino G. G., "mTOR inhibitors in polycystic kidney disease." *New England Journal of Medicine*, vol 363, pp 879-881, 2010.
- 51) Website. (CT vs. MRI), http://www.diffen.com/difference/CT_Scan_vs_MRI.
- 52) Willson T.M., Brown P.J., Sternbach D.D., et al., "The PPAR γ 's: from orphan receptors to drug discovery." *Journal of Medicinal Chemistry*, vol 43, pp 527-550, 2000.

- 53) Xu H.E., Lambert M.H., Montana V.G., et al., "Molecular recognition of fatty acids by peroxisome proliferator-activated receptors." *Molecular Cell*, vol 3, pp 397-403, 1999.
- 54) Ye M., Grant M., Sharma M., et al., "Cyst fluid from human autosomal dominant polycystic kidneys promotes cyst formation and expansion by renal epithelial cells in vitro." *Journal of American Society of Nephrology*, vol 3, pp 984-994, 1992.
- 55) Ye M. and Grantham J.J., "The secretion of fluid by renal cysts from patients with autosomal dominant polycystic kidney disease." *New England Journal of Medicine*, vol 329, pp 310-313, 1993.
- 56) Zhang H., Zhang A., Kohan D.E., et al., "Collecting duct-specific deletion of peroxisome proliferator-activated receptor gamma blocks thiazolidinedione-induced fluid retention." *Proceedings of the National Academy of Sciences-USA*, vol 102, pp 9406-9411, 2005.

TABLES

Table 1: Summary of overall data completed for the 24 week, rosiglitazone study on the PCK rat model..

PCK rats were fed a control of rosiglitazone-supplemented diet (mg/kg BW) for a total of 24 weeks). The values given are averages ± SEM.

Abbreviations in the table include: KW% BW: total kidney weight as a percentage of total body weight; LW% BW: liver weight as a percentage of total body weight.

P-values are for the comparison of control versus rosiglitazone-supplemented diets by Anova, one-way test a P value less than .05 is considered significant. NS: not significant, S: Significant.

24 Week Diet	Control	Rosiglitazone	Significance	Rosiglitazone	Significance	Rosiglitazone	Significance
	Diet	4.0mg/kg BW		0.4 mg/kg BW		0.04mg/kg BW	
	n=12	n=3		n=8		n=8	
Body Weight (BW) g	340.68 ± 5.55	378.5 ± 2.47	S	338.94 ± 6.94	NS	342.11 ± 10.10	NS
Kidney Weight (KW) g	4.33 ± 0.18	3.56 ± 0.26	S	4.27 ± 0.22	NS	3.68 ± 0.14	S
KW % BW	1.22 ± 0.04	0.94 ± 0.06	S	1.27 ± 0.08	NS	0.95 ± 0.15	S
% Cyst Volume	12.70 ± 1.32	7.58 ± 0.72	S	18.53 ± 2.55	S	8.49 ± 1.92	S
Renal Cyst Volume (mL)	0.53 ± 0.06	0.27 ± 0.05	S	0.82 ± 0.14	S	0.33 ± 0.09	S
Liver Weight (LW) g	23.11 ± 1.44	22.66 ± 5.39	NS	22.05 ± 2.07	NS	24.23 ± 0.10	NS
LW % BW	6.77 ± 0.43	5.97 ± 1.38	NS	6.50 ± 0.57	NS	7.11 ± 0.27	NS
Liver % Fibrocystic	31.10 ± 2.02	36.17 ± 0.38	NS	36.81 ± 3.61	NS	35.36 ± 3.74	NS
Heart Weight (HW)	1.29 ± 0.03	1.25	Ns	1.15 ± 0.05	NS	1.23 ± 0.03	NS

Table 2: Summary of overall 10 day data completed for the pioglitazone study on the W-WPK rat model.

W-WPK rats were fed a control of pioglitazone-supplemented diet (mg/kg BW) from day 5 until day 10 of age. The values given are averages \pm SEM.

Abbreviations in the table include: KW% BW: total kidney weight as a percentage of total body weight; LW% BW: liver weight as a percentage of total body weight; HW%BW: heart weight as a percentage of total body weight.

P-values are for the comparison of control versus pioglitazone-supplemented diets by Anova, one-way test a P value less than .05 is considered significant. NS: not significant, S: Significant.

W-WPK 10 Day	Control	Pioglitazone	Significance	Pioglitazone	Significance
	Diet	20.0 mg/kg BW		2.0 mg/kg BW	
	n=7	n=2		n=4	
Glucose (mg/dL)	343 \pm 43.962	298 \pm 32	NS	312.75 \pm 67.24	NS
	n=7	n=6		n=5	
Hematocrit	26.13 \pm 0.65	25.81 \pm 1.08	NS	26.28 \pm 0.99	NS
	n=9	n=6		n=5	
Body Weight (BW) g	18.61 \pm 0.881	18.97 \pm 1.046	NS	20.732 \pm 0.66	NS
Kidney Weight (KW) g	0.607 \pm 0.074	0.703 \pm 0.073	NS	0.748 \pm 0.059	NS
KW % BW	3.20 \pm 0.15	3.67 \pm 0.20	S	3.59 \pm 0.21	NS
% Cyst Volume	45.125 \pm 2.104	46.99 \pm 2.92	NS	44.042 \pm 4.42	NS
Renal Cyst Volume (mL)	0.278 \pm 0.036	0.337 \pm 0.0498	NS	0.338 \pm 0.0586	NS
	n=7	n=5		n=5	
Liver Weight (LW) g	0.663 \pm 0.036	0.676 \pm 0.04	NS	0.714 \pm 0.02	NS
LW % BW	3.54 \pm 0.14	3.16 \pm 0.15	NS	3.46 \pm 0.16	NS
Heart Weight (HW)	0.143 \pm 0.005	0.168 \pm 0.007	S	0.166 \pm 0.005	S
HW % BW	0.77 \pm 0.04	0.91 \pm 0.07	NS	0.80 \pm 0.02	NS
	n=2	n=2		n=1	
Renal Cyst Volume (CT Scans)	41.891 \pm 0.809	46.457 \pm 12.15	NS	41.204	NS

Table 3: Summary of overall 18 day data completed for the pioglitazone study on the W-WPK rat model.

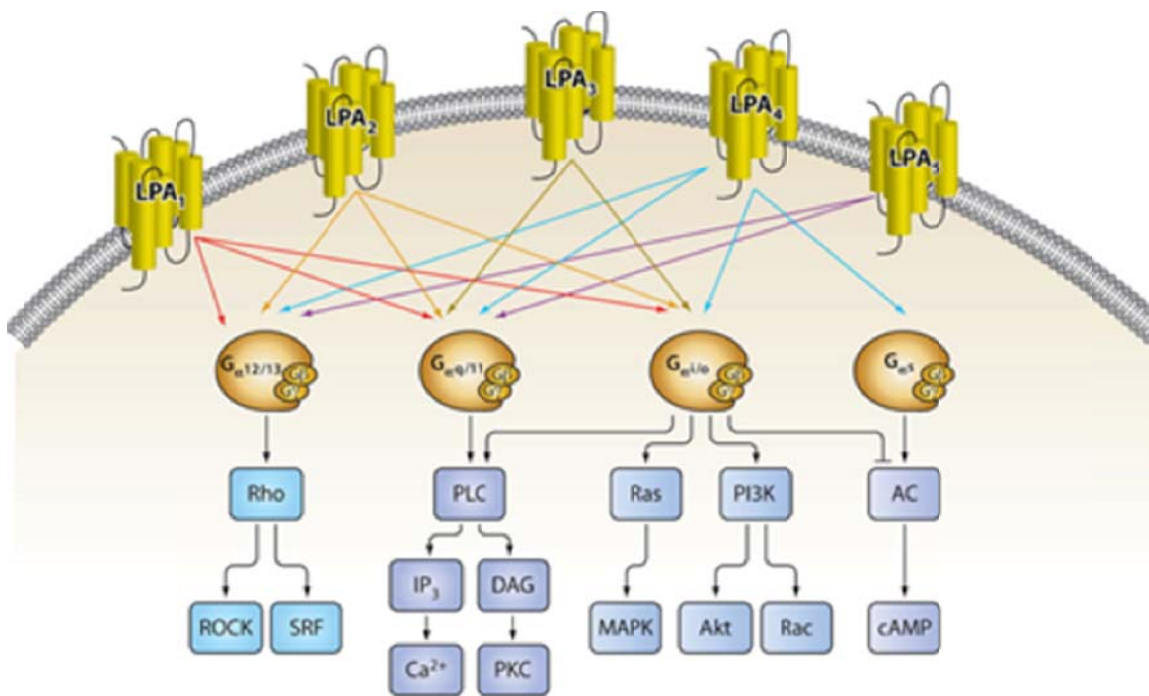
W-WPK rats were fed a control of pioglitazone-supplemented diet (mg/kg BW) from day 5 until day 18 of age. The values given are averages \pm SEM.

Abbreviations in the table include: KW% BW: total kidney weight as a percentage of total body weight; LW% BW: liver weight as a percentage of total body weight; HW%BW: heart weight as a percentage of total body weight.

P-values are for the comparison of control versus pioglitazone-supplemented diets by Anova, one-way test a *P* value less than .05 is considered significant. NS: not significant, S: Significant.

W-WPK 18 Day	Control	Pioglitazone	Significance	Pioglitazone	Significance
	Diet	20.0 mg/kg BW		2.0 mg/kg BW	
	n=11	n=8		n=10	
Glucose (mg/dL)	255.7 \pm 16.6	193 \pm 8.91	S	213.4 \pm 13.0	S
Hematocrit	28.83 \pm 1.12	28.89 \pm 0.76	NS	27.45 \pm 1.17	NS
Body Weight (BW) g	29.91 \pm 2.11	26.41 \pm 0.677	NS	27.02 \pm 0.948	NS
Kidney Weight (KW) g	4.51 \pm 0.477	4.22 \pm 0.13	NS	3.53 \pm 0.1704	S
KW % BW	14.94 \pm 1.02	16.01 \pm 0.45	NS	13.23 \pm 0.78	NS
% Cyst Volume	74.06 \pm 1.021	73.55 \pm 1.343	NS	72.629 \pm 0.15	NS
Renal Cyst Volume (mL)	3.34 \pm 0.357	3.11 \pm 0.134	NS	2.574 \pm 0.145	S
Liver Weight (LW) g	1.36 \pm 0.0698	1.296 \pm 0.03	NS	1.302 \pm 0.02	NS
LW % BW	4.63 \pm 0.23	4.93 \pm 0.19	NS	4.86 \pm 0.14	NS
Heart Weight (HW)	0.30 \pm 0.11	0.275 \pm 0.014	NS	0.242 \pm 0.009	S
HW % BW	1.02 \pm 0.06	1.04 \pm 0.05	NS	0.91 \pm 0.04	NS
	n=7	n=8		n=8	
Brain Perimeter (cm)	4.045 \pm 0.433	4.167 \pm 0.383	NS	4.131 \pm 0.352	NS
Brain Area (cm ²)	0.406 \pm 0.108	0.419 \pm 0.049	NS	0.414 \pm 0.056	NS
	n=3	n=2		n=2	
Renal Cyst Volume (CT Scans)	72.257 \pm 5.932	66.518 \pm 4.980	NS	64.562 \pm 3.289	NS

FIGURES



AR Choi JW, et al. 2010.
Annu. Rev. Pharmacol. Toxicol. 50:157–86

Figure 1: Postulated LPA receptors (LPA₁-LPA₅) pathways from Choi, et al. (9)

Schematic of the various pathways in which LPA receptors 1-5 potentially are activated or inhibited.

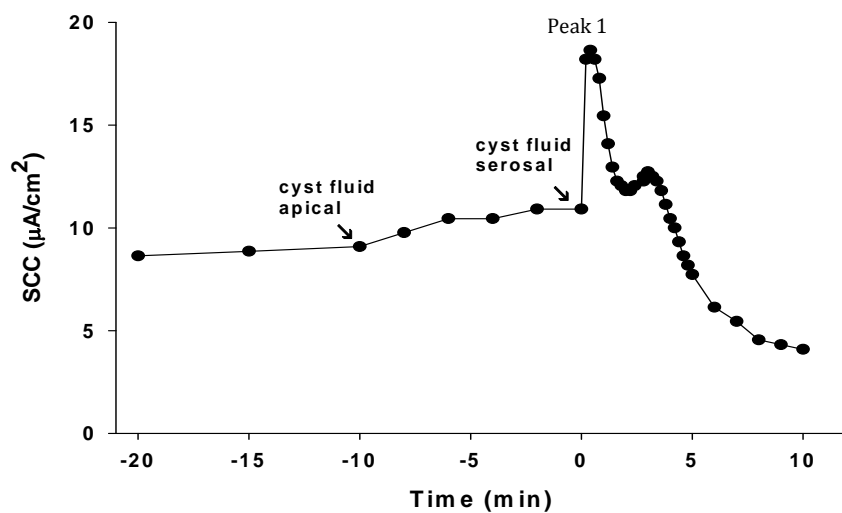


Figure 2: Human Cyst Fluid Addition to Apical and Basolateral side of the mpkCCD_{cl4} renal cell line

The apical and basolateral cyst fluid stimulation of ion transport (SCC) of a monolayer of mpkCCD_{cl4} cells grown on transwells. At time = -10 minutes, cyst fluid was added to the apical side to obtain a final concentration of 10%. At time = 0 minutes, cyst fluid was added to the basolateral side to obtain a final concentration of 10%. In both cases an equal amount of serum-free media was added to the opposing side to balance the addition of cyst fluid.

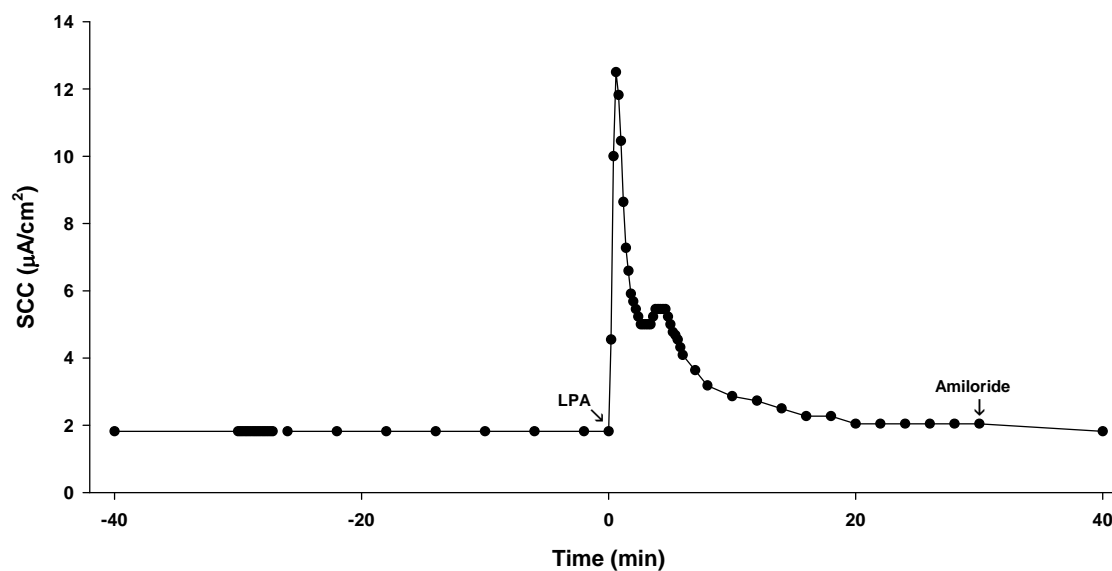


Figure 3: Stimulatory response to the addition of $50\mu\text{M}$ LPA to the basolateral side of the mpkCCD_{c14} renal cell line

Confluent monolayers cultures were kept in normal conditions assembled into the Ussing chambers, until the vehicle (DMSO) was added at $t = -30$ minutes to the apical side. At time=0 minutes, $50\mu\text{M}$ LPA was added to the basolateral side. 1×10^{-5} M Amiloride was added apically after 30 minutes to inhibit sodium flux.

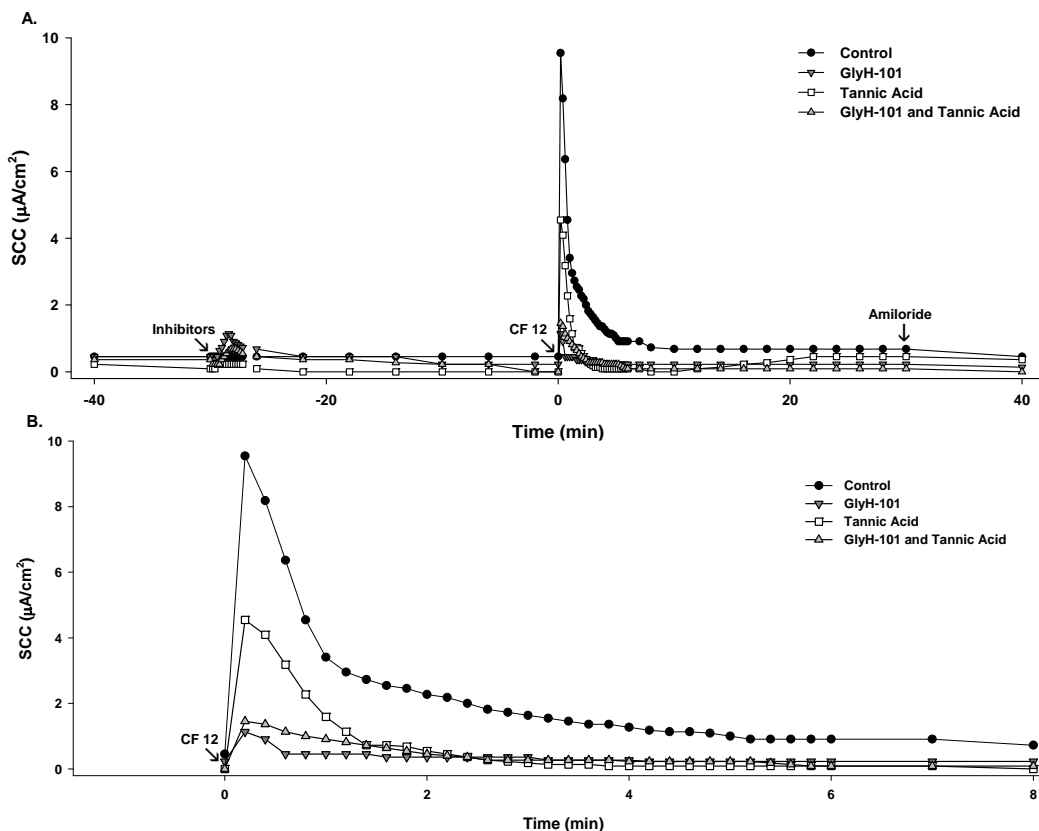


Figure 4: Inhibition of cyst fluid (CF-12) stimulated chloride secretion in mpkCCD_{c14} cells with known inhibitors of CFTR and CaCCs

A. Confluent monolayers of mpkCCD_{c14} renal cells grown on permeable supports, they were excised and mounted into Ussing chambers. The cells were allowed appropriate amount of time to develop a stable basal short circuit current (SCC). The graph shows the measurement of SCC, net ion transport. 50 μM GlyH-101 and 20 μM tannic acid were added at time = -30 minutes to the apical side as indicated. At time = 0 minutes, CF-12 was added to the basolateral side to obtain a final concentration of 10%, subsequently an equal amount of serum free media was added to the basolateral side to equal out the pressure. 1×10^{-5} M Amiloride was added apically 30 minutes after the LPA addition to inhibit sodium flux. B. The second graph depicts the ion transport events in an expanded time frame.

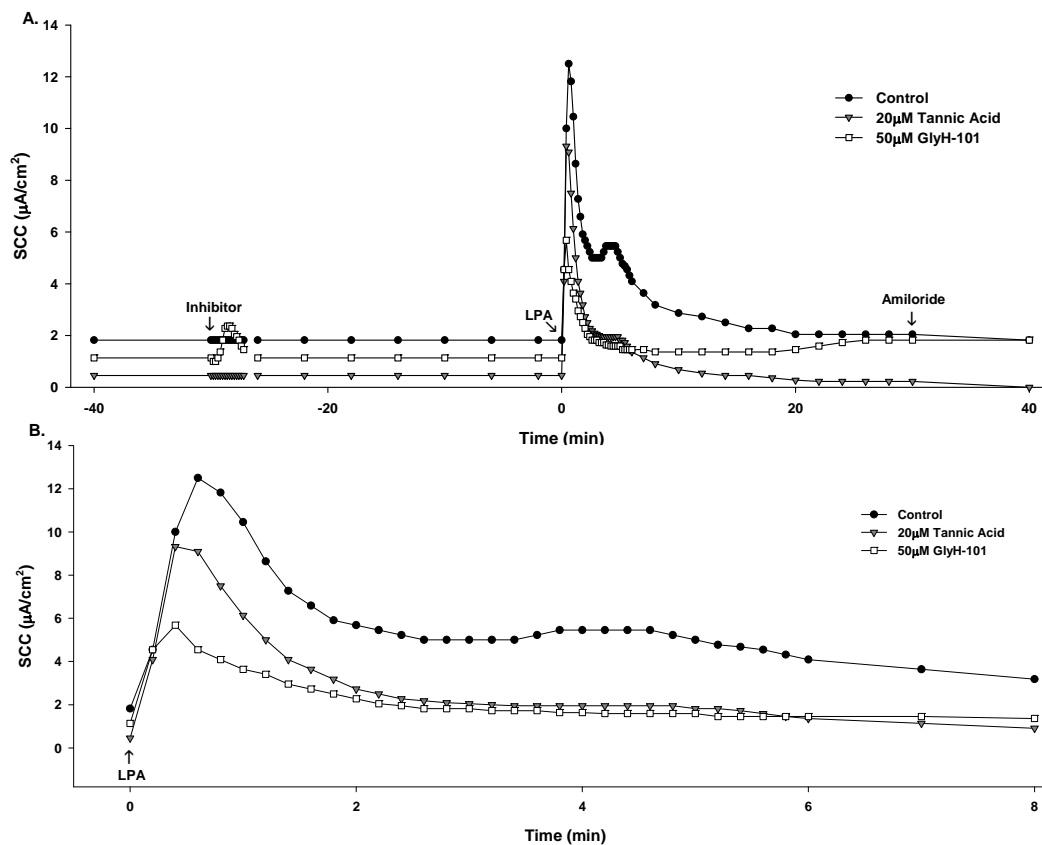


Figure 5: Inhibition of LPA stimulation with CFTR and CaCC inhibitors

A. Confluent monolayers of mpkCCD_{cl4} renal cells grown on permeable supports, they were excised and mounted into Ussing chambers. The cells were allowed appropriate amount of time to develop a stable basal short circuit current (SCC). The graph shows the measurement of SCC, net ion transport. 50 μM GlyH-101 and 20 μM tannic acid were added at time= -30 minutes to the apical side as indicated. At time=0 minutes, 50 μM LPA was added basolaterally. 1×10^{-5} M Amiloride was added to the apical side 30 minutes after the LPA addition to inhibit sodium flux. B. The second graph depicts the ion transport events in an expanded time frame.

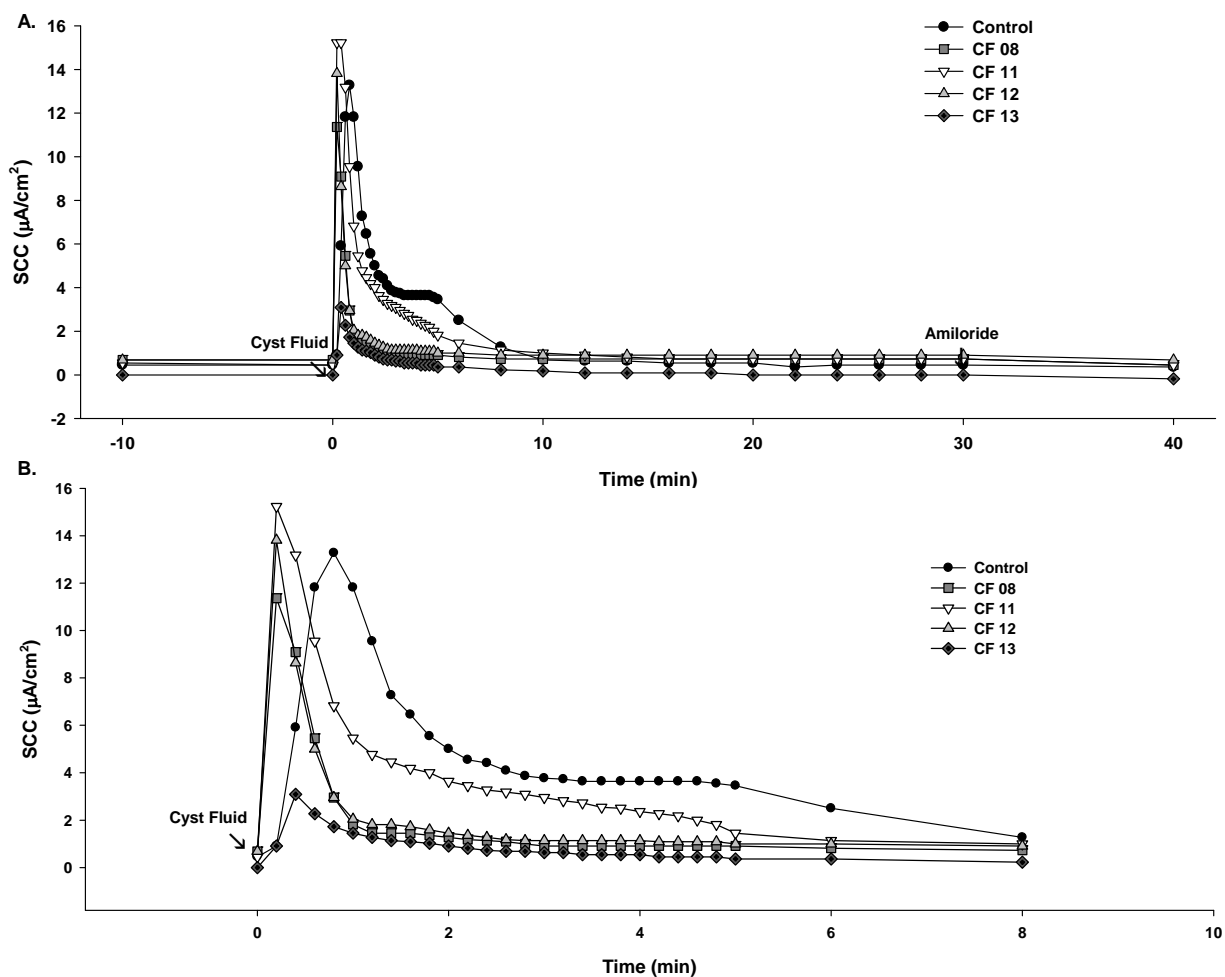


Figure 6: Testing the Stimulatory Capacity of Human Cyst Fluid from Multiple Patients

A. Confluent monolayers of mpkCCD_{cl4} renal cells grown on permeable supports, they were excised and mounted into Ussing chambers. The cells were allowed appropriate amount of time to develop a stable basal short circuit current (SCC). The graph shows the measurement of SCC, net ion transport. At time= 0 different cyst fluids from different patients were added to the basolateral bathing media. For control, at time=0, 50 μM LPA was added to the basolateral bathing media. 1×10^{-5} M Amiloride was added apically after 30 minutes to inhibit sodium flux. Each plot represents a single experiment. B. The second graph depicts the ion transport events in an expanded time frame.

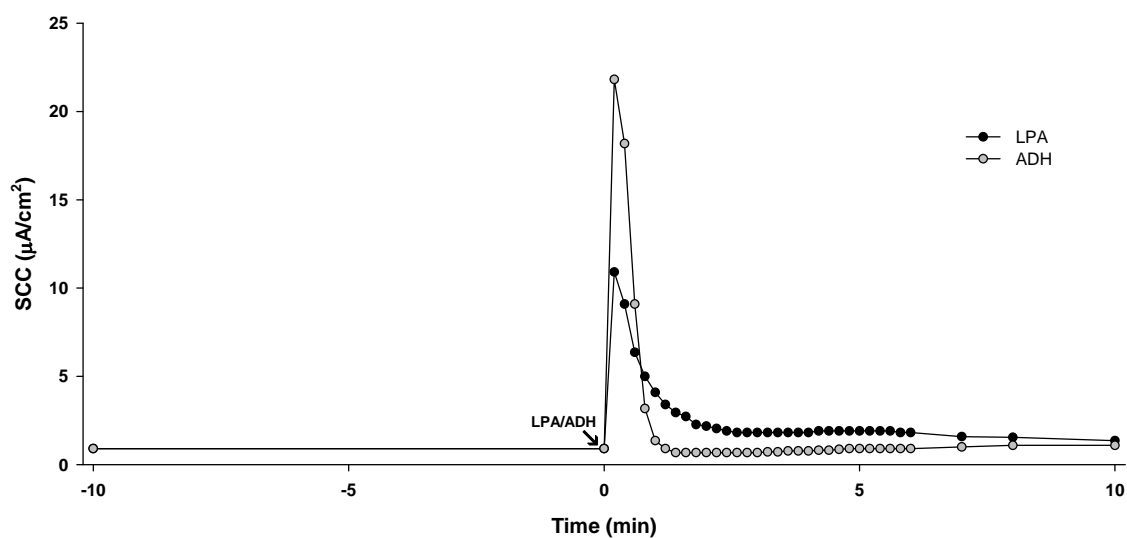


Figure 7: Comparison of LPA and ADH stimulation of ion transport in the mpkCCD_{cl4} renal cell line

Confluent monolayers of mpkCCD_{cl4} renal cells grown on permeable supports, they were excised and mounted into Ussing chambers. The cells were allowed appropriate amount of time to develop a stable basal short circuit current (SCC). The graph shows the measurement of SCC, net ion transport. At time= 0, 50 μM LPA or 100 mU/mL ADH was added to the basolateral bathing media. 1×10^{-5} M Amiloride was added apically after 30 minutes to inhibit sodium flux.

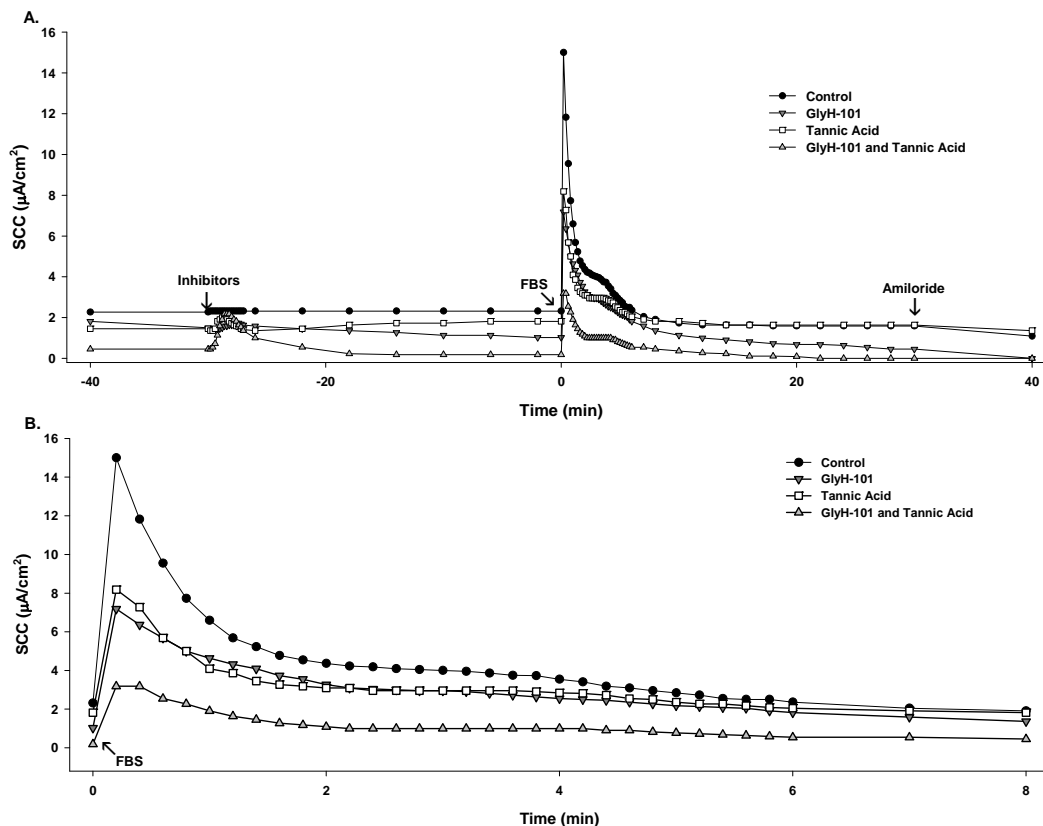


Figure 8: Inhibition of the fetal bovine serum (FBS) stimulation with CFTR and CaCC inhibitors

A. Confluent monolayers of mpkCCD_{cl4} renal cells grown on permeable supports, they were excised and mounted into Ussing chambers. The cells were allowed appropriate amount of time to develop a stable basal short circuit current (SCC). The graph shows the measurement of SCC, net ion transport. 50 μM GlyH-101 and 20 μM tannic acid were added at time= -30 minutes to the apical side as indicated. At time=0 minutes, 10% FBS was added basolaterally, subsequently an equal amount of serum free media was added to the basolateral side to equal out the pressure. 1×10^{-5} M Amiloride was added to the apical side 30 minutes after the LPA addition to inhibit sodium flux. B. The second graph depicts the ion transport events in an expanded time frame.

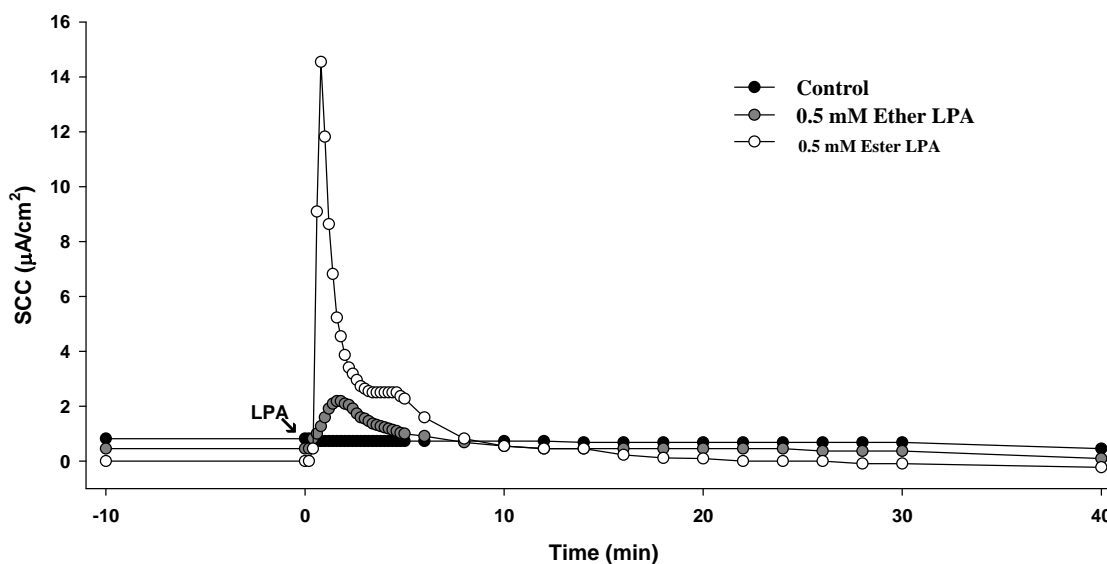


Figure 9: Comparison of the basolateral stimulatory response of ether LPA and ester LPA

Confluent monolayers of mpkCCD_{cl4} renal cells grown on permeable supports, they were excised and mounted into Ussing chambers. The cells were allowed appropriate amount of time to develop a stable basal short circuit current (SCC). The graph shows the measurement of SCC, net ion transport. 50 μM ester or ether LPA was added basolaterally at time= 0 minutes as indicated by the arrow. 1x10⁻⁵ M Amiloride was added to the apical 30 minutes after LPA was added to inhibit sodium flux. The experiment was also conducted at 50 nM LPA with a minor ion transport response (data not shown).

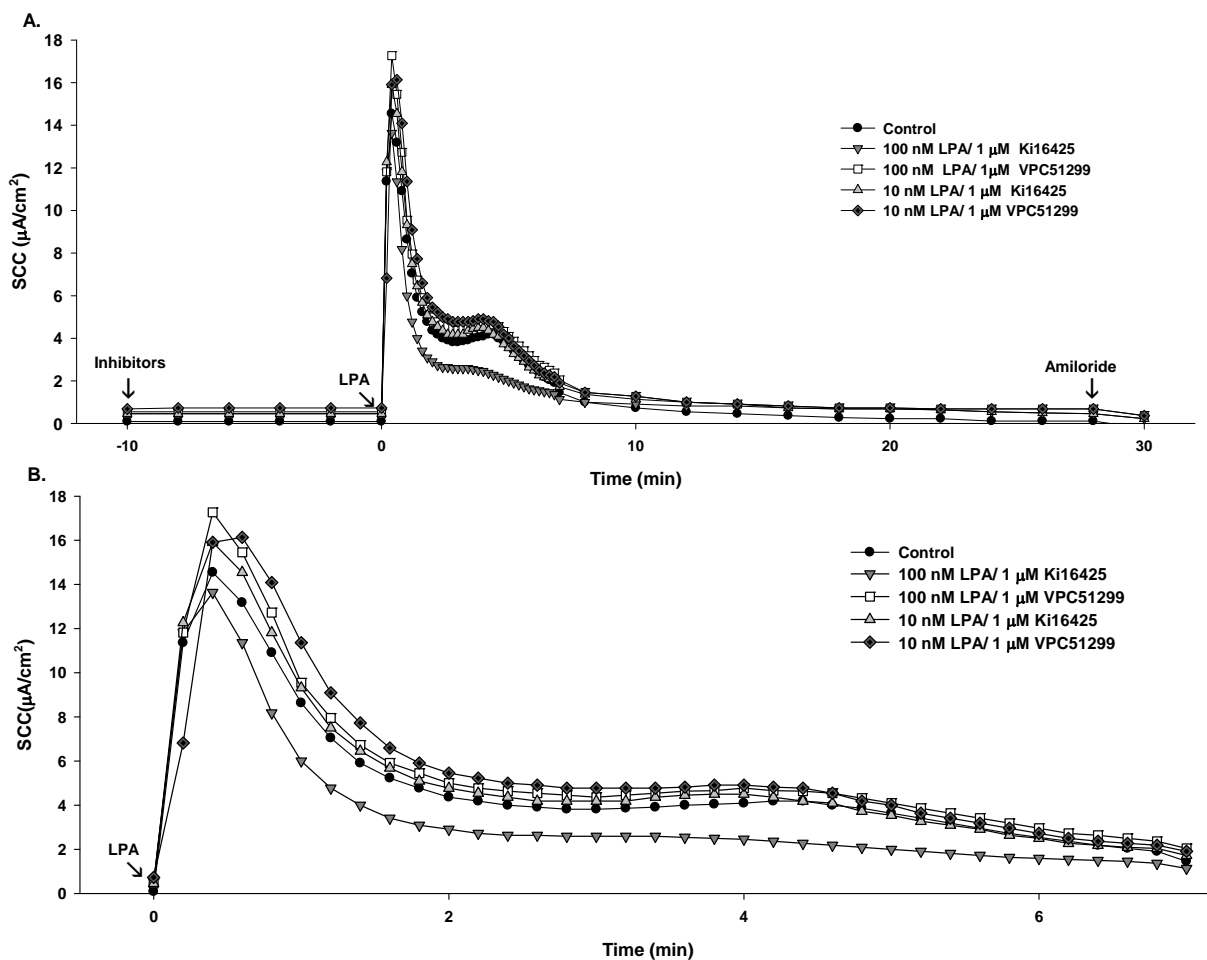


Figure 10: Inhibition of LPA stimulation with LPA 1/3 Receptor Antagonists (Ki6425 and VPC51299)

A. Confluent monolayers of mpkCCD_{c14} renal cells grown on permeable supports, they were excised and mounted into Ussing chambers. The cells were allowed appropriate amount of time to develop a stable basal short circuit current (SCC). The graph shows the measurement of SCC, net ion transport. At time= -30 minutes the LPA 1/3 receptor antagonists (Ki6425 and VPC51299) were added to the basolateral side as indicated. At time= 0 minutes the 50 μM LPA was added to the basolateral side. 1×10^{-5} M Amiloride was added after 30 minutes to inhibit sodium flux. B. The second graph depicts the peaks in an expanded time frame.

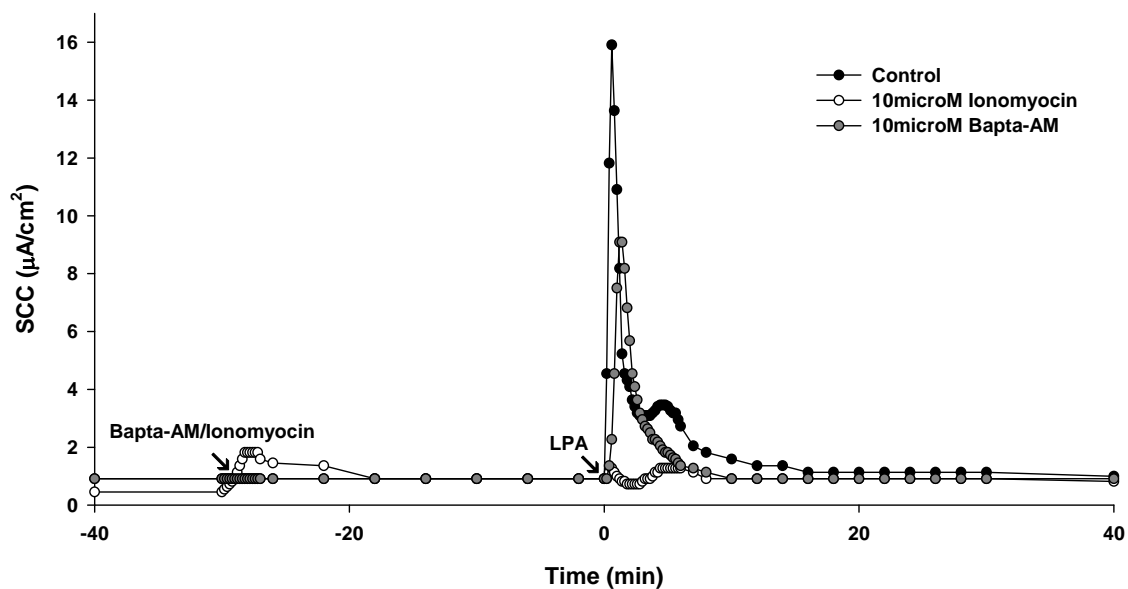


Figure 11: Basolateral addition of Bapta-AM and Ionomycin with LPA

Confluent monolayers of mpkCCD_{cl4} renal cells grown on permeable supports, they were excised and mounted into Ussing chambers. The cells were allowed appropriate amount of time to develop a stable basal short circuit current (SCC). The graph shows the measurement of SCC, net ion transport. At time = -30, either 0.1 mM Ionomycin or 100 mM Bapta-AM was added basolaterally. At time = 0 minutes the 50 μM LPA was added to the basolateral side. 1×10^{-5} M Amiloride was added after 30 minutes to inhibit sodium flux.

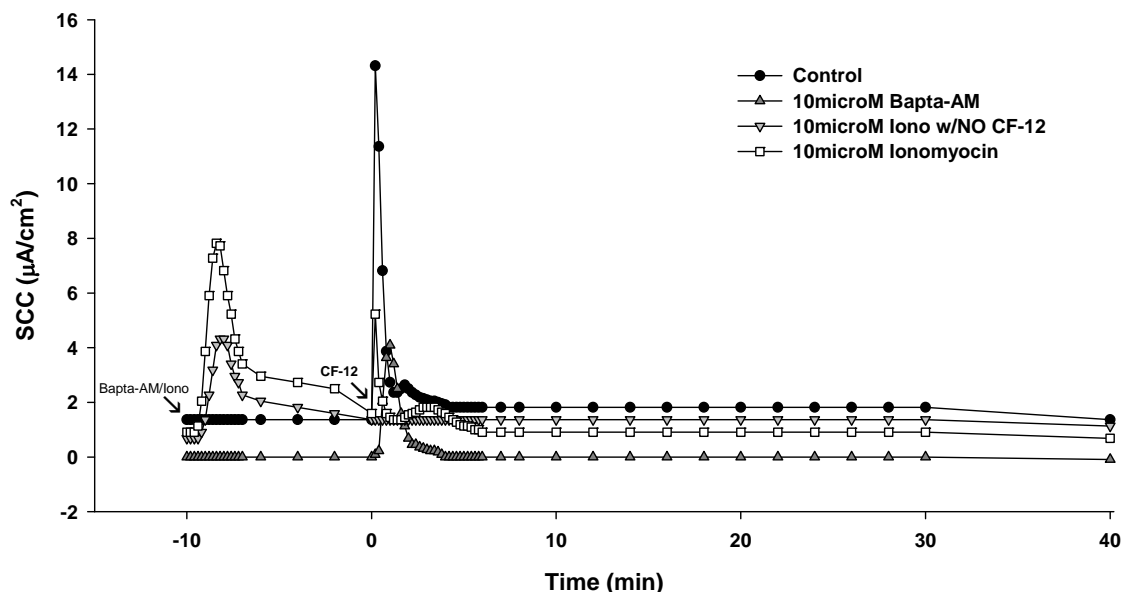


Figure 12: Basolateral addition of Bapta-AM and Ionomycin with CF-12

Confluent monolayers of mpkCCD_{cl4} renal cells grown on permeable supports, they were excised and mounted into Ussing chambers. The cells were allowed appropriate amount of time to develop a stable basal short circuit current (SCC). The graph shows the measurement of SCC, net ion transport. At time= -30, either 0.1 mM Ionomycin or 100 mM Bapta-AM or a vehicle was added basolaterally. At time= 0 minutes 10% CF-12 was added basolaterally, subsequently an equal amount of serum free media was added to the basolateral side to equal out the pressure. 1×10^{-5} M Amiloride was added after 30 minutes to inhibit sodium flux.

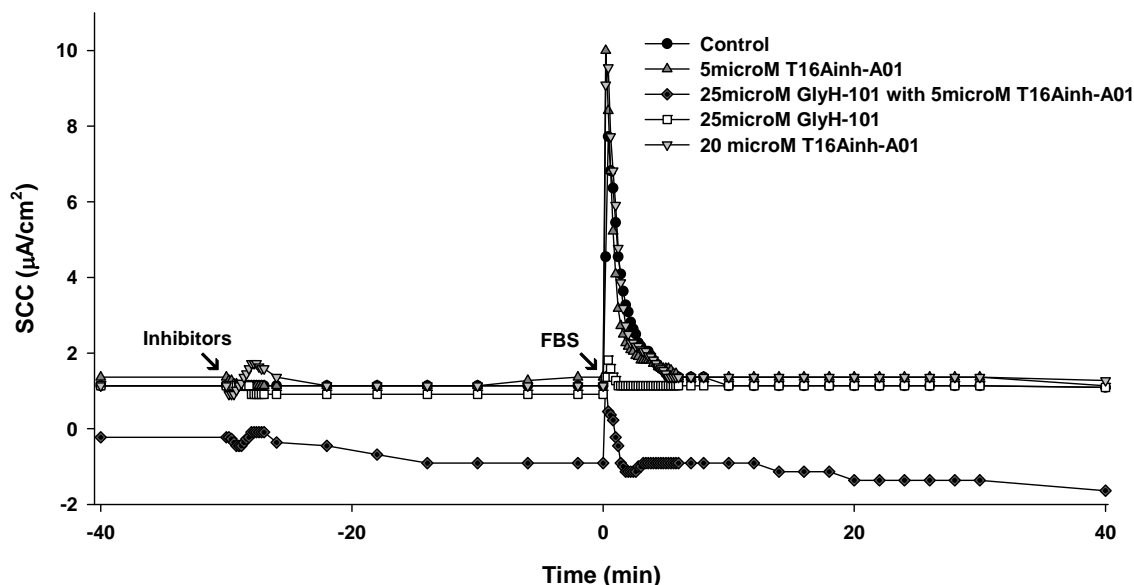


Figure 13: Inhibition of the fetal bovine serum (FBS) stimulation with T16AinhA-01

Confluent monolayers of mpkCCD_{cl4} renal cells grown on permeable supports, they were excised and mounted into Ussing chambers. The cells were allowed appropriate amount of time to develop a stable basal short circuit current (SCC). The graph shows the measurement of SCC, net ion transport. At time= -30 minutes, the chloride channel inhibitors were added (5 μM T16Ainh-A01, 20 μM T16Ainh-A01, 25 μM GlyH-101, 25 μM GlyH-101/ 5 μM T16Ainh-AO1) to the apical side. At time= 0 minutes, 10% FBS was added basolaterally, subsequently an equal amount of serum free media was added to the basolateral side to equal out the pressure. 1×10^{-5} M Amiloride was added after 30 minutes to inhibit sodium flux.

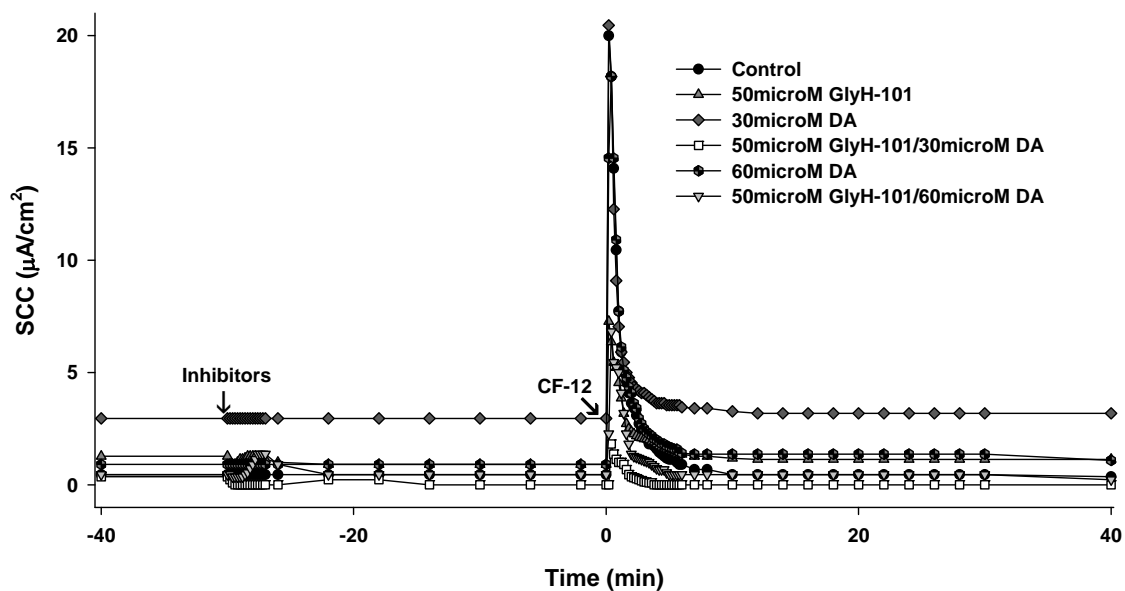


Figure 14: Inhibition of the cyst fluid (CF-12) stimulation with digalliac acid (DA)

Confluent monolayers of mpkCCD_{cl4} renal cells grown on permeable supports, they were excised and mounted into Ussing chambers. The cells were allowed appropriate amount of time to develop a stable basal short circuit current (SCC). The graph shows the measurement of SCC, net ion transport. At time= -30 minutes, the chloride channel inhibitors were added (50 μM GlyH-101, 30 μM digalliac acid, 60 μM digalliac acid, 50 μM GlyH-101/ 30 μM digalliac acid, 50 μM GlyH-101/ 60 μM digalliac acid) to the apical side. At time= 0 minutes, 10% CF-12 was added basolaterally, subsequently an equal amount of serum free media was added to the basolateral side to equal out the pressure. 1×10^{-5} M Amiloride was added after 30 minutes to inhibit sodium flux.

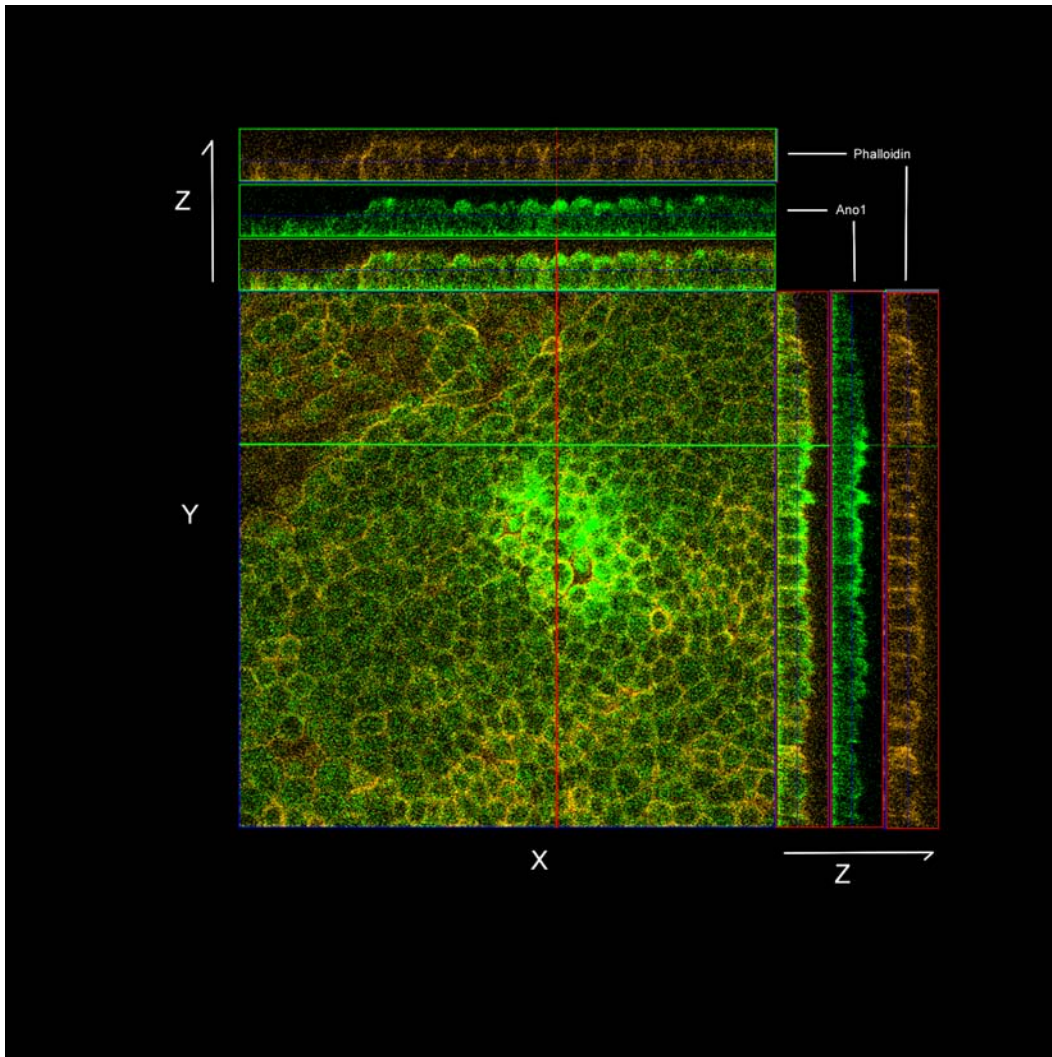


Figure 15: Immunohistochemical confocal staining of the mpkCCD_{cl4} renal cell line for TMEM16A

Confluent monolayers of mpkCCD_{cl4} renal cells were grown on permeable supports at which they cells were fixed using 4% paraformaldehyde. The cells were immunolabeled with antibodies specific for TMEM16A and AN01 (green) and actin (red). The center image is the 2-dimensional view, while the side images are a composite of the confocal images, to represent the 3-dimensional staining on the cells.

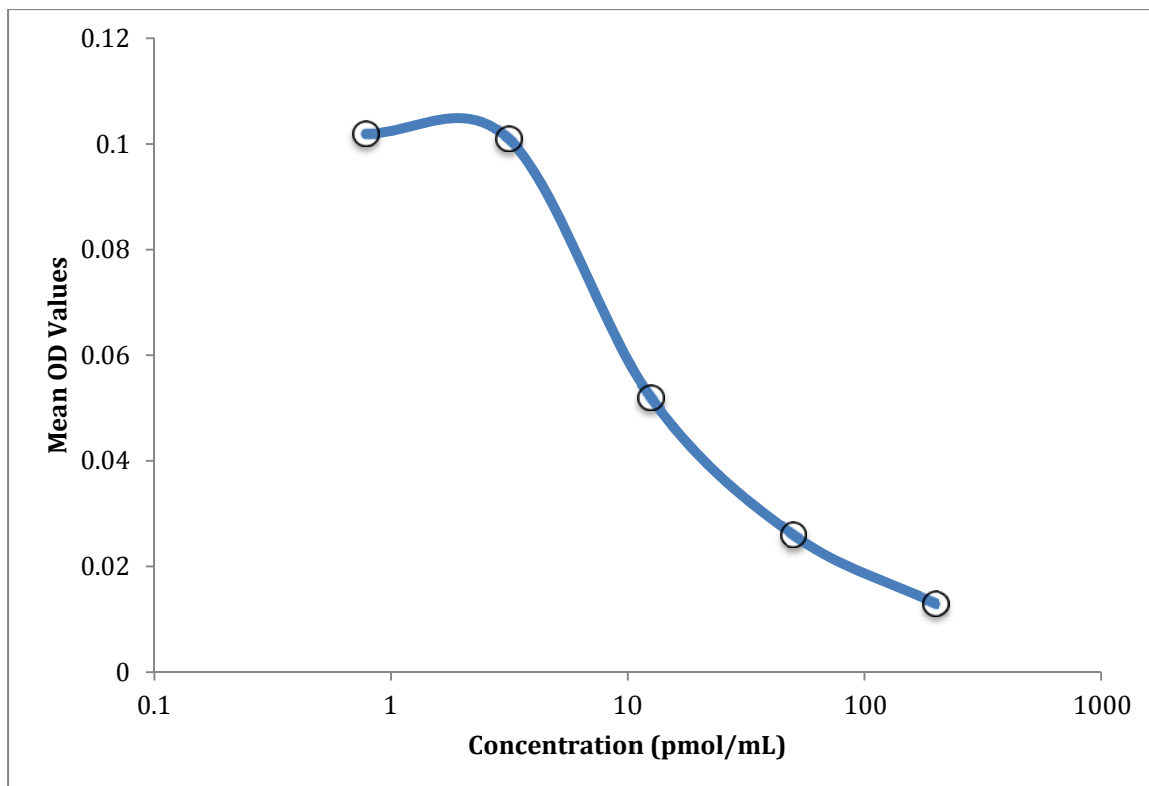


Figure 16: Standard curve generated from the cAMP standard solutions solutions

The cAMP standard (2,000 pmol/mL) was diluted down into 5 cAMP concentrations, 200 pmol/mL, 50 pmol/mL, 12.5 pmol/mL, 3.13 pmol/mL, 0.78 pmol/mL. A cAMP assay was completed on two duplicates of each of the standards and their optical density was determined at 405 nm. Using a log scale, the concentration of cAMP (pmol/mL) was graphed against the mean optical density (OD) to generate a standard curve.

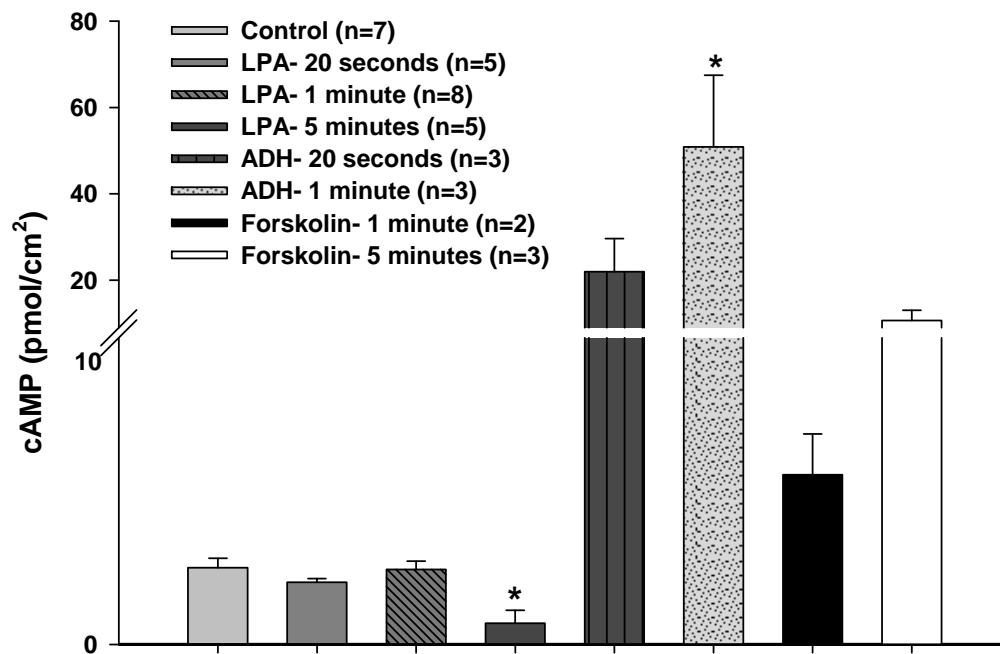


Figure 17: Concentration of cAMP (pmol/cm²) determined after stimulation of various agents with the mpkCCD_{cl4} renal cell line

Samples were collected from after stimulation with various reagents (LPA, ADH, and Forskolin) for the time frames of 20 seconds, 1 minute, and 5 minutes. A cAMP assay was completed on duplicates of the samples and their optical density was determined at 405 nm. Using a log scale, the concentration of cAMP (pmol/mL) was determined by using the standard curve and graphing the mean optical density (OD) to determine the corresponding concentration. Significance was determined by comparing the samples to the control using a students t-test, *p value* less than 0.05 were considered significant.

Fluid Secretion with mpkCCD_{cl4} renal cells

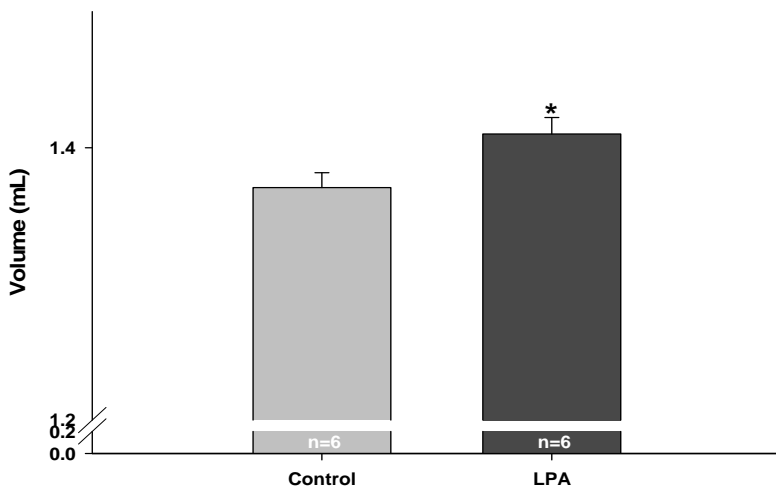


Figure 18: Fluid secretion after 5 minutes of LPA stimulation on the basolateral side of the mpkCCD_{cl4} renal cell line

Confluent monolayers of mpkCCD_{cl4} renal cells were grown on permeable supports. The feeding media was changed 24 hours prior to experiment. The cells were stimulated with 0.114 mM LPA on the basolateral side, after 5 minutes of gently swirling the secreted fluid, along with the original 1.5 mL of media was collected and weighed. Significance was completed by comparing the control LPA stimulated mass, in which 1 μ L of fluid is 1 μ g of mass. A student's t-test was used in which a *p* value of less than 0.05 is considered significant.

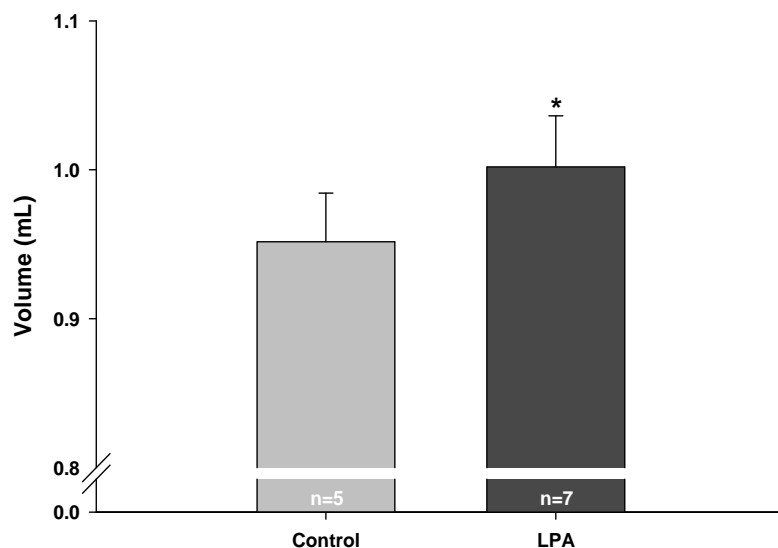


Figure 19: Fluid secretion after 24 hours of LPA stimulation on the basolateral side of the mpkCCD_{c14} renal cell line

Confluent monolayers of mpkCCD_{c14} renal cells were grown on permeable supports. The cells were stimulated with 0.114 mM LPA on the basolateral side for 24 hours. 500 μ L of mineral oil was added to reduce the loss of fluid due to evaporation. secreted fluid along with the original 1.5 mL of media was collected, and was centrifuged to removed the oil, then weighed. Significance was completed by comparing the control LPA stimulated mass, in which 1 μ L of fluid is 1 μ g of mass. A students t-test was used in which a *p value* of less than 0.05 is considered significant.

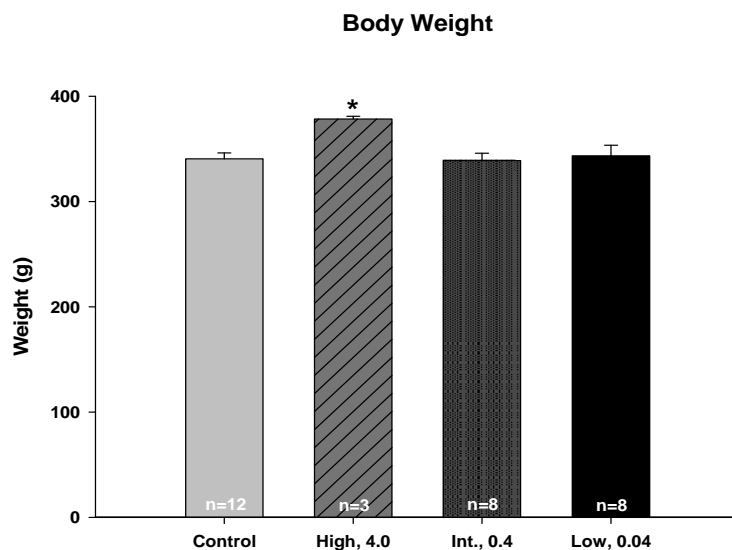


Figure 20: Rosiglitazone treated PCK rats body weight comparison for control, high, intermediate, and low dose treatment

Animals were fed rosiglitazone at the concentrations listed starting at the time of weaning (4 weeks) for 24 weeks. Body weight data are plotted as means \pm SEM. Statistics were completed using Prostat, using one-tailed Anova, using a student t-test a *p* value less than 0.05 was considered significant. Further statistics were completed using the Anova one-way testing and Anova F-test, in which the null hypothesis of the control vs. rosiglitazone treated were equal, if rejected, the data was significant.

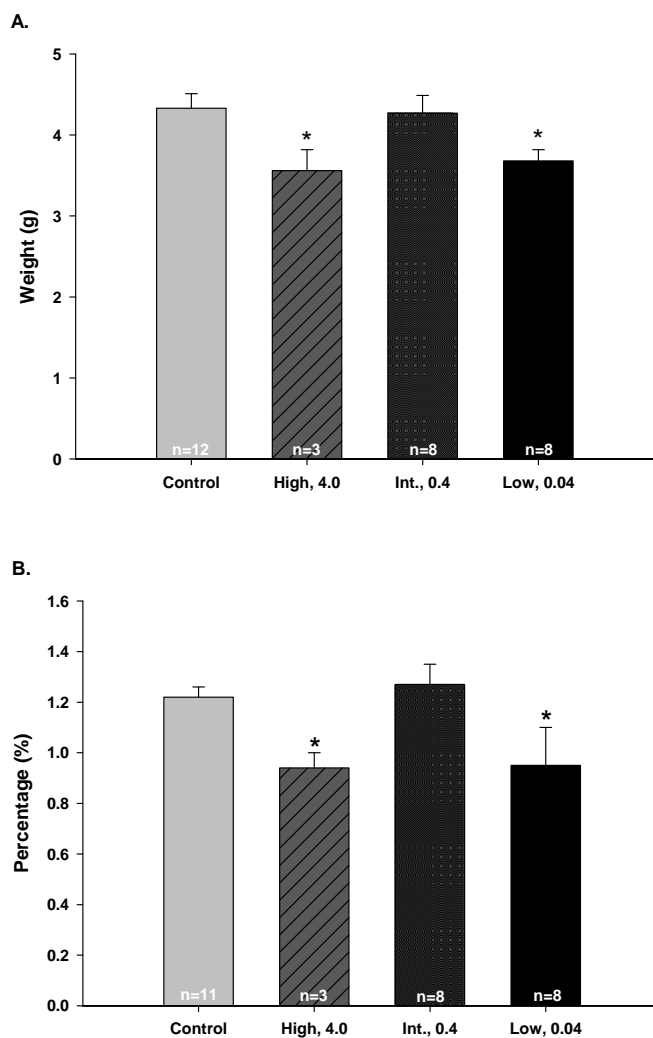


Figure 21: Rosiglitazone treated PCK rats total kidney weight (A) and kidney weight as a percent of Body weight (KW%BW) (B) comparison for control, high, intermediate, and low dose treatment

Animals were fed rosiglitazone at the concentrations listed starting at the time of weaning (4 weeks) for 24 weeks. Total Kidney Weight (A) and KW%BW (B) data are plotted as means \pm SEM. Statistics were completed using Prostat, using one-tailed Anova, using a student t-test a *p* value less than 0.05 was considered significant. Further statistics were completed using the Anova one-way testing and Anova F-test, in which the null hypothesis of the control vs. rosiglitazone treated were equal, if rejected, the data was significant.

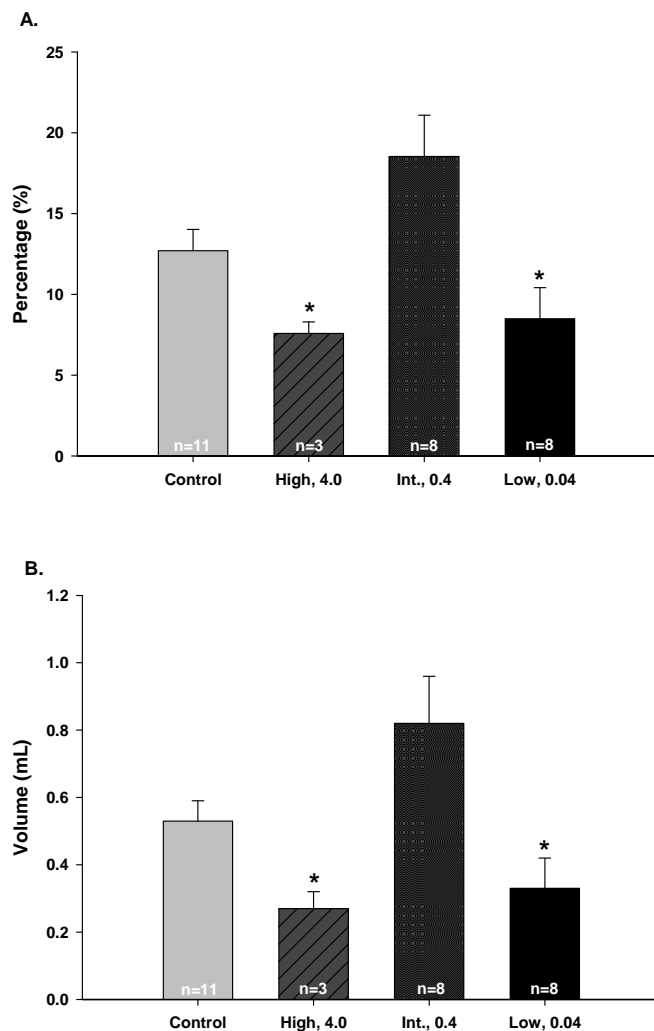


Figure 22: Rosiglitazone treated PCK rats renal cyst volume percentage (Vv) (A) and renal cyst volume (B) comparison for control, high, intermediate, and low dose treatment

Animals were fed rosiglitazone at the concentrations listed starting at the time of weaning (4 weeks) for 24 weeks. Renal cyst volume percentage (Vv) (A) and renal cyst volume (B) data are plotted as means \pm SEM. Statistics were completed using Prostat, using one-tailed Anova, using a student t-test a *p* value less than 0.05 was considered significant. Further statistics were completed using the Anova one-way testing and Anova F-test, in which the null hypothesis of the control vs. rosiglitazone treated were equal, if rejected, the data was significant.

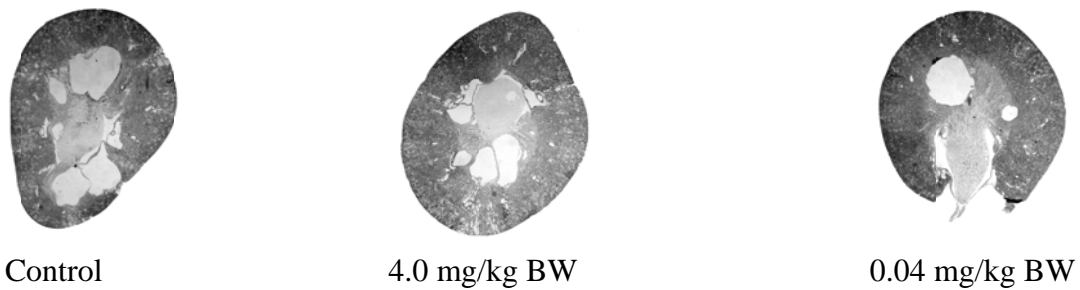


Figure 23: Histological Kidney Sections from Rosiglitazone (Control, High, Low), treated PCK rats

The images show transverse histological sections of kidneys from the PCK rats after 24 weeks of a diet supplemented with Rosiglitazone. A daily treatment of 0 mg/kg BW or control, 4.0 mg/kg BW or high, 0.04 mg/kg BW or low.

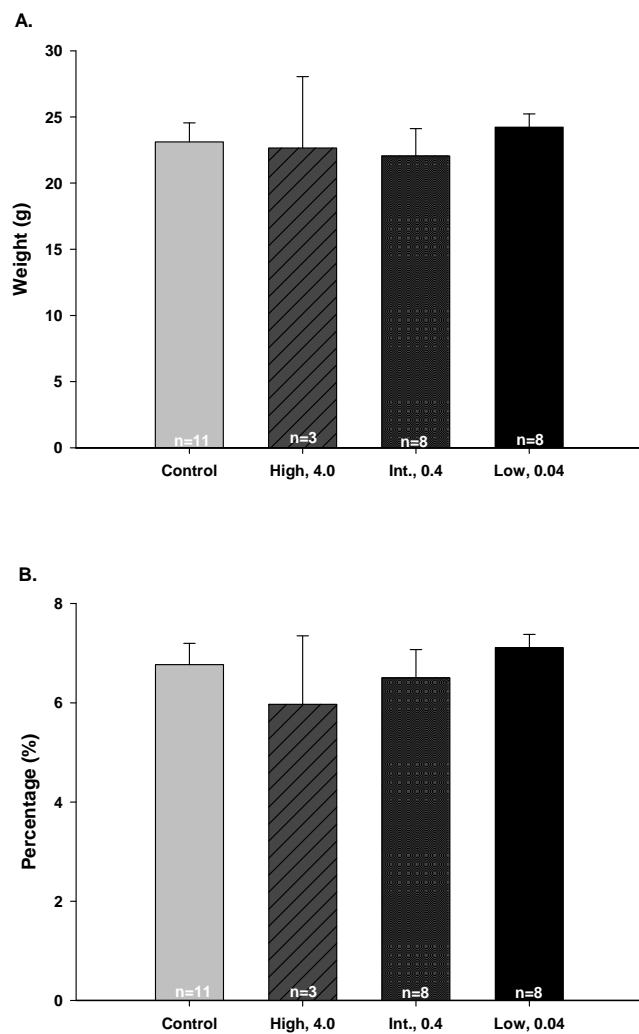


Figure 24: Rosiglitazone treated PCK rats total liver weight (A) and liver weight as a percent of Body weight (LW%BW) (B) comparison for control, high, intermediate, and low dose treatment

Animals were fed rosiglitazone at the concentrations listed starting at the time of weaning (4 weeks) for 24 weeks. Total liver weight (A) and LW%BW (B) data are plotted as means \pm SEM. Statistics were completed using Prostat, using one-tailed Anova, using a student t-test a *p* value less than 0.05 was considered significant. Further statistics were completed using the Anova one-way testing and Anova F-test, in which the null hypothesis of the control vs. rosiglitazone treated were equal, if rejected, the data was significant.

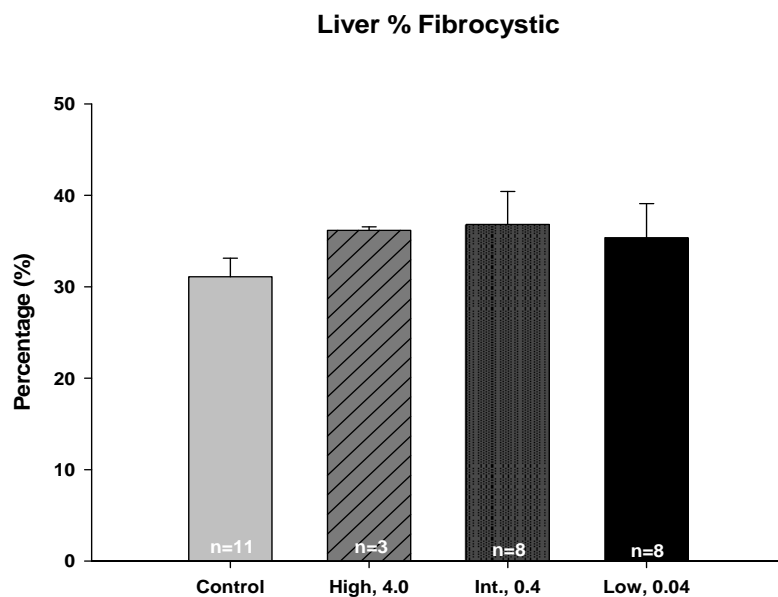


Figure 25: Rosiglitazone treated PCK rats liver percent fibrocystic comparison for control, high, intermediate, and low dose treatment

Animals were fed rosiglitazone at the concentrations listed starting at the time of weaning (4 weeks) for 24 weeks. Liver percent fibrocystic data are plotted as means \pm SEM. Statistics were completed using Prostat, using one-tailed Anova, using a student t-test a *p* value less than 0.05 was considered significant. Further statistics were completed using the Anova one-way testing and Anova F-test, in which the null hypothesis of the control vs. rosiglitazone treated were equal, if rejected, the data was significant.

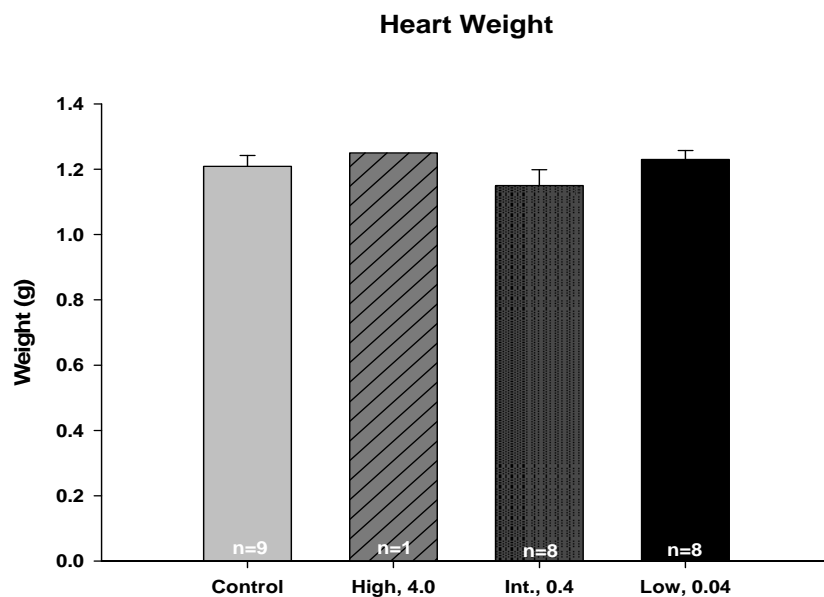


Figure 26: Rosiglitazone treated PCK rats heart weight comparison for control, high, intermediate, and low dose treatment

Animals were fed rosiglitazone at the concentrations listed starting at the time of weaning (4 weeks) for 24 weeks. Heart weight data are plotted as means \pm SEM. Statistics were completed using Prostat, using one-tailed Anova, using a student t-test a *p* value less than 0.05 was considered significant. Further statistics were completed using the Anova one-way testing and Anova F-test, in which the null hypothesis of the control vs. rosiglitazone treated were equal, if rejected, the data was significant.

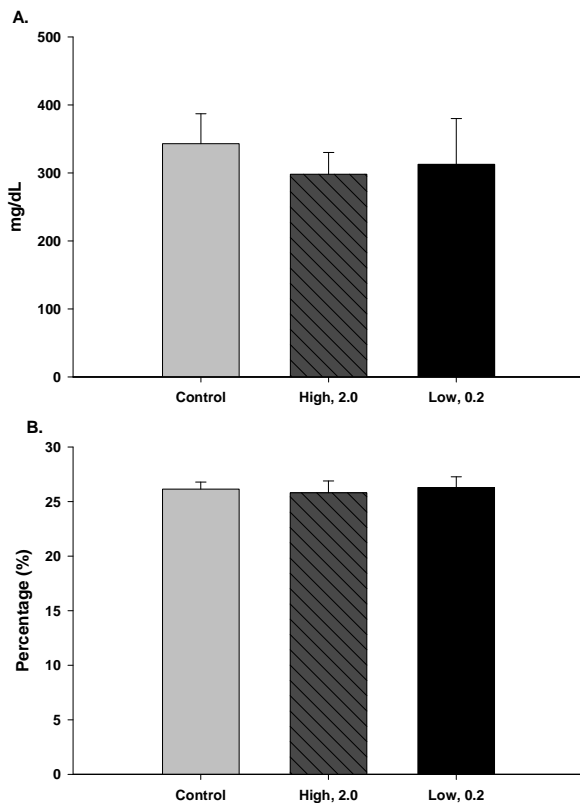


Figure 27: 10 Day Pioglitazone treated W-WPK rats glucose (A) and hematocrit (B) comparison for control, high, and low dose treatment

Animals were fed pioglitazone at the concentrations listed starting at day 5 of age and continued on treatment till day 10. Glucose (A) and hematocrit (B) data are plotted as means \pm SEM. Statistics were completed using Prostat, using one-tailed Anova, using a student t-test a *p* value less than 0.05 was considered significant. Further statistics were completed using the Anova one-way testing and Anova F-test, in which the null hypothesis of the control vs. rosiglitazone treated were equal, if rejected, the data was significant.

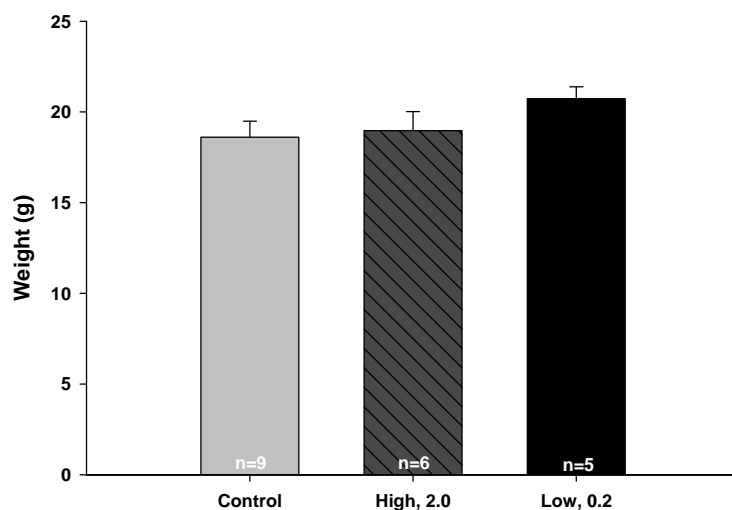


Figure 28: 10 Day Pioglitazone treated W-WPK rats body weight comparison for control, high, and low dose treatment

Animals were fed pioglitazone at the concentrations listed starting at day 5 of age and continued on treatment till day 10. Body weight data are plotted as means \pm SEM. Statistics were completed using Prostat, using one-tailed Anova, using a student t-test a *p* value less than 0.05 was considered significant. Further statistics were completed using the Anova one-way testing and Anova F-test, in which the null hypothesis of the control vs. rosiglitazone treated were equal, if rejected, the data was significant.

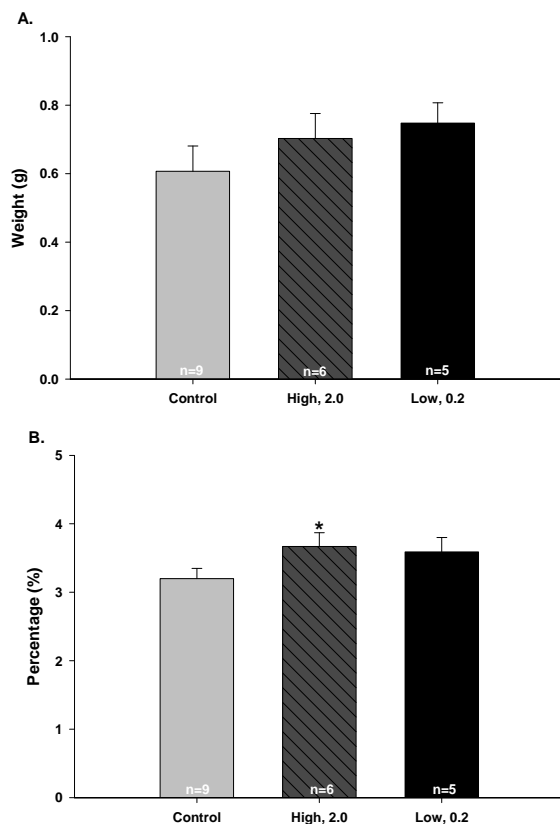


Figure 29: 10 Day Pioglitazone treated W-WPK rats total kidney weight (A) and kidney weight as a percent of body weight (KW%BW) (B) comparison for control, high, and low dose treatment

Animals were fed pioglitazone at the concentrations listed starting at day 5 of age and continued on treatment till day 10. Total kidney weight (A) and KW%BW (B) data are plotted as means \pm SEM. Statistics were completed using Prostat, using one-tailed Anova, using a student t-test a *p* value less than 0.05 was considered significant. Further statistics were completed using the Anova one-way testing and Anova F-test, in which the null hypothesis of the control vs. rosiglitazone treated were equal, if rejected, the data was significant.

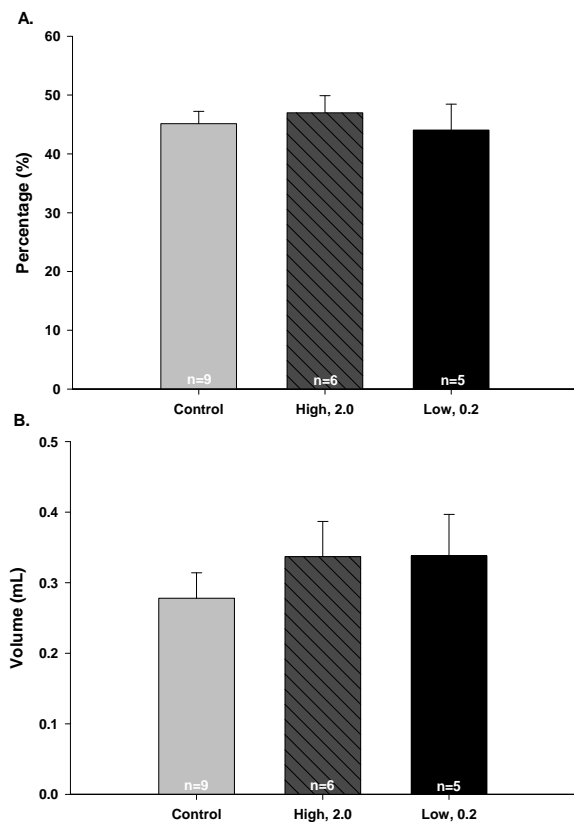


Figure 30: 10 Day Pioglitazone treated W-WPK rats renal cyst volume percentage (Vv) (A) and renal cyst volume (B) comparison for control, high, and low dose treatment

Animals were fed pioglitazone at the concentrations listed starting at day 5 of age and continued on treatment till day 10. Renal cyst volume percentage (Vv) (A) and renal cyst volume (B) data are plotted as means \pm SEM. Statistics were completed using Prostat, using one-tailed Anova, using a student t-test a *p* value less than 0.05 was considered significant. Further statistics were completed using the Anova one-way testing and Anova F-test, in which the null hypothesis of the control vs. rosiglitazone treated were equal, if rejected, the data was significant.

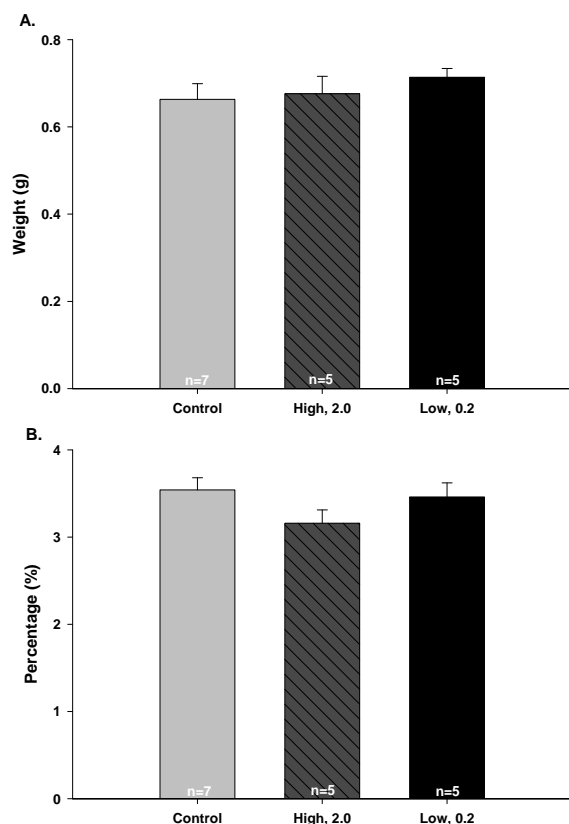


Figure 31: 10 Day Pioglitazone treated W-WPK rats total liver weight (A) and liver weight as a percent of body weight (LW%BW) (B) comparison for control, high, and low dose treatment

Animals were fed pioglitazone at the concentrations listed starting at day 5 of age and continued on treatment till day 10. Total liver weight (A) and LW%BW (B) data are plotted as means \pm SEM. Statistics were completed using Prostat, using one-tailed Anova, using a student t-test a *p* value less than 0.05 was considered significant. Further statistics were completed using the Anova one-way testing and Anova F-test, in which the null hypothesis of the control vs. rosiglitazone treated were equal, if rejected, the data was significant.

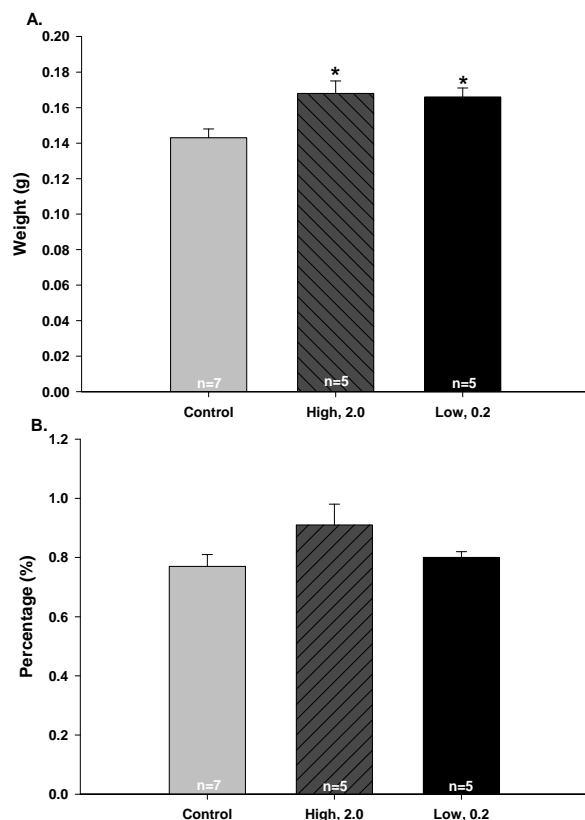


Figure 32: 10 Day Pioglitazone treated W-WPK rats total heart weight (A) and heart weight as a percent of body weight (HW%BW) (B) comparison for control, high, and low dose treatment

Animals were fed pioglitazone at the concentrations listed starting at day 5 of age and continued on treatment till day 10. Total heart weight (A) and HW%BW (B) data are plotted as means \pm SEM. Statistics were completed using Prostat, using one-tailed Anova, using a student t-test a *p* value less than 0.05 was considered significant. Further statistics were completed using the Anova one-way testing and Anova F-test, in which the null hypothesis of the control vs. rosiglitazone treated were equal, if rejected, the data was significant.

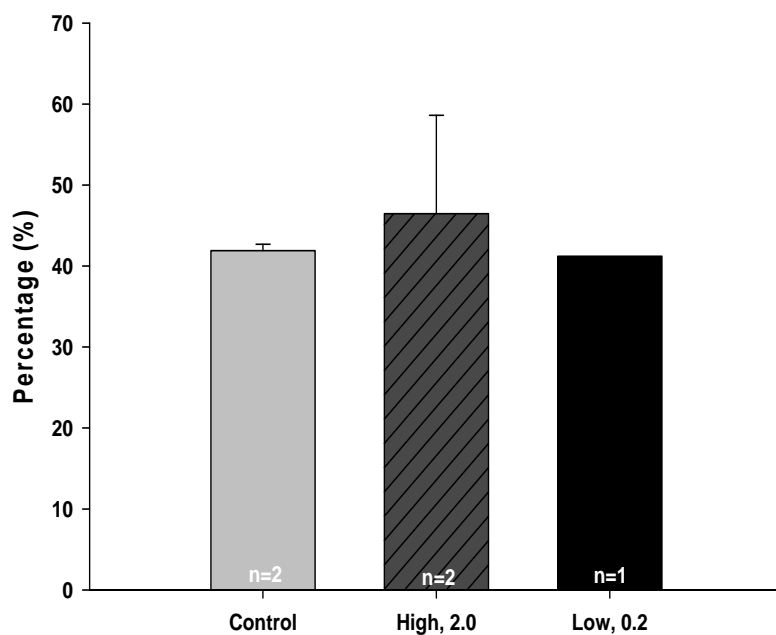


Figure 33: 10 Day Pioglitazone treated W-WPK rats CT renal cyst volume percentage comparison for control, high, and low dose treatment

Animals were fed pioglitazone at the concentrations listed starting at day 5 of age and continued on treatment till day 10. CT renal cyst volume percentage are plotted as means \pm SEM. Statistics were completed using Prostat, using one-tailed Anova, using a student t-test a *p value* less than 0.05 was considered significant. Further statistics were completed using the Anova one-way testing and Anova F-test, in which the null hypothesis of the control vs. rosiglitazone treated were equal, if rejected, the data was significant.

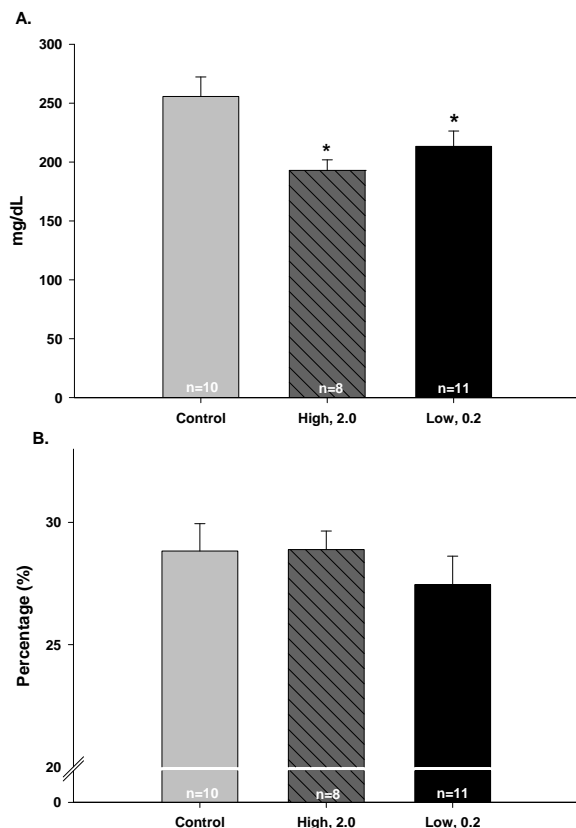


Figure 34: 18 Day Pioglitazone treated W-WPK rats glucose (A) and hematocrit (B) comparison for control, high, and low dose treatment

Animals were fed pioglitazone at the concentrations listed starting at day 5 of age and continued on treatment till day 18. Glucose (A) and hematocrit (B) data are plotted as means \pm SEM. Statistics were completed using Prostat, using one-tailed Anova, using a student t-test a *p* value less than 0.05 was considered significant. Further statistics were completed using the Anova one-way testing and Anova F-test, in which the null hypothesis of the control vs. rosiglitazone treated were equal, if rejected, the data was significant.

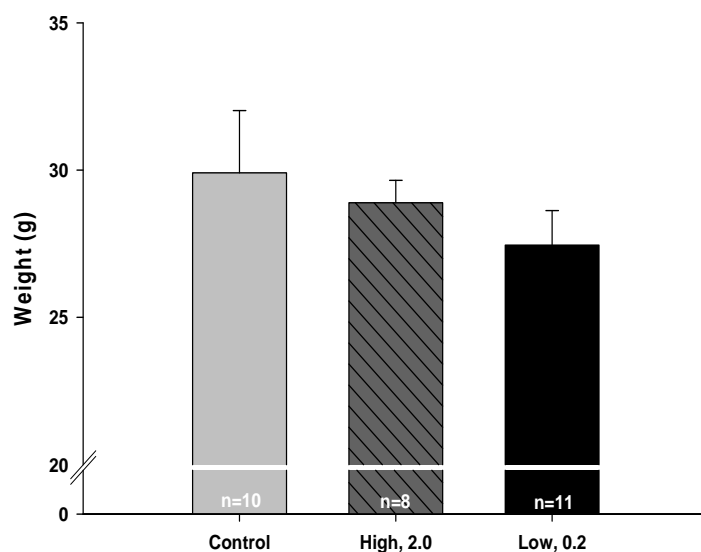


Figure 35: 18 Day Pioglitazone treated W-WPK rats body weight comparison for control, high, and low dose treatment

Animals were fed pioglitazone at the concentrations listed starting at day 5 of age and continued on treatment till day 18. Body weight data are plotted as means \pm SEM. Statistics were completed using Prostat, using one-tailed Anova, using a student t-test a *p* value less than 0.05 was considered significant. Further statistics were completed using the Anova one-way testing and Anova F-test, in which the null hypothesis of the control vs. rosiglitazone treated were equal, if rejected, the data was significant.

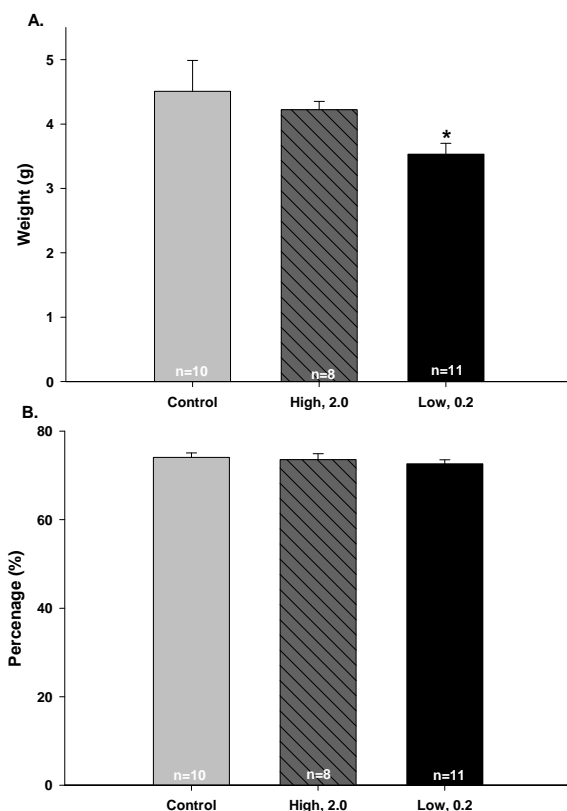


Figure 36: 18 Day Pioglitazone treated W-WPK rats total kidney weight (A) and kidney weight as a percent of body weight (KW% BW) (B) comparison for control, high, and low dose treatment

Animals were fed pioglitazone at the concentrations listed starting at day 5 of age and continued on treatment till day 18. Total kidney weight (A) and KW% BW (B) data are plotted as means \pm SEM. Statistics were completed using Prostat, using one-tailed Anova, using a student t-test a *p* value less than 0.05 was considered significant. Further statistics were completed using the Anova one-way testing and Anova F-test, in which the null hypothesis of the control vs. rosiglitazone treated were equal, if rejected, the data was significant.

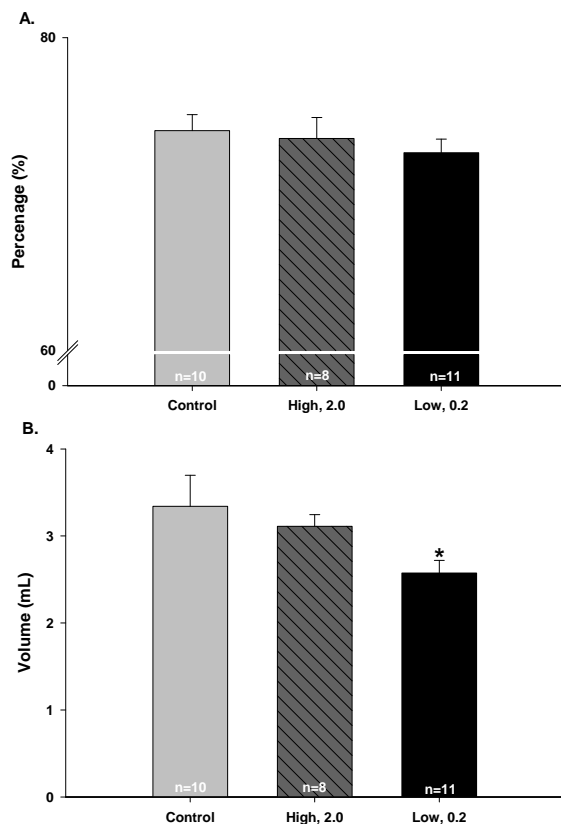


Figure 37: 18 Day Pioglitazone treated W-WPK rats renal cyst volume percentage (Vv) (A) and renal cyst volume (B) comparison for control, high, and low dose treatment

Animals were fed pioglitazone at the concentrations listed starting at day 5 of age and continued on treatment till day 18. Renal cyst volume percentage (Vv) (A) and renal cyst volume (B) data are plotted as means \pm SEM. Statistics were completed using Prostat, using one-tailed Anova, using a student t-test a *p* value less than 0.05 was considered significant. Further statistics were completed using the Anova one-way testing and Anova F-test, in which the null hypothesis of the control vs. rosiglitazone treated were equal, if rejected, the data was significant.

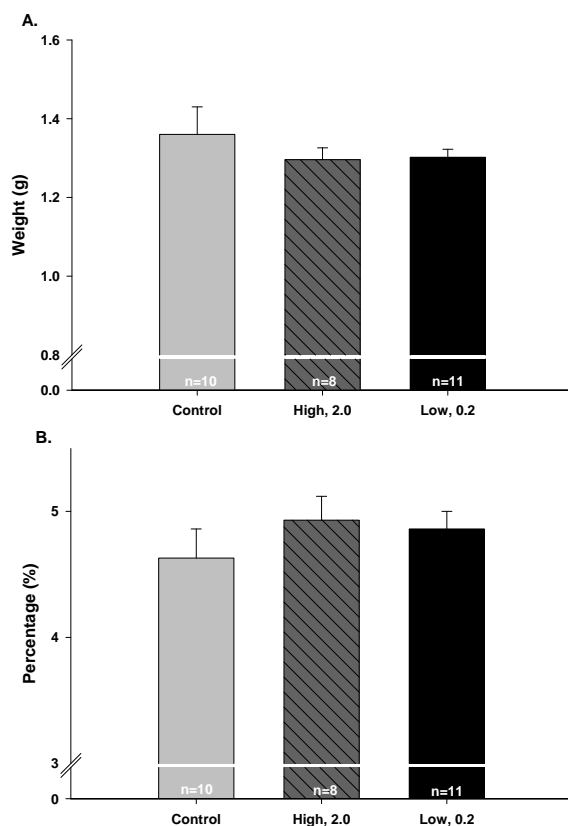


Figure 38: 18 Day Pioglitazone treated W-WPK rats total liver weight (A) and liver weight as a percent of body weight (LW% BW) (B) comparison for control, high, and low dose treatment

Animals were fed pioglitazone at the concentrations listed starting at day 5 of age and continued on treatment till day 18. Total liver weight (A) and LW% BW (B) data are plotted as means \pm SEM. Statistics were completed using Prostat, using one-tailed Anova, using a student t-test a *p value* less than 0.05 was considered significant. Further statistics were completed using the Anova one-way testing and Anova F-test, in which the null hypothesis of the control vs. rosiglitazone treated were equal, if rejected, the data was significant.

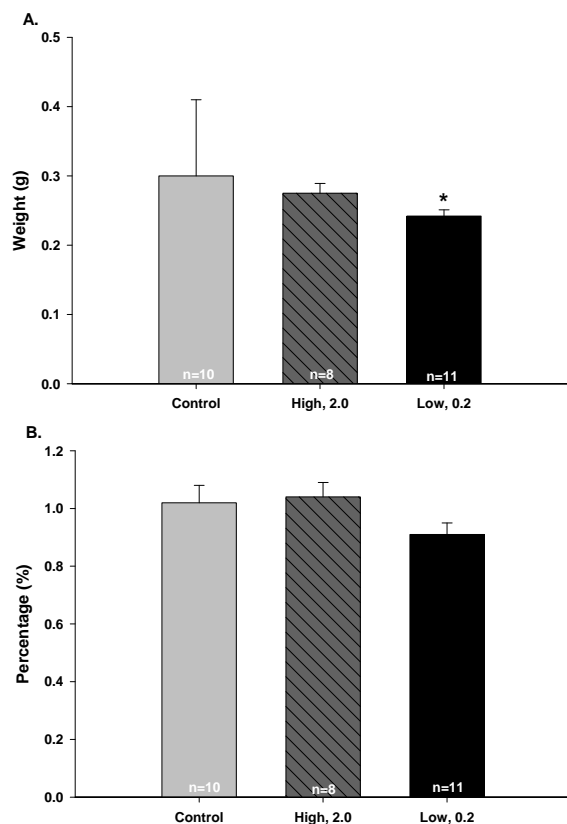


Figure 39: 18 Day Pioglitazone treated W-WPK rats total heart weight (A) and heart weight as a percent of body weight (HW% BW) (B) comparison for control, high, and low dose treatment

Animals were fed pioglitazone at the concentrations listed starting at day 5 of age and continued on treatment till day 18. Total heart weight (A) and HW% BW (B) data are plotted as means \pm SEM. Statistics were completed using Prostat, using one-tailed Anova, using a student t-test a *p* value less than 0.05 was considered significant. Further statistics were completed using the Anova one-way testing and Anova F-test, in which the null hypothesis of the control vs. rosiglitazone treated were equal, if rejected, the data was significant.

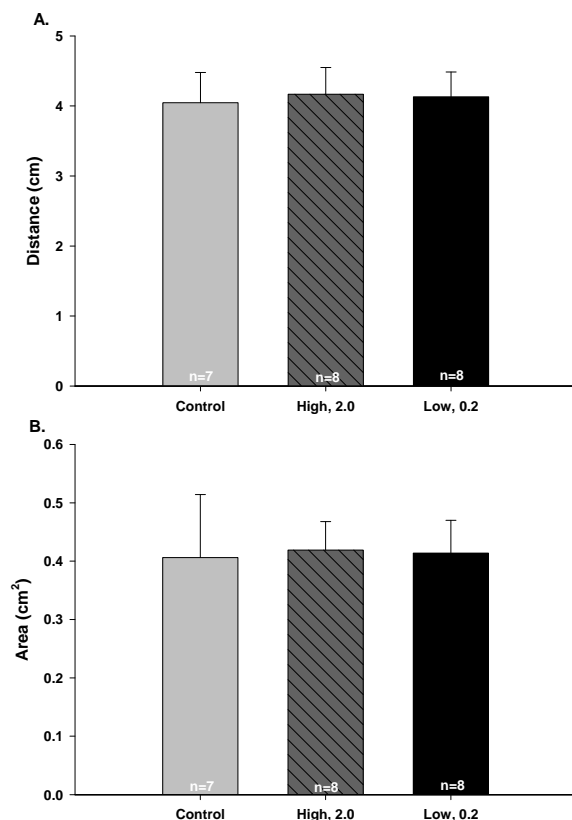


Figure 40: 18 Day Pioglitazone treated W-WPK rats brain perimeter (A) and brain area (B) comparison for control, high, and low dose treatment

Animals were fed pioglitazone at the concentrations listed starting at day 5 of age and continued on treatment till day 18. Brain perimeter (A) and brain area (B) data are plotted as means \pm SEM. Statistics were completed using Prostat, using one-tailed Anova, using a student t-test a *p* value less than 0.05 was considered significant. Further statistics were completed using the Anova one-way testing and Anova F-test, in which the null hypothesis of the control vs. rosiglitazone treated were equal, if rejected, the data was significant.



Figure 41: 18 Day Pioglitazone 3-D Cystic Tissue Image generated from Philips program using CT value ranges

Animals were fed pioglitazone starting at day 5 of age and continued on treatment till day 18. From each treatment group at day 18, some W-WPK rats were randomly chosen to be scanned. The CT scans generated a series of images to generate the whole animal. By analyzing each image in which the kidney was present, a 3-dimensional kidney was built, by only using CT value ranges for cyst tissue.

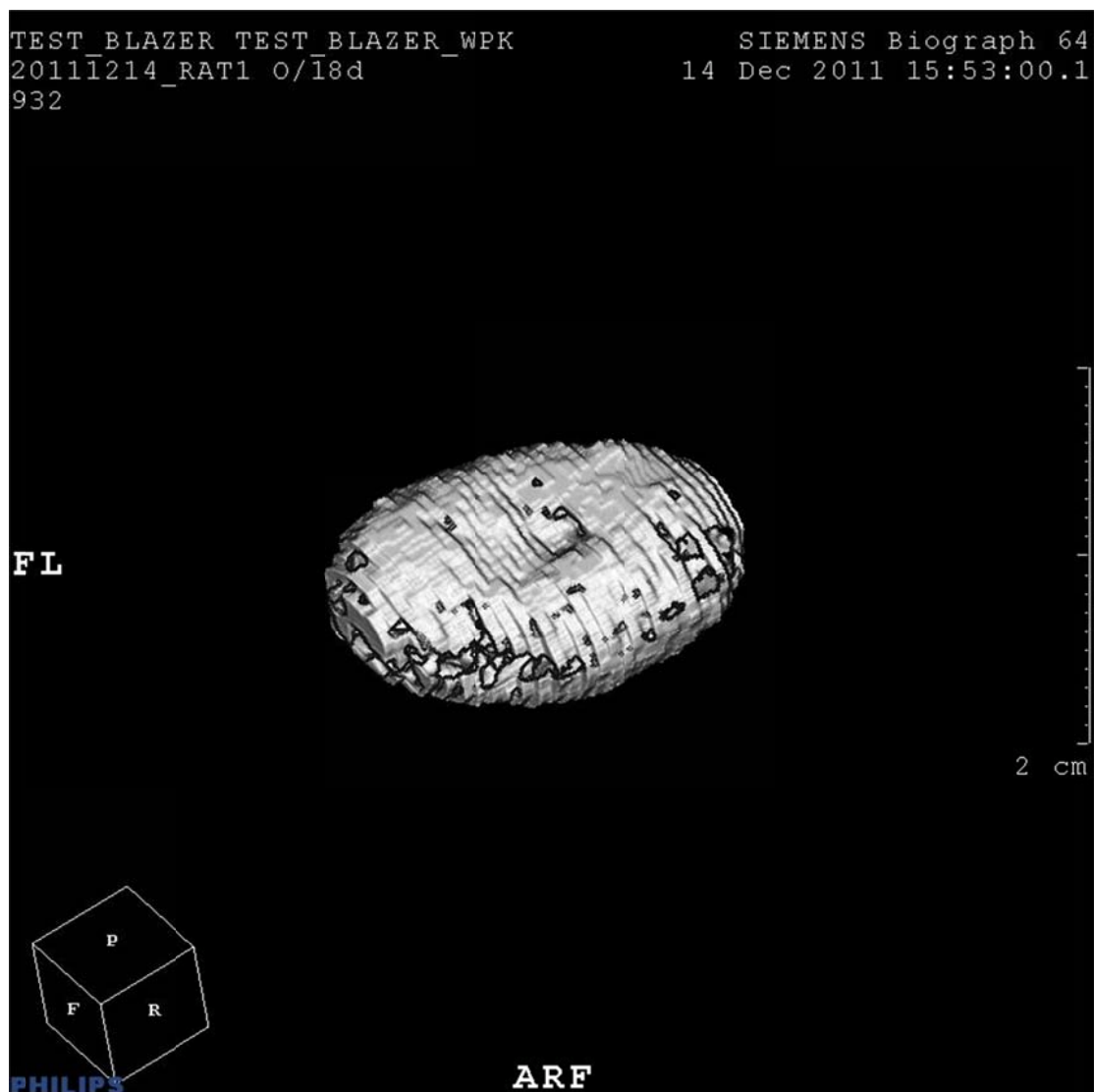


Figure 42: 18 Day Pioglitazone 3-D Cystic Normal Image generated from Philips program using CT value ranges

Animals were fed pioglitazone starting at day 5 of age and continued on treatment till day 18. From each treatment group at day 18, some W-WPK rats were randomly chosen to be scanned. The CT scans generated a series of images to generate the whole animal. By analyzing each image in which the kidney was present, a 3-dimensional kidney was built, by only using CT value ranges for normal tissue.

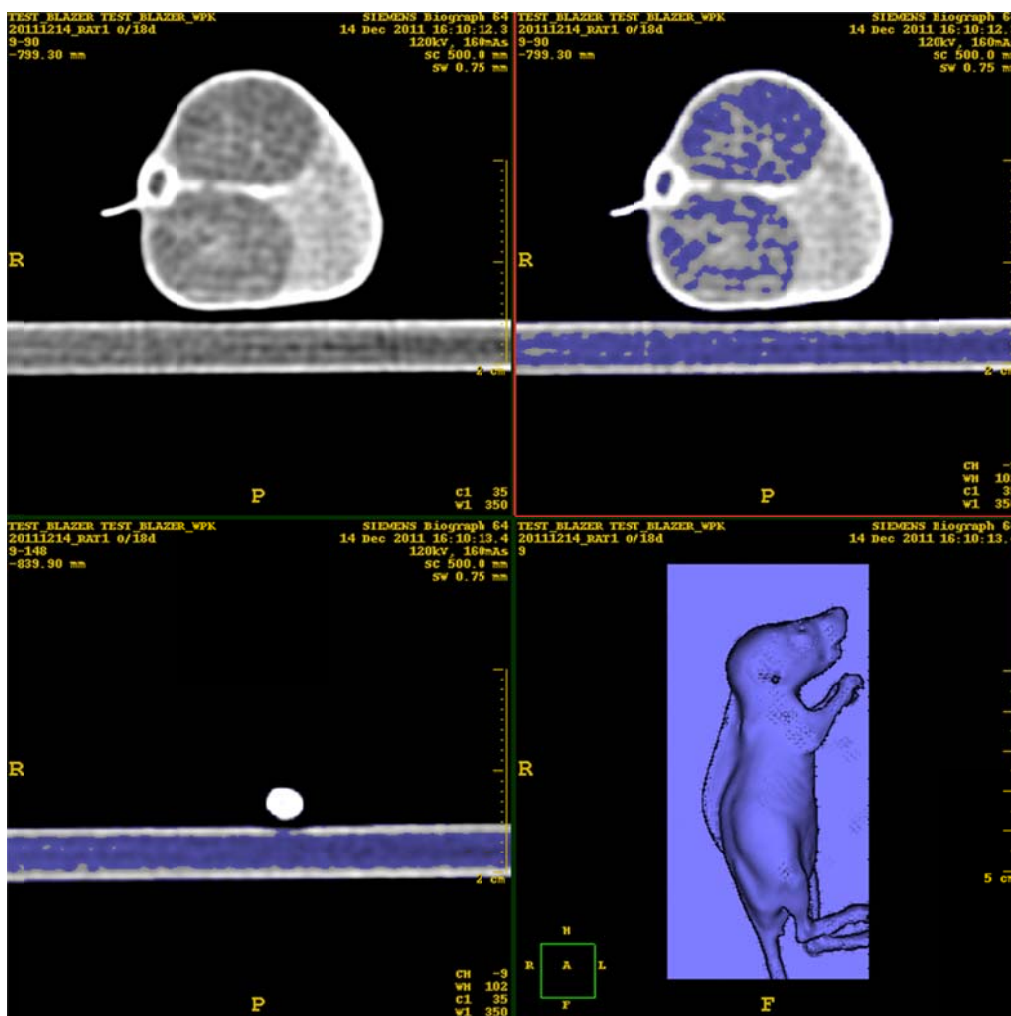


Figure 43: 18 Day Pioglitazone 2-D Image of CT values labeling for cystic tissue from Philips program

Animals were fed pioglitazone starting at day 5 of age and continued on treatment till day 18. From each treatment group at day 18, some W-WPK rats were randomly chosen to be scanned. The CT scans generated a series of images to generate the whole animal. CT value ranges were determined, in which only the cystic tissue in the kidney was labeled blue (upper right panel), and could be applied to the whole animal for analysis to generate a 3-dimensional kidney (lower right panel). The other images were other views to help aid in the analysis

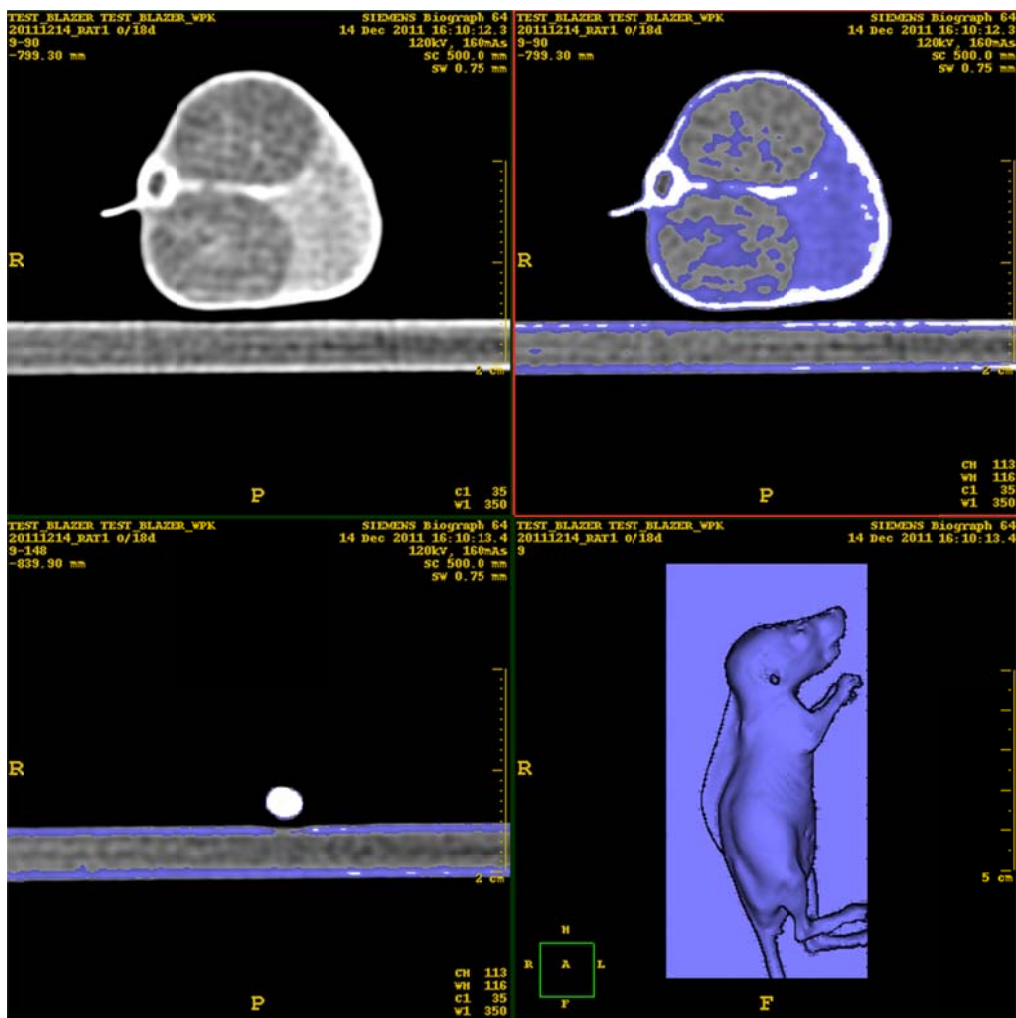


Figure 44: 18 Day Pioglitazone 2-D Image of CT values labeling for normal tissue from Philips program

Animals were fed pioglitazone starting at day 5 of age and continued on treatment till day 18. From each treatment group at day 18, some W-WPK rats were randomly chosen to be scanned. The CT scans generated a series of images to generate the whole animal. CT value ranges were determined, in which only the normal tissue in the kidney was labeled blue (upper right panel), and could be applied to the whole animal for analysis to generate a 3-dimensional kidney (lower right panel). The other images were other views to help aid in the analysis

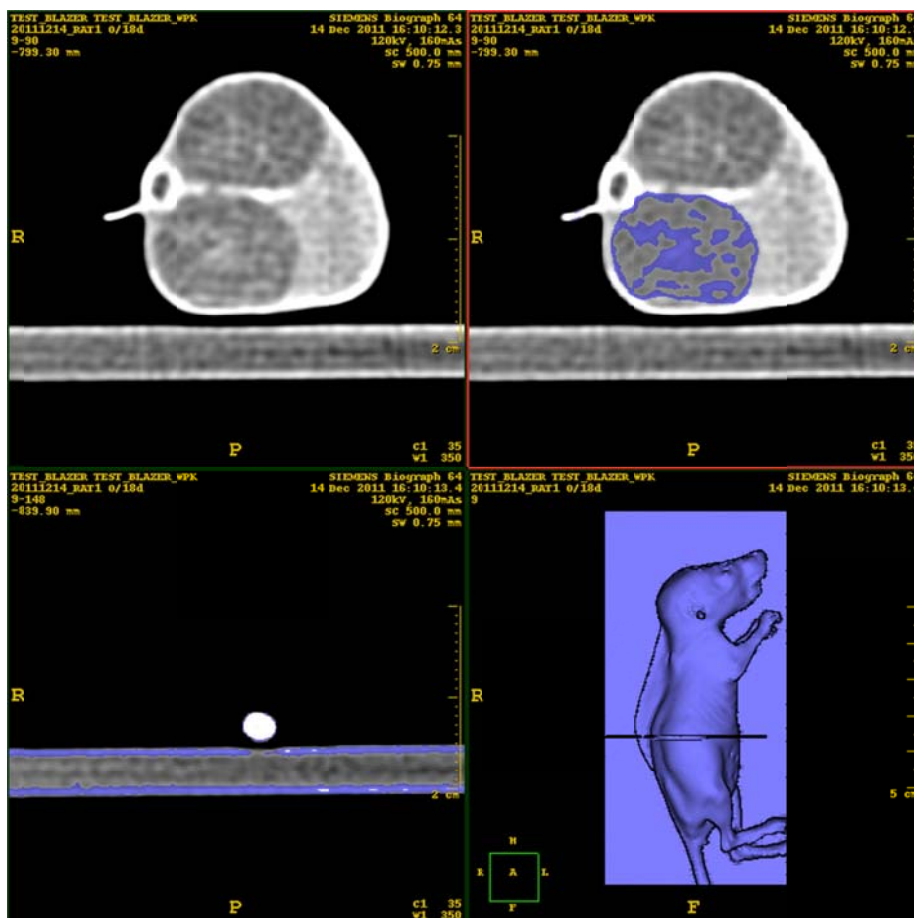


Figure 45: 18 Day Pioglitazone 2-D Image of CT values labeling for normal tissue from Philips program, with all other CT labeled tissue removed, besides the kidney

Animals were fed pioglitazone starting at day 5 of age and continued on treatment till day 18. From each treatment group at day 18, some W-WPK rats were randomly chosen to be scanned. The CT scans generated a series of images to generate the whole animal. CT value ranges were determined, in which only the normal tissue in the kidney was labeled blue and by using the tools of the program the other labeled regions of the 2-dimensional image was removed, leaving only the normal functioning tissue of the kidney labeled blue (upper right panel). This could be applied to the whole animal for analysis to generate a 3-dimensional kidney, in which the areas that were removed from the one 2-dimensional image are now removed from the 3-dimensional image (lower right panel). The other images were other views to help aid in the analysis

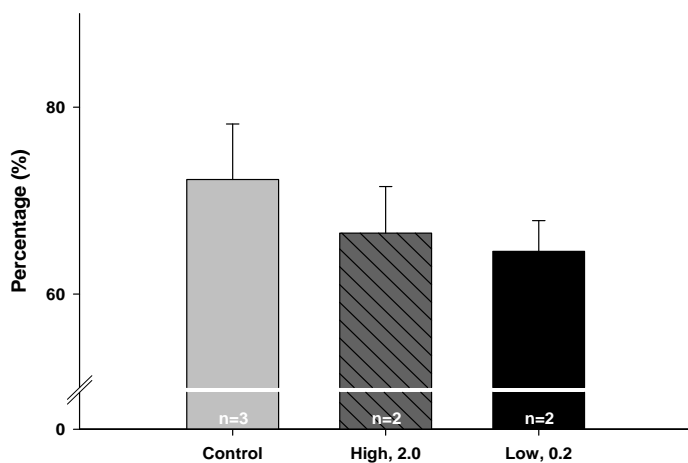


Figure 46: 18 Day Pioglitazone treated W-WPK rats CT renal cyst volume percentage comparison for control, high, and low dose treatment

Animals were fed pioglitazone at the concentrations listed starting at day 5 of age and continued on treatment till day 10. CT renal cyst volume percentage are plotted as means \pm SEM. Statistics were completed using Prostat, using one-tailed Anova, using a student t-test a *p* value less than 0.05 was considered significant. Further statistics were completed using the Anova one-way testing and Anova F-test, in which the null hypothesis of the control vs. rosiglitazone treated were equal, if rejected, the data was significant.

VITA

VITA

Stephanie Marge Flaig

EDUCATION

Indiana University Purdue University at Indianapolis, Indianapolis, IN
 “Development of Therapies to Treat Polycystic Disease”
M.S. in BiologyDecember 2012

Indiana University Purdue University at Indianapolis, Indianapolis, IN
B.S. in Biology/ Minor in ChemistryAugust 2010

AWARDS & HONORS

Indiana University Purdue University at Indianapolis, Indianapolis, IN
 Educational Enhancement Grant by Graduate Student OrganizationSpring 2012
 School of Science Graduate Student Council Travel AwardSpring 2012
 Student Travel Grant by Center of Membrane SciencesSpring 2011
Ball State University, Muncie, IN
 Indiana Physiological Society
 Graduate Student Research AwardFebruary 2012

UNIVERSITY SERVICE

Indiana University Purdue University at Indianapolis, Indianapolis, IN
Biology Graduate Student Organization
 President Fall 2011-Spring 2012
 Member Fall 2010-Spring 2011
IUPUI Science Apprenticeship Camp
 Team LeaderJune 2011, June 2012
IU School of Medicine Camp MD
 Research Demonstrator May 2012

COMMUNITY SERVICE

Indianapolis Humane Society

Medical Screening Volunteer March 2012-Current
Indiana University Purdue University at Indianapolis, Indianapolis, IN

24th Hoosier Science and Engineering Fair

Senior Judge April 2012
Ivy Technical University, Bloomington, IN

23rd Hoosier Science and Engineering Fair

Senior Judge April 2011

TEACHING EXPERIENCE

Indiana University Purdue University at Indianapolis, Indianapolis, IN

Teaching Assistant

Human Biology Laboratory Spring 2012

Anatomy Laboratory Spring 2011

RESEARCH EXPERIENCE

Indiana Nanotech, Indianapolis, IN

Research Technician January 2010-April 2011

Indiana School of Dentistry, Indianapolis, IN

Research Intern – Windsor Research Laboratory August 2008-April 2009

ORAL PRESENTATIONS

Indiana University Purdue University at Indianapolis, Indianapolis, IN

Department of Biology Annual Retreat

“TRPV4 treatment in the W-WPK rat model of hydrocephalus” October 2012

Experimental Biology 2012, San Diego, CA

“Low dose Low dose PPAR γ agonist inhibition of cyst growth in the PCK model of polycystic kidney disease” April 2012

Lake Cumberland Biological Transport Group of the American Physiological Society Annual Meeting, Jamestown, KY

“Low dose PPAR γ agonist inhibition of cyst growth in the rat models of polycystic kidney disease” June 2012

“Activation of chloride channels in the mpkCCD_{cl4} renal cell line in response to lysophosphatidic acid (LPA)” June 2011

POSTER PRESENTATIONS

- Experimental Biology 2012, San Diego, CA
 “Low dose Low dose PPAR γ agonist inhibition of cyst growth in the PCK model of polycystic kidney disease” April 2012
- IUPUI Research Day, Indianapolis, IN
 “Low dose Low dose PPAR γ agonist inhibition of cyst growth in the PCK model of polycystic kidney disease” April 2012
- Indiana Physiological Society 2nd Annual Meeting, Muncie, IN
 “Low dose Low dose PPAR γ agonist inhibition of cyst growth in the PCK model of polycystic kidney disease” February 2012
- Experimental Biology 2011, Washington D.C.
 “Activation of chloride channels in the mpkCCD_{cl4} renal cell line in response to lysophosphatidic acid (LPA)” April 2011
- Indiana Physiological Society 1st Annual Meeting, Indianapolis, IN
 “Activation of chloride channels in the mpkCCD_{cl4} renal cell line in response to lysophosphatidic acid (LPA)” February 2011

PUBLISHED PAPERS

- Blazer-Yost B.L., Blacklock B.J., Flaig S.M., et al., “Lysophosphatidic Acid is a Modulator of Cyst Growth in Autosomal Dominant Polycystic Kidney Disease.” *Cellular Physiology and Biochemistry*, vol 28, pp 1255-1264, 2011.
- Karlinsey R.L., Mackey A.C., Walker T.J., Frederick K.E., Blanken D.D., Flaig S.M., and Walker E.R., “*In vitro* remineralization of human and bovine white-spot enamel lesions by NaF dentifrices: A pilot study.” *Journal of Dentistry and Oral Hygiene*, vol 3, no 2, pp 22-29, 2011.

PUBLISHED ABSTRACTS

- Flaig S.M., Carr A., Gattone V.H., and Blazer-Yost B.L., “Low dose PPAR γ agonist inhibition of cyst growth in the PCK rat model of polycystic kidney disease.” *The Journal of the Federation of American Societies for Experimental Biology*, vol 26, pp 868.4, 2012.
- Flaig S.M. and Blazer-Yost B.L., “Activation of chloride channels in the mpkCCD_{cl4} renal cell line in response to lysophosphatidic acid (LPA).” *The Journal of the Federation of American Societies for Experimental Biology*, vol 25, pp 839.1, 2011.